Enhancement of Polymer-mediated Gene Expression using Chemotherapeutic Modulators of Intracellular Trafficking and Cell Cycle Progression

by

Sutapa Barua

A Dissertation Presented in Partial Fulfillment
of the Requirements for the Degree
Doctor of Philosophy

Approved April 2011 by the
Graduate Supervisory Committee:

Kaushal Rege
Deirdre Meldrum
Christina Voelkel-Johnson
Lenore Dai
Michael Sierks

ARIZONA STATE UNIVERSITY

May 2011

ABSTRACT

Gene therapy is a promising technology for the treatment of various nonheritable and genetically acquired diseases. It involves delivery of a therapeutic gene into target cells to induce cellular responses against diseases. Successful gene therapy requires an efficient gene delivery vector to deliver genetic materials into target cells. There are two major classes of gene delivery vectors: viral and non-viral vectors. Recently, non-viral vectors such as cationic polymers have attracted more attention than viral vectors because they are versatile and non-immunogenic. However, cationic polymers suffer from poor gene delivery efficiency due to biological barriers. The objective of this research is to develop strategies to overcome the barriers and enhance polymer-mediated transgene expression.

This study aimed to (i) develop new polymer vectors for gene delivery, (ii) investigate the intracellular barriers in polymer-mediated gene delivery, and (iii) explore new approaches to overcome the barriers. A cationic polymer library was developed by employing a parallel synthesis and high-throughput screening method. Lead polymers from the library were identified from the library based on relative levels of transgene expression and toxicity in PC3-PSMA prostate cancer cells. However, transgene expression levels were found to depend on intracellular localization of polymer-gene complexes (polyplexes). Transgene expression was higher when polyplexes were dispersed rather than localized in the cytoplasm.

Combination treatments using small molecule chemotherapeutic drugs, e.g. histone deacetylase inhibitors (HDACi) or Aurora kinase inhibitor (AKI)

increased dispersion of polyplexes in the cytoplasm and significantly enhanced transgene expression. The combination treatment using polymer-mediated delivery of p53 tumor-suppressor gene and AKI increased p53 expression in PC3-PSMA cells, inhibited the cell proliferation by ~80% and induced apoptosis. Polymer-mediated p53 gene delivery in combination with AKI offers a promising treatment strategy for *in vivo* and clinical studies of cancer gene therapy.

DEDICATION

To Banabhante,
my father (Jinadatta Barua), mother (Smrity Kana Chowdhury),
Dipak, Uma and Dibbya

ACKNOWLEDGMENTS

First of all, I am immensely grateful to my advisor Dr. Kaushal Rege for his continuous support and guidance throughout the project. I gratefully thank Dr. Deirdre Meldrum, Dr. Roger Johnson and Dr. Honor Glenn of the Center for Biosignatures Discovery Automation at the Biodesign Institute at Arizona State University (ASU) for the training and access to the Nikon confocal microscope used in several studies in this research. Many thanks to Dr. Christina Voelkel-Johnson at the Medical University of South Carolina (MUSC) in Charleston, SC, and Dr. Michael Sierks of Chemical Engineering at ASU for helpful discussions and insights related to this work. Thanks are due to Dr. Lenore Dai for agreeing to be in my committee.

I thank Dr. Michel Sadelain and Gertrude Gunset at the Memorial Sloan Kettering Cancer Center in New York, NY for their generous donation of the PC3-flu and PC3-PSMA cells employed in this research. Many thanks to Professor Vinod Labhasetwar and Dr. Blanka Sharma of the Lerner Research Institute at the Cleveland Clinic in Cleveland, OH for kindly providing the p53 plasmid DNA and pCEP4 control vector. The EGFP plasmid DNA was obtained from Dr. Voelkel-Johnson's laboratory at MUSC. Special thanks to Professor Stuart Schreiber at the Broad Institute in Boston, MA for generously providing the tubacin and niltubacin, and Dr. Haiyong Han and Professor Daniel D. Von Hoff at Translational Genomics Research Institute in Phoenix, AZ for the VX-680 aurora kinase inhibitor molecules.

I am grateful to Milen Vitanov, Dr. Laura Gonzalez and Professor Joshua LaBaer at the Biodesign Institute of ASU for assistance and providing the facilities with Western blots and an automated cell counter. I acknowledge Carlos Bentanzos and Dr. Sergei Sarovsky for access to the DLS instrument. Thanks to Dr. Christine Pauken at the Harrington Department of Bioengineering at ASU for the training in the cell and tissue culture laboratory and providing murine osteoblast cells when I first started at ASU. Thanks to Bret Judson of the W. M. Keck Bioimaging Laboratory, ASU (currently at Cornell University) for his invaluable assistance with confocal microscopy. Thanks to Kenneth Mossman of the LeRoy Eyring Center for Solid State Science laboratory, ASU for all the help in carrying out the FT-IR experiments. In the daily routine lab work, I was fortunate to receive continuous support from the fellow students: Joe, David and Jimmy, a number of FURI undergraduate students, and a few talented high school students. Thanks to the people (Phil, Srinath, Shanta and Sharareh) in Dr. Sierks's laboratory for their instant help and advice. I am thankful to be financially supported by the start-up funds from the state of Arizona, the Arizona Biomedical Research Commission (ABRC), and National Science Foundation (NSF).

Finally, I am greatly indebted to my parents who encouraged and supported me throughout my life. I would also like to appreciate the support and love from my husband, younger sister, brother, friends and relatives.

TABLE OF CONTENTS

CHAPTER Page

Appendix Page

LIST OF TABLES

LIST OF FIGURES

Chapter 1

INTRODUCTION

1.1 Description of Gene Therapy

Gene therapy, the delivery of exogenous nucleic acids to diseased cells, has evolved as a potential therapeutic tool for the treatment of both inherited and acquired diseases. A wide variety of nucleic acids, for example, plasmid deoxyribonucleic acids (pDNA) (1, 2), oligonucleotides (2-4), ribozymes (5) or small interfering ribonucleic acids (siRNA) (6-9) have been examined to alter biological outcomes of a defective gene. The commonly used nucleic acid-based therapeutic agents are negatively charged plasmid DNA (pDNA). pDNA are large (3-15kbp), hydrophilic macromolecules that encode a specific therapeutic protein's gene expression system and control the functioning of the gene within a target cell. However, pDNA cannot penetrate biological membranes that necessitate the formulation of gene delivery vector systems to deliver the gene into target cells. A vector can deliver therapeutic genes to a specific cell population and express encoded proteins at the target site. In consideration of this, gene delivery systems should be designed optimizing the following steps:

i) bind and transport DNA to the target cells,

ii) evade immune systems of a body,

iii) release DNA into cytoplasm,

iv) transport DNA through cytoskeletal network within the cytoplasm, and

v) transfer DNA across the nucleus for efficient transcription and translation

At each step of the journey, the number of transferring DNA decreases resulting in poor efficiency of DNA delivery. Thus, knowledge of intracellular transport barriers and cellular delivery of pDNA are important concerns in developing therapeutically effective gene delivery and identifying successful vectors.

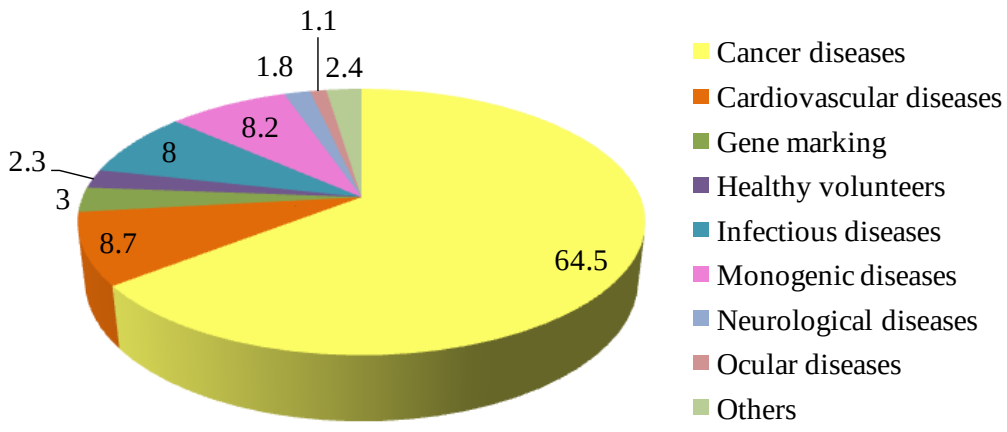

Figure 1.1. Statistics of various diseases targeted by gene therapy clinical trials. Most of the trials are designed to treat cancer. Adopted from Ref. (10)

1.2 Cancer Gene Therapy

The possibility of human gene therapy was first suggested in 1970 for the treatment of inherited single-gene disorders (11). A decade later, when it was realized that cancer is also a disease of genetic disorders, there was a strong feeling that the technology could be applied to a widespread genetic disorders such as cystic fibrosis and some other cancers. The first cancer gene therapy clinical trial was performed in 1991 by Steven A. Rosenberg and R. Michael Blaese's groups (12). The genetically modified human tumor-infiltrating lymphocytes were infused into five patients with metastatic melanoma (12). The study successfully showed tumor regression in patients and the feasibility of

human gene transfer in a clinical setting. Since then remarkable progresses have been made in the past twenty years to meet the therapeutic needs of conventional treatments that are toxic, ineffective or most commonly, both. To date, 1644 gene therapy clinical trials have been approved for treating cancer, cardiovascular, monogenic, infectious, and other diseases (Figure 1.1) (10). More than 60% of the trials aim for cancer gene therapy.

The number of strategies that have been designed and tested for cancer gene therapy are as follows (10, 13):

1. replacing defective tumor suppressor genes such as p53;
2. inactivate oncogenes e.g. ras to block transcription and translation;
3. delivering drug sensitivity genes that can convert a prodrug to a cytotoxic drug upon their expression in cancer cells;
4. stimulating immune responses to activate cytotoxic effects on cancer cells; and
5. delivering multidrug resistance genes to normal cells that allow higher doses of chemotherapy to be given to the cancer cells

Although introducing these genetic materials to correct a specific genetic defect is an attractive strategy, the lack of targeting tumor cells and poor efficiency of gene transfer vectors has rendered this approach clinically less effective. The vast majority of gene therapy clinical trials are in phase I, phase II and combination of phase I/II trials (10, 13). In phase I testing, maximum tolerable doses of gene delivery vectors and transgene products are determined. Phase II efficacy studies involve identification of any antitumor activity of the new agents in patients with

advanced diseases. Evaluation of phase III, phase IV and single subject gene therapy clinical trials are limited but work is now in progress to develop and translate a non-invasive technique into a clinical reality.

1.3 Gene Delivery Vectors

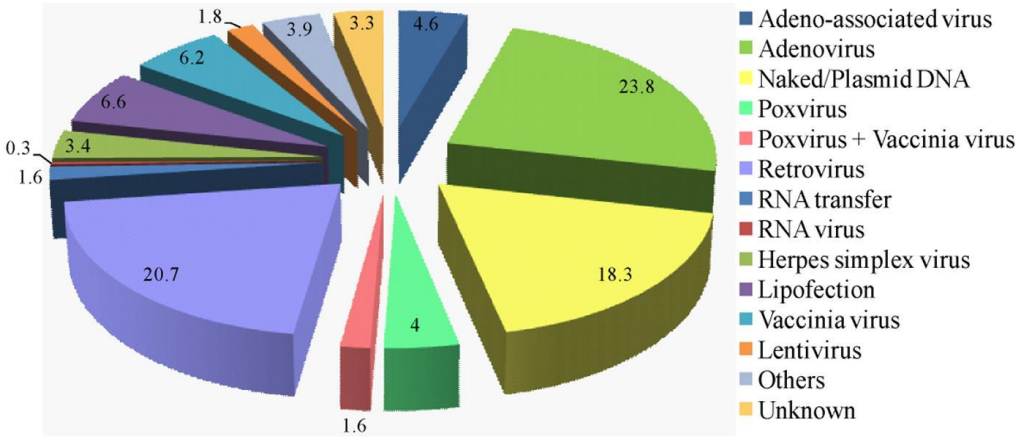

Figure 1.2. Gene delivery vectors used in clinical trials. The most commonly used vectors in gene-transfer trials are the retrovirus and adenovirus vectors. Non-viral gene transfer, including naked DNA and lipofection has occupied 25% of all the trials. Adopted from Ref. (10)

Effective gene therapy of genetic disorders requires a vector that can deliver transgenes into target cells safely and produce the gene of interest in substantial quantities. Unfortunately, gene transfer vectors for clinical use do not possess these desirable properties. Currently, gene therapy in clinical trials is based on viral and non-viral delivery systems, each with its own characteristic advantages and disadvantages (10, 13). Viral vectors are biological systems that possess efficient machinery for delivering DNA into mammalian cells and are the most efficient gene delivery vectors known (14-17). Commonly used viral vectors are retroviruses (including lentiviruses), adenovirus, herpes simplex virus (HSV),

adeno-associated virus (AAV), and vaccinia (or pox) virus (Figure 1.2). Viral vectors have been widely investigated as vehicles for transgene delivery. However, they are plagued by the issues of recognition by the host's immune defense mechanism and limited capacity of carrying genetic materials (18). The safety concern of viral vectors was highlighted when a 18-year old young patient, Jesse Gelsinger died in 1999 following an infusion of genetically altered adenoviral vectors for the treatment of an inherited enzyme deficiency (19). In another incidence Children with X-linked SCID developed leukemia after receiving a retroviral gene therapy (20). These clinical trials demanded investigations of less immunogenic non-viral vector systems than viral vectors. Other important reasons for switching towards non-viral vectors are the capacity of carrying low transgene size, relatively expensive production of viral titers and difficulty in scale up.

Non-viral gene delivery systems do not have limitations in the size of transgenes to be delivered and in recognition by the immune system. However, inefficient targeting and delivery to specific tissues, and dose-dependent inflammatory responses are the major important limiting steps for effective non-viral gene therapy. A wide variety of non-viral agents have been investigated extensively for exploring potential gene delivery vectors. Cationic molecules, such as lipids (21), polymethacrylates (22), polypeptides (23, 24), celluloses (25), chitosan (26-28), dendrimers including polyamidoamine or PAMAM dendrimers (2, 29), poly(vinyl pyrrolidone) (30), and polyamine polymers (31) are attractive agents. The polymers condense DNA to nanoscale complexes in aqueous

solutions by neutralizing the negative charges on the DNA. The complexes possess an excess positive charge and interact with anionic mammalian cell membranes leading to efficient cellular uptake into target cells. An effective gene delivery vector is then able to disassemble and release DNA by escaping the intracellular degradation processes (32).

1.4 Non-viral Vectors: Cationic Polymers

Polymers are synthetic gene delivery vectors which possess the ability to deliver genetic materials to target cells (9, 33-35). Cationic polymers neutralize the negative charge on pDNA resulting in the formation of nanoscale polymer-DNA complexes (polyplexes). The advantages of using polymeric vectors are their flexibility in design, the easy production of large sets of compounds and the ability to screen them in parallel for transgene delivery. High-throughput screening techniques have been widely employed in the pharmaceutical industry for facilitating the rapid evaluation and identification of novel small molecule drugs (36-41). Combinatorial chemistry and parallel screening techniques have recently evolved as attractive options for rapidly generating polymer libraries consisting of candidates that possess a wide range of physicochemical diversities. Table 1.1 summarizes some small-to-medium sized polymer libraries that have been synthesized by different research groups using high-throughput screening and combinatorial approaches.

Table1.1 Summary of cationic polymer libraries for gene delivery vectors

Polymer Vector (Ref.)	Number of polymers in a library	Monomers used	Target cells	# of lead polymers; and the highest transgene expression levels	Relative transgene expression compared to control(s)
Polyethyle-ne imine (pEI) (42)	144	Linear pEI (423Da) or a pEI polymer mixture of 423Da linear and 1.8kDa branched pEIs (1:1 w/w ratio), and 24 bi- and oligo-acrylates	COS-7 monkey kidney cells	9; Absolute values of the highest gene expression levels were not reported	850-3670 fold enhancement in luciferase expression compared to those using non-crosslinked pEI
pEI (43)	435	Functionaliza-tion of the primary, secondary and tertiary amines of 25kDa pEI (pEI-25) by methylation, benzylation and n-dodecylation	CHO-K1 chinese hamster ovary cells	3; 19-28% enhanced green fluorescent protein (EGFP) positive cells	Same expression levels as that of jet pEI, Lipofectamine and unmodified pEI-25
Poly-β-amino esters (PBAE) (44)	2350	Ninety four different amine monomers and 25 diacrylate monomers	COS-7 cells	46; absolute values were not reported.	2-50 fold higher than those using pEI-25
PBAE (45)	486	The top performing polymers in the library described in Ref. (44)	Human Umbili-cal Vein Endotheli al cells (HUV-EC)	3 (C32, JJ32 and C28); 25-47% green fluorescent protein (GFP) cells	5 and 1.6 fold more GFP using C32 than pEI-25 and Lipofectamine, respectively
PBAE (46)	36	End-modified C32 polymers using 36 different amine group containing small molecules as end-capping reagents	COS-7 cells	5; ~$1.2x10^5$ RLU of luciferase expression	10-20 fold higher than those of unmodified C32 and pEI-25

Table1 continued

Polymer Vector	Number of polymers in a library	Monomers used	Target cells	# of lead polymers; and the highest transgene expression levels	Relative transgene expression compared to control(s)
C32 PBAE (47, 48)	60	Modification of the di-amine end-groups of C32 polymer	HeLa, HepG2, DC 2.4, HUVEC, hMSC and COS-7 cells	5; 75-90% GFP positive cells	70-90 fold enhancement compared to those using pEI-25
Polyamino esters (PAE) (49)	16	Amine-containing γ-aminopropyl-triethoxysilane (APES) and polyethylene glycol diacrylate (PEGDA; 258Da)	Human embryonic kidney (293T) and HeLa cervical cancer cells	5; $1x10^5$-$5x10^8$ and $1x10^5$-$5x10^6$RLU/mg in absence and presence of serum, respectively	10-100 fold more luciferase expression than those of pEI-25
Cyclodextrin (CD) (50)	7	β-CD and pEI-25 derivatives with varying degree of CD grafting onto pEI polymers	PC3 prostate cancer cells	15-25% EGFP positive cells	Similar levels of expression using pEI-25
Chitosan (CS) (51)	12	*N*-maleated chitosan grafted oligoamine derivatives	293T and HeLa cells	10^8-10^9 RLU/mg luciferase expression	Similar efficacy like pEI-25
Polysaccharide based polyamines (52)	11	Schizophyllan-based oligoamine polymers	COS-1, CHO-K1, and HeLa cells	1; $5x10^5$RLU/mg	5 fold higher than that of pEI-25

The combinatorial library approaches result versatile polymer libraries in a rapid fashion to identify effective gene delivery vectors. Although screening of

these cationic polymers and/or their derivatives has been carried out, the diversity of chemical structures among these polymers has made it difficult to find a correlation between the polymer physicochemical properties, transfection efficiencies, and differential cellular responses. Further developments in polymer chemistries, elucidation of physicochemical factors, cellular responses to delivery and interactions with various cell types will facilitate the identification of efficient polymeric vectors for gene delivery. These investigations in concert with *in vivo* studies will be critical to advance polymeric vectors towards clinical applications. Recently, a polymer based on cyclodextrin (CD) has been used by Davis et. al (9, 53) in phase I clinical trials for siRNA nucleic acid delivery. The researchers demonstrated a nanoparticle delivery system (CALAA-01) consisting of CD-siRNA complexes, polyethylene glycol (PEG)-adamantane groups and human transferrin protein targeting ligands. The nanoparticles carried siRNA for the reduction of ribonucleotide reductase subunit 2 (RRM2) anti-cancer targets in patients with solid tumors. Systemic injections of the complexes in three patients resulted in successful intracellular localization of the CALAA-01in tissues and a decrease in RRM2 mRNA and protein levels. In this preclinical evaluation of CALAA-01, no signs of toxicity were seen. The results demonstrate that cationic polymer based nanoparticles represent an attractive approach for developing safe and effective polymeric gene delivery vectors. However, target cells have biological barriers that inhibit expression of the foreign gene products. The following sections describe some of the biological barriers to the uptake of genes to their effective expression in the target cells.

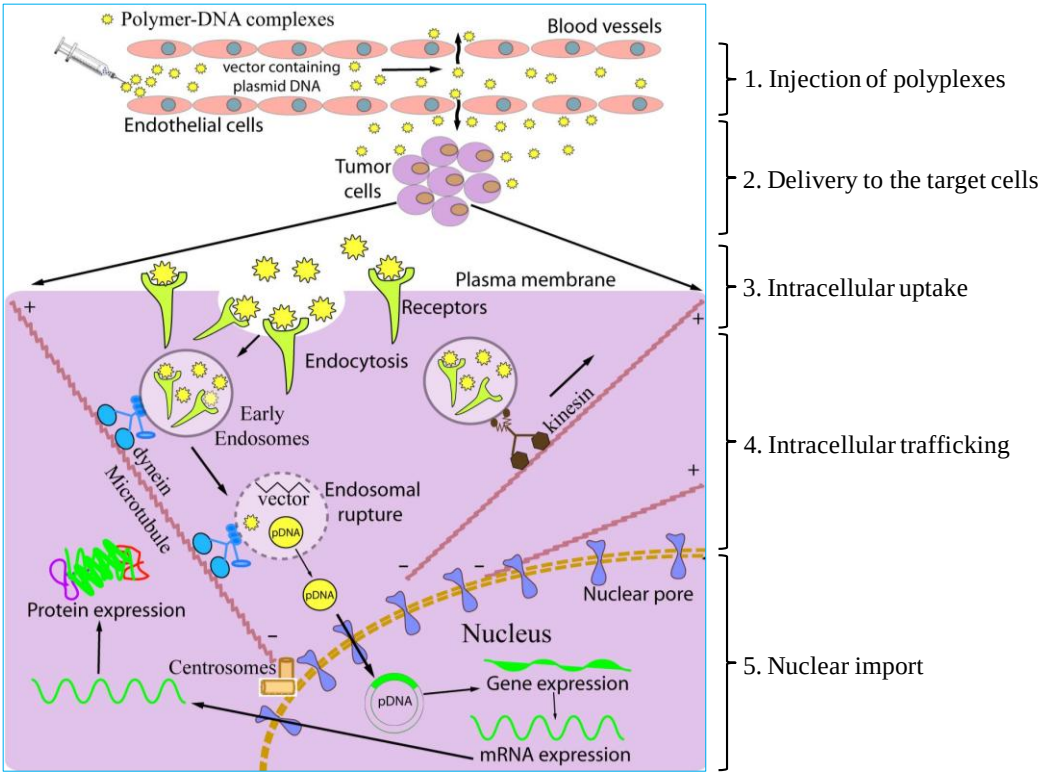

Figure 1.3. Schematic of the transport of polyplexes from an extracellular environment into the nucleus of a cell and the biological barriers to non-viral gene delivery. (1) Administration and injection of polyplexes into the blood vessels; (2) delivery of the polyplexes to the targeted tumor cells by passing through the blood vessel walls and avoiding any non-specific binding or degradation; (3) uptake and internalization of the polyplexes from the plasma membrane through endocytosis; (4) sequestration of polyplexes to endosomes and trafficking along microtubules towards the nucleus. Microtubule dependent directional transport of cargoes involves the dynein motor that moves cargoes from the plasma membrane towards to the minus end of the microtubules or centrosomes. Kinesin motors typically move towards the microtubule plus ends. The polyplexes must escape from the acidic endosomal vesicles generally by endosomal rupture in order to avoid DNA degradation; and (4) DNA should cross the nuclear pore complexes in order to be transcribed inside the nucleus.

1.5 Biological Barriers to Gene Transfer

For efficient DNA delivery, a non-viral vector should carry exogenous DNA stably from the lab bench test tubes into the intracellular nucleus without any DNA degradation. Several biological hurdles that involve in non-viral gene delivery are (i) serum stability, (ii) cell-specific targeting, (iii) route of administration, (iv) cellular uptake, (v) intracellular trafficking, (vi) endosomal

escape, (vii) dissociation of pDNA from the polyplexes, (viii) nuclear import of pDNA, and (ix) regulation of gene expression (Figure 1.3). Topics related to steps (i)-(iii) are not discussed in this thesis because the objective of this research project is to summarize the critical steps in intracellular trafficking of polyplexes. The cellular level barriers are described in the following section.

1.5.1 Endocytosis: The Primary Uptake Route

The plasma membrane consists of a lipid bilayer that poses the first barrier towards polyplexes in reaching the intracellular environment. Most non-viral DNA complexes first associate with cell membranes through electrostatic interactions with anionic cell surface proteoglycans (54). The complexes enter cells via endocytosis such as clathrin-dependent endocytosis, clathrin-independent endocytosis, macropinocytosis and phagocytosis (21, 55-57). Endocytosis is essentially the invagination of plasma membrane with the formation of endocytic vesicles. This invagination occurs at specific domains in the plasma membrane, characterized by a specific lipid and/or protein composition for the different endocytic pathways. In clathrin-dependent endocytosis, the specific domain is characterized by the presence of clathrin and is called a clathrin-coated pit (55, 58-61). Plasma membrane folding at these coated pits results in the formation of clathrin-coated vesicles. These vesicles lose their clathrin coat upon internalization and fuse with each other or with pre-existing endosomal compartments to form early endosomes (31). Early endosomes can either recycle their cargo to the extracellular environment or mature to late endosomes which is accompanied by a decrease in pH from 7.0 to 5.9 (55, 62). Late endosomes

deliver their cargoes to the lysosomes with an additional pH drop from pH 6.0 to 5.0 (55, 62). The average time to mature from early to late endosomes is approximately 5 min, while late endosomes progress to lysosomes in 30 min (55).

The mechanism of endocytosis, however, depends on the size of external materials and the cell type. Rejman et al. found that latex beads of less than 200nm were taken up by the clathrin-dependent pathway, whereas larger beads (200-500nm) entered the cells through caveolae or lipid-raft mediated endocytosis (63). Particles larger than 500nm preferably enter cells by macropinocytosis, a mechanism of endocytosis in which large droplets of fluid are trapped underneath the cell surface by ruffling (64). PLGA-DNA polyplexes (65), pEI polyplexes (66), histidylated polylysine particles (67) with a size range of 70-200nm are internalized via clathrin-dependent pathways. Transgene expression using lipoplexes and polyplexes were reported to be abolished by the inhibitors of clathrin and caveolae mediated endocytosis (68). Nanoparticles of alginate-chitosan-DNA complexes were reported to be endocytosed via a clathrin-mediated pathway in 293T and COS-7 cells but were internalized by a caveolae-mediated pathway in CHO cells (69).

1.5.2 Cytoplasmic Trafficking

Polyplexes encapsulated in endosomal vesicles are carried from the plasma membrane towards the nucleus by trafficking along long microtubule fibers that provide the highway or 'tracks' for transport of the vesicles (63, 70). The direction of endosomal vesicle trafficking depends on the functions of two motor proteins of microtubules, the dynein and kinesin (71). Dyneins move cargo

towards the minus end of microtubules (towards the nucleus), while kinesins move cargo towards the plus end of the microtubules (towards the plasma membrane) (step 4; Figure 1.3). The movement can also be bi-directional by switching between two motor proteins (72). Numerous viruses exploit the bi-directional intracellular transport system and utilize dynein-mediated trafficking for intracellular translocation to nuclear periphery (72). A study on pEI-pGL3 DNA polyplex mediated transfection of MDA-MB-231 human breast carcinoma and HEK293 human embryonic kidney cell lines has shown that microtubule stabilization using paclitaxel enhances luciferase gene expression by 20-fold (73). Disruption of microtubules using colchicine decreases the luciferase gene expression by 75%. Transgene expression was also decreased by greater than 80% by inhibiting the activities of dynein and kinesins. The results indicated that both polyplex delivery and transgene expression are dependent on intact microtubules and its two motor proteins.

1.5.3 Endolysosomal Escape of Polyplexes

Escape of polyplexes before maturation of endosomes to degradative lysosomal acidic environments is considered a key rate-limiting step in the success of non-viral gene delivery and expression (Figure 1.3). Endosomal disruption by the proton sponge mechanism (Figure 1.4) has been proposed for the polyplexes of polyamidoamine (PAMAM) (74) and pEI (74) due to the presence of protonable amines incorporated into the branched polymers. pEI has one protonable amino nitrogen in every third atom. This nitrogen is protonated during acidification, which imparts a high buffering capacity inside acidic late

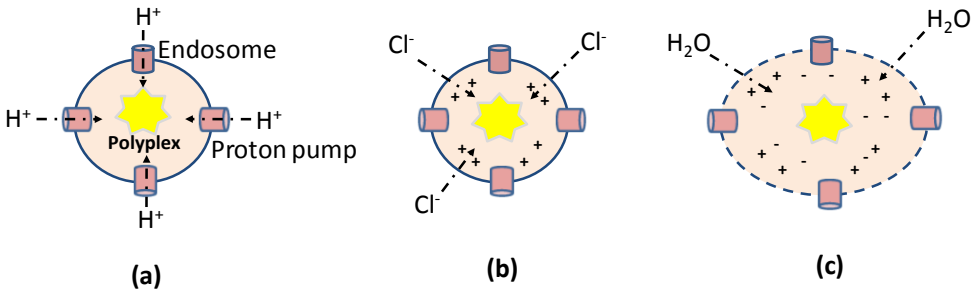

Figure 1.4. Proton sponge effects. (a) Proton accumulation into endosomes by proton pumps; (b) the protons are accompanied with chloride ion influx; and (c) builds up osmotic pressure of water that eventually ruptures the endosomes.

endosomes (74). Massive proton accumulation is accompanied by high chloride ion influx into the endosome, causing osmotic swelling of the endosome and eventual vesicle lysis (Figures 1.4). Sonawane et al. used a chloride-sensitive fluorophore to monitor the chloride accumulation and swelling in endosomes (74). Their work revealed that enhanced endosomal buffering of pEI relative to polylysine resulted in increased chloride ion retention and endosomal swelling. Likewise, it has been shown that the addition of the buffering agent chloroquine to cells transfected using non-buffering polymers results in increased transgene expression; however, chloroquine had no effect when added to known proton-sponge buffering polymers (4, 75). Blocking vacuolar proton pumps by inhibitors such as bafilomycin A1 lowers pEI-mediated transgene expression in a cell type-specific manner (76). However, the proton sponge hypothesis has remained controversial suggesting that pEI polyplexes show higher transfection efficiency than other agents because of their escaping nature from lysosomal trafficking, not because of their buffering capacity (77).

1.5.4 Nucleocytoplasmic Trafficking of pDNA

Nuclear trafficking of pDNA is the next hurdle for efficient transfection. pDNA, that are escaped from degradation and delivered to the perinuclear region, has to be imported into the host cell nucleus for transcription. The translocation of pDNA to the interior of the nucleus depends on its size as revealed by the size-dependent nuclear diffusion of oligonucleotides through nuclear pore complexes (NPC) (78). While small (< 250bp) DNA fragments enter into the nucleus by passive diffusion without any specific interactions, larger DNAs (up to 1kb) require active transport to overcome the lateral mobility in the highly viscous cytoplasm. Several groups have reported that active transport of large DNA fragments through NPC is an extremely inefficient process (79). Attachment of nuclear localization sequences (NLS; PKKKRKV) to pDNA can stimulate the nuclear entry and expression of large DNA (80, 81). Dean et al. showed that transfection efficiency can be augmented by coupling of single or multiple NLS to pDNA and transporting pDNA into the nucleus. Another possibility for the nuclear entry of pDNA is the entry during mitotic cell division when the nuclear membrane breaks down. No matter what the route, DNA has to reach the nucleus to have any therapeutic effect.

1.5.5. Regulation of Gene Expression

Effective expression of a transgene is also a big issue in gene therapy. Acetylation and deacetylation of histones and other proteins associated with condensed chromosomes inside the nucleus have been shown to be important in the regulation of transgene expression (82-85). Histones are a family of nuclear

proteins that interact with DNA resulting in DNA being wrapped around a core of histone octamer within the nucleosome (86, 87). Deacetylation of the histone lysine residues is associated with compact binding of DNA around core histones following which the transcription apparatus cannot access the promoter regions, and expression of the corresponding genes cannot be started (88). The mechanisms in controlling regulation of transgene expression by histone acetylation or deacetylation have not been fully delineated. Nan et al. showed that transiently transfected GFP DNA was assembled with chromatin containing acetylated histones in histone deacetylase inhibitor (HDACi) treated cells (89). Another mechanism of enhancing gene expression using HDACi is the activation of transcription factors by HDACi that can bind to the promoter site of transgene and start transcription (90, 91). HDACi such as trichostatin A (TSA), MS-275 and depsipeptide have been shown to enhance adenovirus-mediated gene expression in bladder and prostate cancer cells by restoring coxsackie-adenovirus receptor protein expression on the surface of the cancer cells (92, 93). The results suggest that epigenetic regulation is an important factor to enhance transgene expression.

1.6 Conclusions

An ideal gene delivery system should bind DNA effectively, increase cellular uptake, help DNA to escape from endosomal compartments, and facilitate their internalization inside the nucleus. Numerous research activities have been conducted to identify and improve cationic polymer vectors that increase DNA stability and transfection. However, polymeric vectors still have orders of lower magnitude efficacy than viral vectors. The other bottlenecks are cytotoxicity of

polymers, intracellular delivery, and poor understanding of biological processes in cancer cells to regulate transgene expression. The first objective of this thesis is to develop a library of polymeric gene delivery vectors that demonstrate high delivery efficacies and low toxicities. The second objective of this thesis is to address the major intracellular trafficking barriers to polymer-mediated gene delivery. The final goal is to explore combination treatment strategies to overcome these cellular barriers and enhance transgene expression.

Chapter 2 of the thesis describes the synthesis and screening of polymer vectors for gene delivery using parallel synthesis and screening techniques (13). Chapter 3 of this thesis discusses intracellular transport and the fate of quantum dot nanoparticles in two prostate cancer cell lines (94). This is followed by the investigation of how intracellular nanoparticle transport is correlated with differential transgene expression in these two cell lines (Chapter 4) (95).

Combination treatments of HDACi and polymer-mediated gene delivery are discussed in Chapter 4. The roles of HDACi in mediating intracellular localization of polyplexes and enhancing transgene expression in prostate cancer cells have been discussed. Further strategies for enhancing polymer-mediated transgene expression by modulating intracellular localization and cell cycle have been described in Chapter 5. Polymer-mediated p53 gene delivery in combination with a chemotherapeutic modulator of cell cycle has been shown to induce apoptosis in prostate cancer cells (Chapter 5). Chapter 6 highlights some future directions. Appendix A of this thesis summarizes additional works on polymer coating of viruses and transduction using polymer-coated viruses.

Chapter 2

PARALLEL SYNTHESIS AND SCREENING OF POLYMERS FOR NON-VIRAL GENE DELIVERY

2.1 Introduction

Novel strategies, including both rational and semi-rational discovery approaches, can lead to the accelerated identification of highly efficient and safe vectors for non-viral gene delivery. Combinatorial / parallel synthesis has gained immense popularity as a means to rapidly synthesize large numbers of small-molecule compounds as potential drug candidates (96, 97). The approach has recently been extended to the synthesis of diverse oligomer and polymer libraries (98-102) for a variety of applications including gene transfer (103-107). In the current work, the parallel synthesis and screening techniques were employed for the rapid identification of novel DNA-binding cationic polymers for gene delivery. A library of eighty polymers was synthesized in parallel; the ring-opening polymerization of diglycidyl ethers by amines (108) was employed in the generation of the library. Primary screening involved the parallel evaluation of the DNA-binding efficacies of the library constituents using the ethidium bromide displacement assay (109-112). *In vitro* transfection, using representative polymers that demonstrated high DNA-binding efficacies, resulted in the identification of a candidate polymer that showed significantly higher transfection activities and lower cytotoxicities than poly(ethylene imine), both in the presence and absence of serum.

2.2 Experimental Procedures

2.2.1 Materials

Eight diglycidyl ethers, 1,4 butanediol diglycidyl ether (1,4 B), 1,4-cyclohexanedimethanol diglycidyl ether (1,4 C), 4-vinylcyclohexene diepoxide (4VCD), ethyleneglycol diglycidyl ether (EDGE), glycerol diglycidyl ether (GDE), neopentylglycol diglycidyl ether (NPDGE), poly(ethyleneglycol) diglycidyl ether (PEGDE), and poly(propyleneglycol) diglycidyl ether (PPGDE) were purchased from Sigma-Aldrich and were used without any further purification. Ten amines, 1-(2-aminoethyl) piperidine, 1,4-bis(3-aminopropyl) piperazine, (1,4 Bis), 3,3'-diamino-N-methyl dipropylamine (3,3'), 4,7,10-trioxa-1,13-tridecanediamine, aniline, butylamine, diethylenetriamine (DT), ethylenediamine (ED), N-(2-aminoethyl)-1,3-propanediamine (N-2amino), and pentaethylenehexamine were also purchased from Sigma-Aldrich and used as received. Calf-thymus DNA, ethidium bromide, 25 kDa poly(ethylene imine) (Mn=10 kDa, Mw=25 kDa; henceforth called pEI-25), 750 kDa poly(ethylene imine) (Mn=60 kDa, Mw=750 kDa ; henceforth called pEI-750), were purchased from Sigma-Aldrich. The pGL3 control vector and the Bright Glo kit were purchased from Promega.

2.2.2 Polymer Synthesis

Eight diglycidyl ethers (2.3M) were reacted with equimolar amounts of amines; neat as-purchased solutions were employed for both reactants. In the case of pentaethylenehexamine, the low solubility of the resulting polymers at a 1:1 ratio of diglycidyl ether to amine necessitated the use of a 10:1 diglycidyl

ether:amine molar ratio in subsequent experiments. The polymerization was carried out in 7mL glass scintillation vials for 16h. After 16h, the resulting polymer was diluted to a concentration of 2mg/mL in 20mM Tris buffer, pH 7.4. The solution pH was adjusted to 7.4 using 30% hydrochloric acid in de-ionized (DI) water to compensate for the alkalinity of the polymers. Only those polymers that were soluble at a concentration of 2mg/mL at pH 7.4 were evaluated for their DNA-binding efficacies.

2.2.3 Parallel Screening of DNA-Binding Activity

The ethidium bromide displacement assay (109-112) was employed to evaluate the DNA-binding affinity of the cationic polymer library in parallel. Briefly, 1.5mL of 6µg/mL double-stranded, calf-thymus DNA was equilibrated with 15µL of 0.5mg/mL ethidium bromide (all solutions were prepared in 20mM Tris buffer, pH 8.0). After equilibration, 25µL of 2mg/mL polymer was added to the DNA-ethidium bromide mixture and equilibrated for 20min. 150 µL of the polymer-DNA solution was transferred into a 96-well microtiter plate and the fluorescence (excitation at 260nm, emission at 595nm) was measured using a plate reader (Perkin Elmer Lambda 6.0). The decrease in fluorescence intensity (percent fluorescence decreased compared to control) was used to rank DNA-binding efficacies of individual polymers.

2.2.4 Polymer-Mediated Transfections

The pGL3 control vector (Promega Corp., Madison, WI), which encodes for the modified firefly luciferase protein under the control of an SV40 promoter, was used in transfection experiments. *E.coli* (XL1 Blue) cells containing the

pGL3 plasmid DNA were cultured overnight (16h, 37 °C, 150rpm) in 15mL tubes (Fisher) in 5mL Terrific Broth (MP Biomedicals, LLC) containing 100µg/mL ampicillin (Research Products International, Corp.). The cultures were then centrifuged at 5400g and 4°C for 10min. Plasmid DNA was purified according to the QIAprep Miniprep Kit (Qiagen®) protocol; DNA concentration and purity were determined based on absorbance at 260 and 280nm determined using NanoDrop Spectrophotometer (ND-1000; NanoDrop Technologies).

The PC3-PSMA human prostate cancer cell line (113) was a generous gift from Dr. Michel Sadelain of the Memorial Sloan Cancer Center, New York, NY. The cells were cultured in a 5% CO_2 incubator at 37°C using RPMI-1640 medium containing 10% heat-inactivated fetal bovine serum (FBS) and 1% antibiotics (10,000units/mL penicillin G and 10,000µg/mL streptomycin). MC3T3 murine osteoblasts, a kind gift from Dr. Christine Pauken (Harrington Department of Bioengineering, ASU), were cultured in a 5% CO_2 incubator in Dulbecco's Modified Eagle's Medium (DMEM; BioWhittaker®) containing 4.5g/L glucose and L-glutamine, supplemented with 10% fetal bovine serum (FBS; Hyclone) and 1% penicillin/streptomycin (Hyclone). PC3-PSMA and MC3T3 cells were seeded in 24-well plates at a density of 50,000 cells/well and allowed to attach overnight. Polymer:pGL3 control plasmid at weight ratios of 25:1 (polymer concentration 10ng/µL and 200ng pGL3 plasmid in each well) were incubated for 30min at room temperature and the resulting polyplexes were added to cells for 6h either in the absence or presence of serum (10% FBS), at the end of which, fresh serum-containing medium was added to the cells. Following further incubation for 48h,

cells were lysed using the Bright Glo kit (Promega) and analyzed for luciferase protein expression (in relative luminescence units or RLU) using a plate reader (Bio-Tek Synergy 2). The protein content in each well was determined using the BCA assay and the luminescence value (RLU) was normalized by the protein content. Transfection efficacies of different polymers from the library were compared with the normalized value (RLU/mg protein) obtained for pEI-25.

2.2.5 Polyplex and Polymer Cytotoxicity

PC3-PSMA cells were seeded in a 24-well plate at a density of 50,000cells/well and incubated overnight at 37°C. Different weight ratios of polymer-DNA polyplexes (10:1 , 25:1, and 50:1 polymer: pGL3 plasmid) and different concentrations of polymers (4-20ng/µL) were added in the absence of serum and the cells were incubated for 6h to determine polyplex- and polymer-induced cytotoxicity, respectively. Following incubation, cells were treated with 100µL of 4µM ethidium homodimer-1 (EthD-1; Invitrogen) for 15min and imaged immediately using Zeiss AxioObserver D1 inverted microscope (10X/0.3 numerical aperture (NA) objective; Carl Zeiss MicroImaging Inc., Germany). Fluorescence using excitation at 550nm and emission at 670nm were used for the microscopy; dead/dying cells with compromised nuclei stained positive (red) for EthD-1.

Quantitative analysis of polymer/polyplex induced cell death was carried out as follows. The number of dead cells in each case was counted manually for three individual fields of fluorescence microscopy images by means of the Cell Counter plugin in ImageJ software (Rasband, W.S., ImageJ, U. S. National

Institutes of Health, Bethesda, Maryland, USA, http://rsb.info.nih.gov/ij/, 1997-2005). The numbers of dead cells in both dead and live controls were determined for at least two fields of view and their average values were calculated. The number of red fluorescent cells in case of each polymer or the corresponding polyplex) was determined and the percentage of dead cells was calculated by normalizing the number of dead cells in the sample to number of dead cells in the dead control.

2.2.6 Polymer Characterization

a. Polymerization Kinetics: The disappearance of reactive (primary and secondary) amines with time was used to monitor the kinetics of the diglycidyl ether-polyamine reaction (Figure 2.1a); the ninhydrin assay (114) was used to determine the concentration of reactive amines at each time point. The ninhydrin assay results in a yellow-orange color in case of secondary amines and a dark blue/purple color in case of primary amines. Briefly, approximately 2mg of the polymers were weighed into 1.5mL microcentrifuge tubes (Fisher) at different time points (0-24 h) during the polymerization reaction. Ninhydrin reagent (Sigma®; 100µl) and DI water (200µl) were added to the polymers in the centrifuge tubes following which, the tubes were then placed in a boiling water bath for 10min and cooled to room temperature (22°C). The mixture was diluted by adding 500µl of 95% ethanol. The mixtures were further diluted 10 and 100-fold using DI water in order to obtain absorbance values within the calibration range (using glycine standards) employed. Absorbance was measured at 570nm in triplicate for each sample using a microplate reader (BioTek Synergy 2®). The

amine concentration was monitored every 4h and the concentration of amines in the reaction mixture at a given time point was normalized with the concentration of amines at the start of the reaction (t=0) in order to obtain percentage amines.

b. Determination of Polymer Molecular Weight: Polymer molecular weight was determined using gel permeation chromatography (GPC) using a ViscoGEL column (MBLMW, Mixed Bed, dimensions: 7.8 mm x 30 cm) using 5% (v/v) acetic acid in water as the eluent (flow rate 1mL/min) (115). The M_n and M_w values were estimated as an average of two experimental runs using a light scattering Viscotek 270 Trisec Dual Detector; OmniSEC software, $\lambda = 670$ nm.

c. Fourier Transform Infrared (FT-IR) Spectroscopy: FT-IR spectra were obtained at two different polymerization time points (t=0 and t=16h) in order to ascertain the formation of the polymers. Polymer samples were loaded on a germanium attenuated total reflectance (GATR) crystal such that they covered the center area of the crystal. The sample chamber was equilibrated to approximately 4millibar pressure in order to minimize interference from atmospheric moisture and CO_2. The absorption spectrum was measured between 650 and 4,000cm^{-1} using a Bruker IFS 66 v/S FT-IR spectrometer and the background spectrum was subtracted from all sample spectra.

2.2.7 Statistical Analyses

Data are reported as mean ± one standard deviation of independent replicate experiments. Statistical significance was determined for a given polymer using unpaired Student's t-test; p-values < 0.05, with respect to pEI-25, are considered statistically significant.

2.3 Results and Discussion

The identification of efficient non-viral gene delivery agents is a critical limitation in the development of safer alternatives to viral-based delivery of DNA. While combinatorial chemistry and high-throughput screening approaches have been widely established in the discovery of small molecule drugs, their utilities in the discovery of non-viral gene delivery agents is somewhat under-explored. This approach has been employed for the discovery of polymeric transfection agents. A library of eighty cationic polymers was synthesized in parallel using the ring opening polymerization between diglycidyl ethers and amines (108). Primary screening involved the evaluation of the DNA-binding efficacies of each of the individual library components in parallel. Transfection experiments with high DNA-binding polymer leads resulted in the identification of one polymer that possessed significantly higher transfection efficacies than polyethyleneimine (pEI) in addition to the identification of other polymer that possessed similar efficacies compared to pEI.

2.3.1 Parallel Synthesis and Evaluation of the DNA-Binding Activity of the Cationic Polymer Library

The ring opening of the epoxide groups on diglycidyl ethers was chosen by polyamines as a suitable platform reaction for the rapid generation of a cationic polymer in a parallel fashion. Figure 2.1a shows the reaction scheme employed for the generation of the library of eighty cationic polymers. A synergistic combination of chemoenzymatic synthesis and parallel screening have been employed for elucidating structure-property relationships involved in

polyamine-DNA binding (111, 112). However, while small molecular weight (< 2kDa) polyamines are known to bind DNA, their poor transfection efficacies necessitate the use of cationic polymers or cationic lipids for gene delivery.

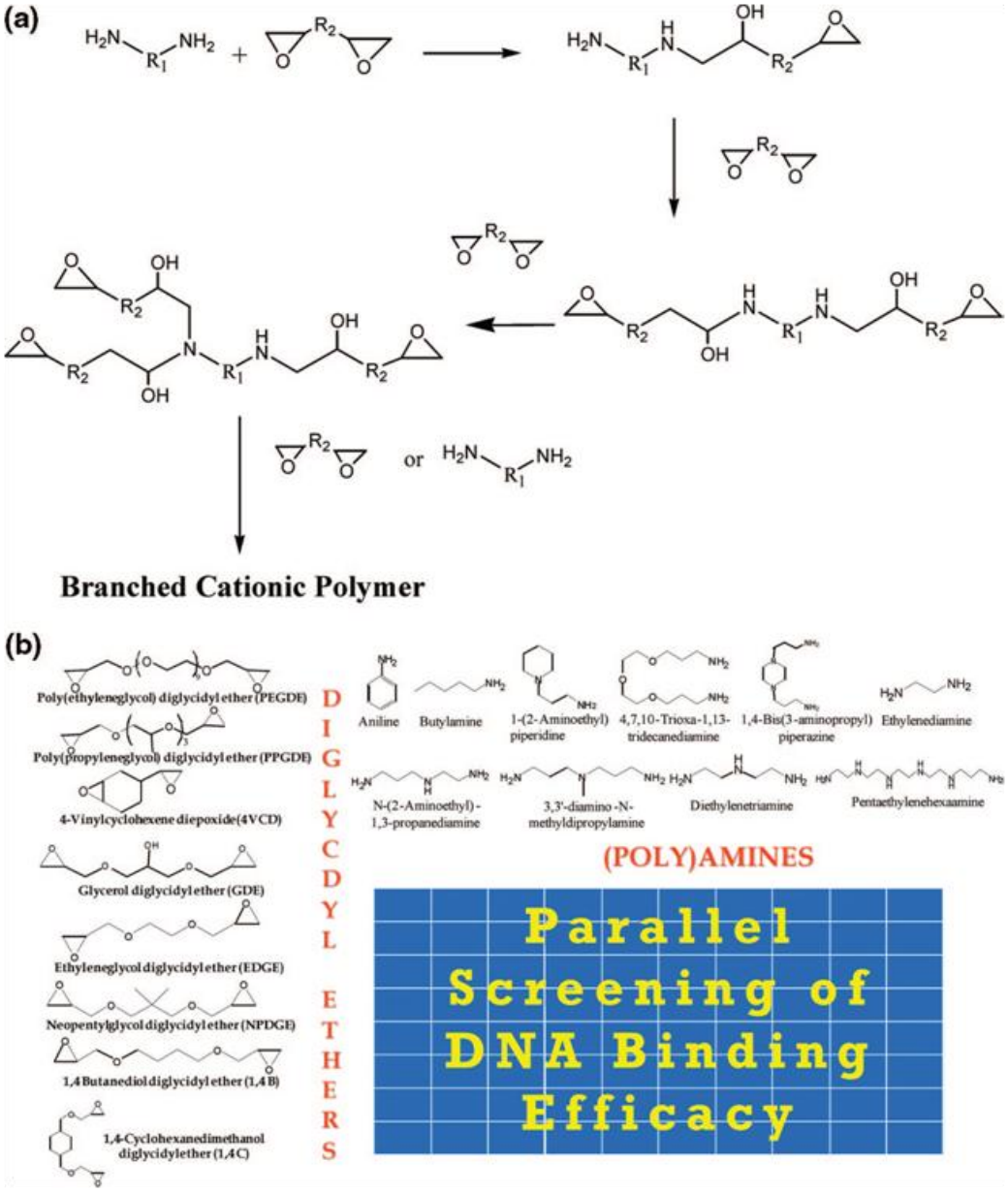

Figure 2.1. a) Schematic of the reaction employed for the generation of the cationic polymer library based on the ring-opening of diglycidylethers by amines. b) Combinatorial matrix of the cationic polymer library composed of diglycidylethers and (poly)amines.

It was hypothesized that the use of diglycidyl ethers to cross-link polyamine molecules can result in diglycidyl ether-polyamine based polymers in which an individual polymer molecule will possess multiple copies of the DNA binding polyamine molecule ultimately resulting in high cellular transfection activities.

Diglycidyl ethers were chosen as co-monomers since epoxide groups readily react with amines and hence can act as linkers between multiple polyamine molecules leading to rapid polymer synthesis. This property of diglycidyl ethers has been exploited for the generation of cross linked polymers and proteins for a variety of biomedical applications (116-119). In addition, the use of a diverse set of diglycidyl ether monomers results in the exploration of a wider chemical space for the resulting polymers. Although most diglycidylethers contained glycol moieties, they differed in the number of methylene ($-CH_2-$) units between the oxygen atoms as well as side chain functionalities. A relatively wider range of chemical diversity was employed in case of amines employed for generating the cationic polymer library. Not only did the amines vary in the nitrogen atom content (from one to six), they also varied in their chemical composition; aromatic (e.g. aniline), cyclic (e.g. 1-(2-aminoethyl) piperidine), and linear polyamines (e.g. diethylenetriamine and pentaethylenehexamine) were employed in the study. As with the diglycidyl ethers, it was hypothesized that exploring a wider chemical space with amine monomers would accelerate the discovery of effective polymeric gene delivery agents. Figure 2.1b shows the combinatorial matrix of the polymer library.

Polymerization reactions were carried out for 16h at 25°C in order to maintain the parallel nature of the synthesis approach. It is acknowledged that different polymerization reactions in the library synthesis can proceed at different rates, resulting in polymers with different molecular weights. However, polymerizations was chosen to carry out for 16h for the following reasons: (1) longer polymerization times (> 24h) resulted in the generation of insoluble polymers in case of a number of higher homologue polyamines, presumably due to extensive cross-linking (not shown); and (2) variability in reaction time was minimized in order to maintain the parallel nature of the polymer synthesis. As a result, all polymerizations with the exception of those based on glycerol diglycidylether-based polymerizations were carried out for 16h; reactions with glycerol diglycidylether were carried out for 4.5h since reaction times greater than 5h resulted in insoluble polymers for all cases.

Sixteen out of the eighty polymers synthesized were not soluble at concentrations of 2mg/ml; in general, the use of higher amine homologues (polyamines) led to lower aqueous solubilities of the resulting polymers. This lower solubility can be attributed to extensive cross-linking that can take place due to the presence of multiple amines. In particular, pentaethylenehexamine-based polymers were insoluble at a concentration of 2mg/ml in buffer when equimolar amounts of the amine and diglycidyl ethers were employed. Therefore, polymers were synthesized with different stoichiometries of pentaethylenehexamine : diglycidylether (10:1, 8:1, 6:1, 4:1, 2:1, and 1:1) and tested their solubilities; a ratio of 10:1 was chosen for subsequent experiments

based on the solubility of the resulting polymers. Sixty-four soluble polymers were employed in the primary screening which involved an evaluation of their respective DNA-binding efficacies using the ethidium bromide displacement assay (109). It is important to mention that the polymers were not characterized at this stage in order to maintain the high-throughput/parallel nature of the current approach; instead, the focus was on the rapid identification of lead candidates that demonstrate high DNA-binding efficacies.

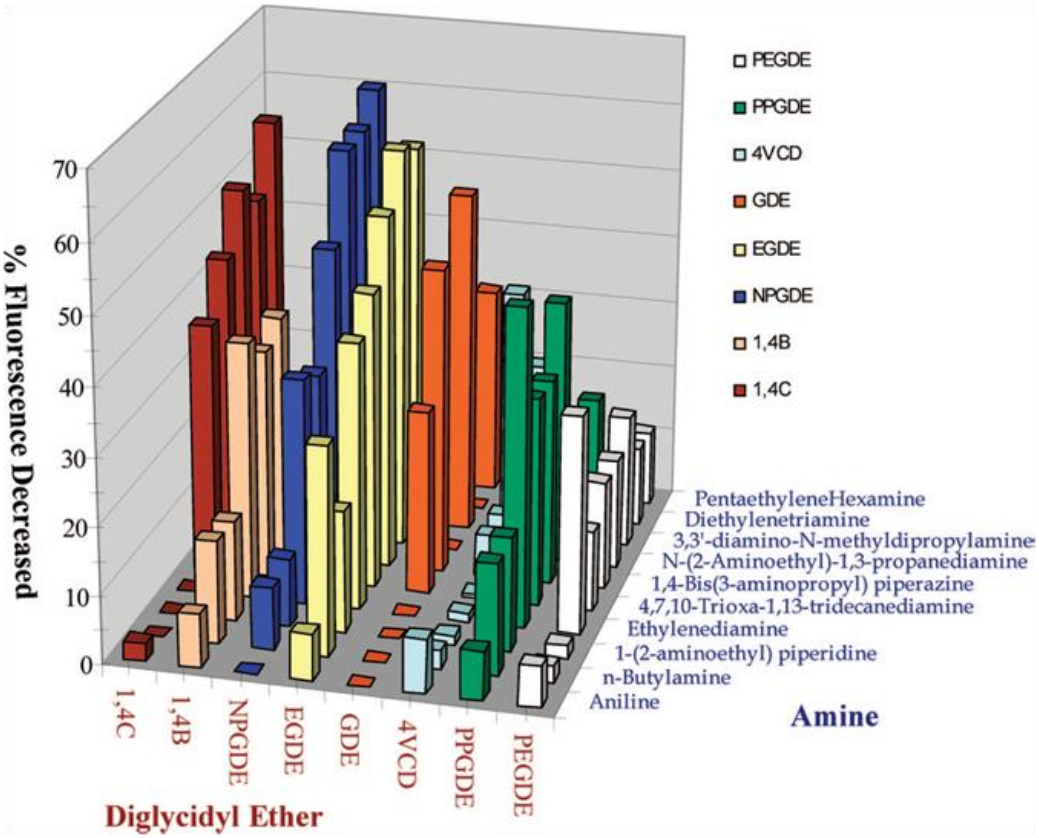

Figure 2.2. DNA-binding activity of the diglycidyl ether based cationic polymer library determined using the ethidium bromide displacement assay. The percent fluorescence decreased upon polymer binding to calf thymus DNA intercalated with ethidium bromide was used to rank polymer efficacy.

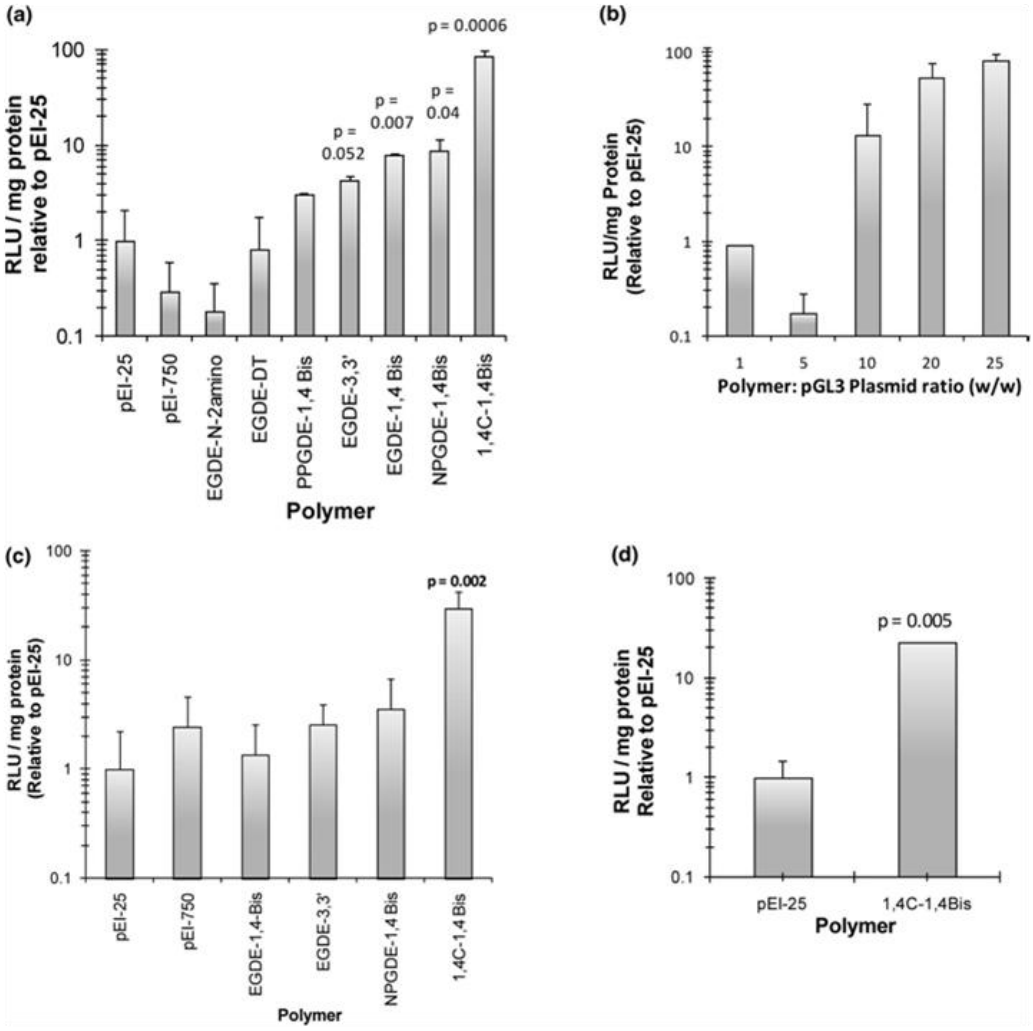

Figure 2.3. Transfection of PC3-PSMA human prostate cancer cells using polymer leads selected from the DNA binding screen. Transfection efficacy of a given polymer was determined from the luciferase expression (relative luminescence units or RLU) normalized by the total protein amount (mg). Polymer transfection efficacies are reported as relative to that of pEI-25. Relative efficacy data are plotted on a logarithmic scale (y-axis) and statistical significance using p-values was determined by comparing data for a given polymer with pEI-25. a. Polymer-mediated transfection of PC3-PSMA cells in the absence of serum using a polymer : pGL3 plasmid ratio of 25:1 (w/w). b. Transfection of PC3-PSMA cells in the absence of serum using different polymer:plasmid ratios of the 1,4C-1,4Bis polymer. c. Polymer-mediated transfection of PC3-PSMA cells in the presence of 10% fetal bovine serum using a polymer:pGL3 plasmid ratio of 25:1. d. Polymer-mediated transfection of murine osteoblasts using 1,4C-1,4Bis and pEI-25 polymers in the presence of 10% fetal bovine serum using a polymer:pGL3 plasmid ratio of 25:1.

Figure 2.2 shows the DNA-binding efficacy of the cationic polymer library determined using the ethidium bromide displacement assay. As expected,

polymers based on monoamines (e.g. aniline and butylamine) demonstrated low values of percent fluorescent decreased (i.e. low DNA-binding efficacies) while those derived from higher homologue polyamines, such as 1,4-Bis(3-aminopropyl)piperazine, 3,3'-diamino-N-methyl dipropylamine, diethylenetriamine, and N-(2-aminoethyl)-1,3-propanediamine demonstrated higher efficacies. While it is possible that the low DNA binding efficacies of some polymers (e.g. polymers based on monoamines) is a result of the lower degree of polymerization, this was not verified further at this stage and discontinued any further analyses with these polymers. Seven representative polymer leads, with different DNA binding efficacies (percent fluorescence decreased values ranging from 30% to 60 %), were chosen for the transfection of PC3-PSMA cells as described below.

2.3.2 *In Vitro* Transfection

Figure 2.3a shows the transfection of PC3-PSMA cells with the pGL3 plasmid using a set of lead polymers selected from the DNA-binding screen. Representative polymer leads that possessed moderate (30% fluorescence decreased) to high (> 60% fluorescence decreased) DNA binding efficacies were employed in the transfection experiments. It is important to point out that calf-thymus DNA was used only as generic double-stranded DNA in the primary DNA binding screen for identifying lead polymers. However, the lack of a constitutive promoter region implies that this DNA cannot be employed as a reporter for transfection. Consequently, transfection was carried out with the pGL3 control vector which codes for luciferase protein. A polymer to plasmid ratio of 25:1 was

employed in order to evaluate the transfection efficacies of the selected polymers. The use of nitrogen:phosphorus (N:P) ratio is common in comparing cationic lipid and cationic polymer meditated gene delivery. However, a w/w ratio was used, which has been previously employed for evaluating polymeric transfection agents (103, 104).

In order to evaluate polymer-mediated transfection efficacy, luminescence (relative light units or RLU) due to the expression of the luciferase normalized to the protein content in each well, and the normalized values were compared to those determined for pEI-25. A number of polymers demonstrated statistically significant higher transfection efficacies than pEI-25 in the absence of serum. In particular, the 1,4C-1,4Bis polymer, based on the monomers, 1,4-cyclohexanedimethanol diglycidyl ether (1,4 C) and 1,4-bis(3-aminopropyl) piperazine (1,4 Bis),demonstrated 80-fold higher transfection efficacy than pEI-25 in the absence of serum. Other polymers demonstrated moderately higher (4-8 fold) or comparable transfection efficacies compared to that of pEI-25 in the absence of serum. For example, neopentyl glycol diglycidyl ether-1,4-bis(3-aminopropyl) piperazine (NPGDE-1,4 Bis) and ethylene glycol diglycidyl ether-1,4-bis(3-aminopropyl) piperazine (EGDE-1,4 Bis) polymers demonstrated approximately eight-fold higher efficacies than pEI-25. Polymers generated using 1,4-bis(3-aminopropyl) piperazine (1,4 Bis) as the amine monomer resulted in candidates with higher gene transfection efficacies than pEI-25.

The transfection efficacy of the 1,4C-1,4Bis polymer was further evaluated as a function of polymer dose (i.e. polymer:pGL3 plasmid) in the

absence of serum (Figure 2.3b). While the polymer demonstrated comparable transfection efficacies to that of pEI-25 at low polymer:plasmid ratios (1:1 and 5:1), transfection efficacies with higher polymer ratios (10:1, 20:1 and 25:1) were significantly higher than those for pEI-25. It is important to note that in addition to the normalized ratios presented in Figure 2.3b, the absolute RLU/mg values using1,4C-1,4Bis polymer were the highest (not shown), indicating that the polymer resulted in greater protein expression than pEI-25 under all conditions.

Next, a sub-set of polymers that demonstrated appreciable transfection efficacies in the absence of serum was employed to transfect PC3-PSMA cells in the presence of serum-containing medium. In the presence of serum, the transfection efficacy dropped in all polymers evaluated. However, the 1,4C-1,4Bis polymer demonstrated 30-fold higher efficacies than pEI-25 in presence of serum (Figure 2.3c). Transfection efficacies of other polymers were not statistically different compared to that of pEI-25. These polymers were not evaluated at higher polymer:pDNA ratios in order to keep 25:1 ratio consistent with that in the experiments carried out in absence of serum. The highest transfection efficiency observed using the 1,4C-1,4Bis polymer makes it an attractive candidate for further evaluation *in vivo*.

Transfection was also carried out in serum-containing medium with murine osteoblast cells in order to compare the efficacy of the 1,4C-1,4Bis polymer to that of pEI-25 in cells unrelated to human prostate cancer cells. Lower transfection efficacies were observed in the MC3T3 murine osteoblast cells for both polymers (not shown) as compared to PC3-PSMA cells, reflecting the

challenges of transfecting these cells using non-viral transfection agents (120). However, as with the PC3-PSMA cells, the 1,4C-1,4Bis polymer was ~23-fold more effective than pEI-25 in transfecting PC3-PSMA cells (Figure 2.3d), indicating that the polymer might be useful in transfecting different cell types. Taken together, these results indicate that transfection using the polymer leads selected from the DNA binding screen resulted in the identification of one polymer-1,4C-1,4Bis that possesses significantly higher transfection efficacies than the current standard pEI-25 polymer (Figures 2.3a-c). In addition, a number of polymers demonstrated moderately higher or comparable transfection efficacies with respect to pEI-25 (Figures 2.3a and 2.3b).

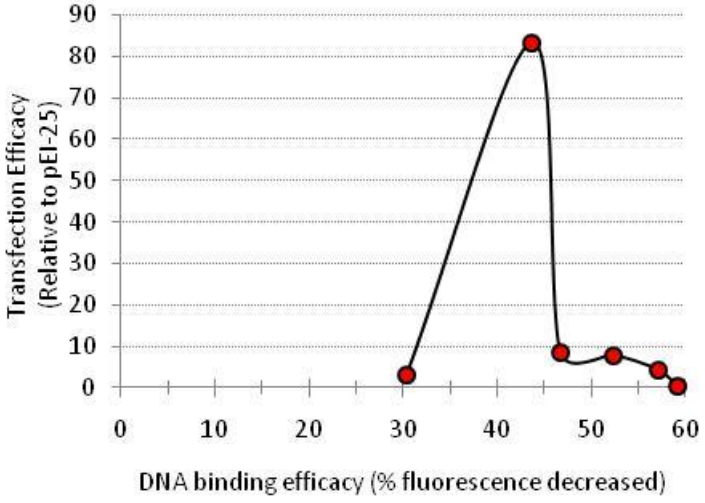

Figure 2.4. Comparison of transfection efficacy of polymers with their respective DNA binding efficacy of polymers leads used in the transfection analysis.

It is important to note that while DNA binding efficacy is indeed necessary for polymer-mediated gene delivery, DNA binding activity of polymers

did not correlate with their transfection efficacies (Figure 2.4). Instead the efficacy depends on the optimum DNA binding affinities of the polymers that regulate cellular uptake and DNA release after endosomal escape.

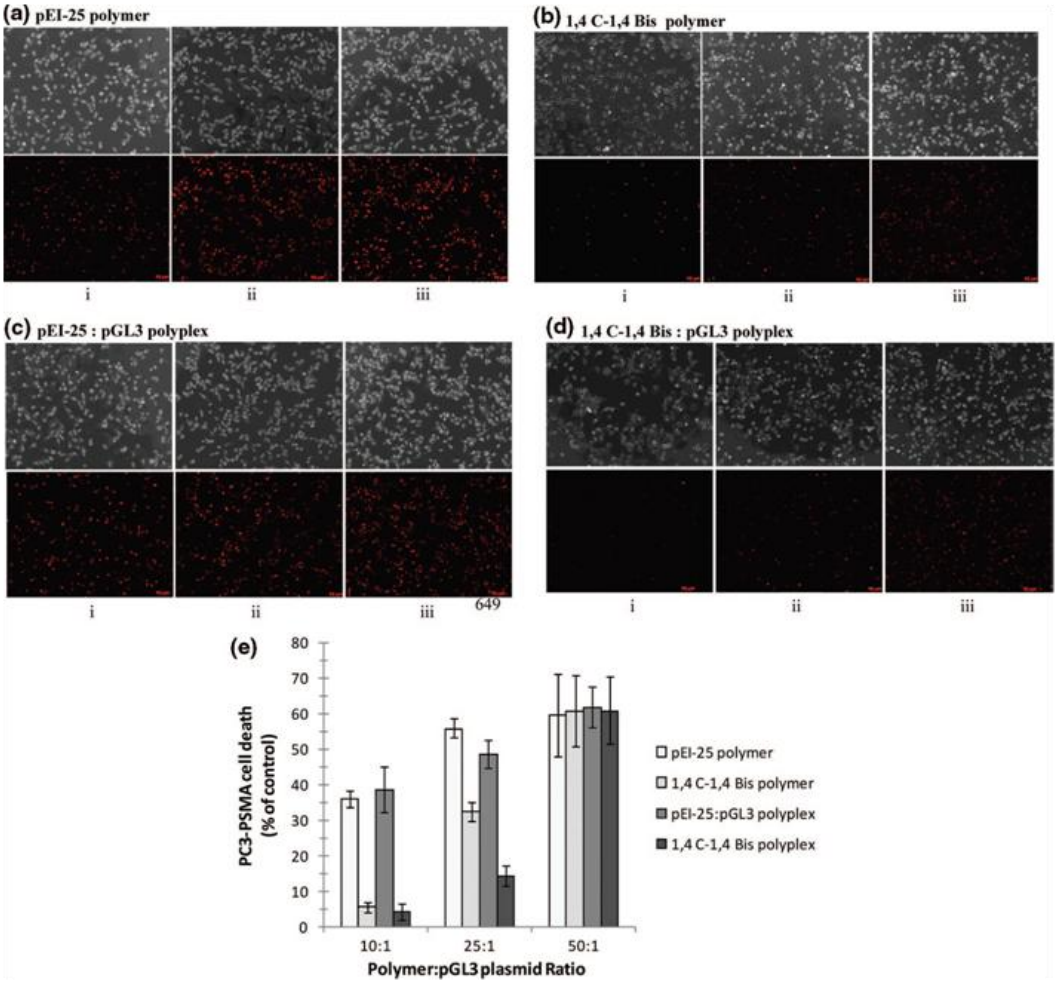

Figure 2.5. Phase contrast and fluorescence microscopic images that show the cytotoxicity of (a) pEI-25 polymer, (b) 1,4C-1,4Bis polymer, (c) pEI-25:pGL3 polyplex, and (d) 1,4C-1,4Bis:pGL3 polyplex towards PC3-PSMA cells in serum-free medium. Red-fluorescent ethidium homodimer, that stains DNA in compromised nuclei, was used for determining cytotoxicity. In figures a ,b: i: 4ng/µl, ii. 10ng /µl, and iii. 20ng/µl polymer. In figures c,d: i. 10:1 polymer: plasmid (or 4ng/µl polymer), ii. 25:1 polymer: plasmid (or 10ng /µl polymer), iii. 50:1 polymer: plasmid (or 20ng /µl polymer). The same amount of pGL3 plasmid (200 ng) was used in all polyplex-mediated cytotoxicity experiments. Representative images of at least three independent experiments and at least three different fields of view per independent experiment are shown in the figure. (e) Percentage of dead PC3-PSMA cells following polymer/polyplex treatment; details are described in the experimental section.

2.3.3 Polymer and Polyplex Cytotoxicity

While cationic polymers are attractive agents for non-viral gene delivery, their toxicity limits their use both *in vitro* and *in vivo*. The cytotoxicity of the 1,4C-1,4Bis polymer was compared with that of pEI-25 in PC3-PSMA cells. Ethidium homodimer is a red-fluorescent dye that stains DNA in cells with compromised nuclei. It is important to note that the MTT assay consistently under-reported PC3-PSMA cell death when compared to what was seen using visual microscopic observation and was therefore not employed for evaluating polymer cytotoxicity with these cells.

Figure 2.5 shows representative fluorescence microscopic images of polymer and polyplex induced cytotoxicity. As seen in Figures 2.5a and b, the 1,4C-1,4Bis polymer was less toxic to PC3-PSMA cells than pEI-25 at all concentrations (4-20ng/µL) investigated. Note that a polymer concentration of 10ng /µL (polymer : pGL3 plasmid 25:1) was used in the transfection experiments in Figure 2.3a. The higher efficacy of the 1,4C-1,4Bis polymer can be explained, in part, due to its lower cytotoxicity compared to pEI-25 under these conditions. While polymer-mediated cytotoxicity is indeed a limiting factor, it was hypothesized that a large number of amine groups responsible for polymer toxicity, are involved in complexation with plasmid DNA. As a result, the cytotoxicity of the polymer :plasmid polyplexes was evaluated in addition to the cytotoxicity due to the polymer alone. As seen in Figures 2.5c and 2.5d, pEI-25-based polyplexes demonstrated significantly higher cytotoxicities towards PC3-PSMA cells compared to polyplexes based on the 1,4C-1,4Bis polymer.

In order to determine the relative toxicities of the two polymers and their polyplexes, polymer and polyplex toxicity based on at least three different fluorescence microscopy images was quantified as described in the experimental section. As seen in Figure 2.5e, pEI-25 is significantly more cytotoxic than the 1,4C-1,4Bis polymer at concentrations of 4ng/µL and 10ng/µL (equivalent to the polymer:pDNA ratios of 10:1 and 25:1, respectively). Both polymers demonstrated similar cytotoxicities at 20ng/µL (equivalent to polymer:pDNA ratio of 50:1). Interestingly, polyplexes of 1,4C-1,4Bis polymer demonstrated lower cytotoxicities than the polymer alone for polymer:pDNA ratios of 10:1 and 25:1. In contrast, polyplexes of pEI-25 showed comparable cytotoxicity with the polymer alone at all polymer:pDNA ratios investigated. It is possible that lower concentrations of pEI-25 are required for complexation with DNA and the excess polymers cause cytotoxicity to cells. The low cytotoxicities of the 1,4C-1,4Bis polymer and its polyplexes are responsible for the higher transfection efficacies of this polymer. Taken together, these results indicate that the 1,4C-1,4Bis polymer demonstrates significantly high efficacies for transfecting PC3-PSMA cells as well as low cytotoxicities that make it an attractive polymeric transfection agent.

2.3.4 Lead Polymer Characterization

Characterization experiments were carried out with the lead polymer (1,4C-1,4Bis) that demonstrated successful cellular transfection. The polymer EGDE-3,3’ was also used in some cases in order to demonstrate the results for a different polymer used in transfection. In order to ascertain that 16h was indeed sufficient time for polymerization, samples of the reaction mixture were evaluated for the

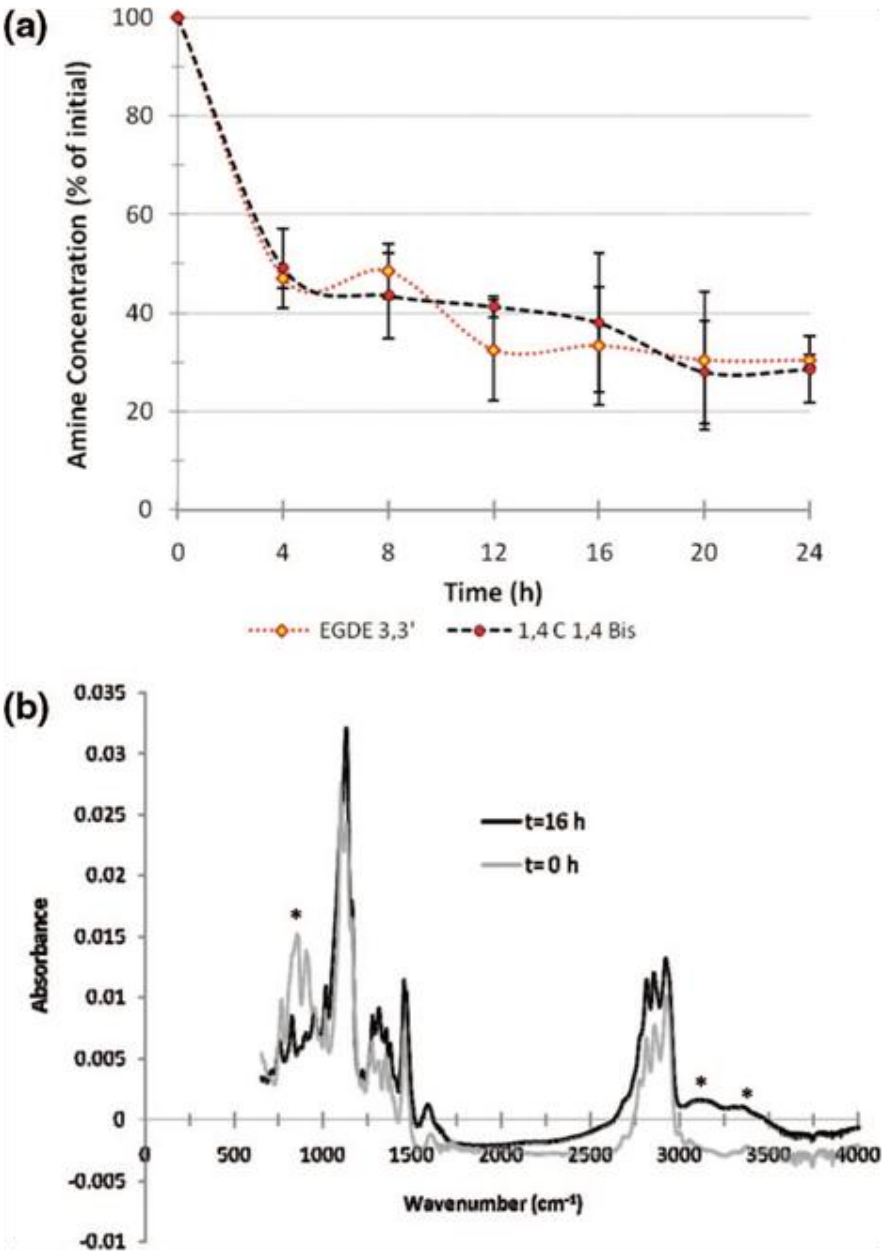

Figure 2.6. Polymer Characterization. a. Polymerization kinetics of the formation of EGDE-3,3' and 1,4C-1,4Bis polymers as reported by the disappearance of amines as a function of time. Formation of dark blue/purple color indicated the presence of primary amines. Primary amine concentration was determined at pre-determined time points using the ninhydrin reagent and compared to the initial primary amine content. Polymerization kinetics of two representative polymer leads 1,4C-1,4Bis and EGDE-3,3' used in transfection experiments are shown in the figure. b. Fourier Transform Infrared (FT-IR) Spectroscopy of 1,4C-1,4Bis polymerization at time t = 0h (monomer mixture) and t =16 h following initiation of the polymer reaction. Polymer formation at 16 h can be seen from the disappearance of the epoxide peak in the 860-950 cm^{-1} region and from the emergence of the hydroxyl peak in the 3000-3500 cm^{-1} region.

disappearance of amines as a function of time (Figure 2.6a) using a ninhydrin assay with glycine standards. The amine concentration remained largely invariant after 12h of reaction time as determined from the using absorbance spectroscopy based on the formation of dark blue/purple color following reaction with primary amines. These results indicated that a reaction time of 16h was appropriate for the generation of polymers that demonstrated moderate to high DNA binding and cellular transfection efficacies. In addition, the presence of residual primary amines (approximately 30% of the initial primary amine concentration, as reported by the dark blue color of the ninhdyrin reaction) indicated the formation of branched polymers with multiple terminal primary amines and not linear polymers. This is consistent with what can be expected from the reaction chemistry employed to generate the polymer library (Figure 2.1a).

Gel permeation chromatography was employed to determine the molecular weight of the 1,4C-1,4Bis polymer which were as follows: M_n = 3.9 kDa and M_w= 23.5 kDa indicating a polydispersity (PD) of 5.96. These values indicate that the molecular weights of 1,4C-1,4Bis are comparable to those of pEI-25 used in the study: M_n = 10kDa, M_w = 25kDa, PD = 2.5 (Sigma). Formation of the 1,4C-1,4Bis polymer was further verified using Fourier Transform-Infrared (FT-IR) spectroscopy by following the appearance and disappearance of certain bands as a function of reaction time. Similar analyses were carried out for other polymers used in the transfection experiments; only results obtained with the 1,4C-1,4Bis polymer that demonstrated high transfection efficacies are described here. The epoxide peak ranging from 858-918 cm^{-1} can be seen in the monomer mixture at

time t=0 h (Figure 2.6b) due to stretching and contraction of C-O bonds in the epoxide moiety (121). However, this peak is significantly reduced after 16h of reaction time, indicating a reduction in the epoxide content upon formation of the cationic polymer (121). Characteristic spectral bands of primary amines were seen at 1100-1128 and 3358-3382 cm^{-1} due to the presence of C-N and N-H bonds, respectively. The broad bands from 3382-3402 cm^{-1} upon 16h of reaction time can be attributed to hydroxyl (-OH) groups generated upon reaction of the epoxy rings with primary and secondary amines (122). Taken together, FT-IR analysis further confirmed that the diglycidyl ether-polyamine reaction resulted in the formation of the 1,4C-1,4Bis polymer that demonstrated high transfection efficacies *in vitro*.

2.4 Conclusions

Parallel polymer synthesis techniques were employed for the rapid generation of a cationic polymer library based on ring opening reactions between diglycidylethers and amines. Polymers were screened in parallel for their DNA-binding affinities using ethidium bromide displacement assay. Parallel screening led to the identification of a number of polymer leads that demonstrated significant DNA-binding properties. *In vitro* transfection experiments indicated that the 1,4C-1,4Bis polymer based on the monomers of 1,4-cyclohexanedimethanol diglycidyl ether (1,4 C) and 1,4-bis(3-aminopropyl) piperazine, (1,4 Bis) resulted in significantly higher transfection efficacies, in both human prostate cancer cells and murine osteoblasts, compared to pEI-25 a current standard for polymer-mediated gene delivery. The 1,4 C-1,4Bis polymer

and resulting polyplexes were lower in cytotoxicity than pEI-25. While previous reports have employed parallel synthesis methods for the accelerated identification of polymeric transfection agents (103, 107, 123-125), a direct comparison of our polymers with those used in previous studies is difficult due to differences in the cell lines used, transfection protocols, and / or the plasmids that have been employed. In addition to the polymer described above, this approach resulted in the identification of a number of other polymers that demonstrated moderately higher or comparable efficacies to pEI-25.

Chapter 3

CANCER CELL PHENOTYPE DEPENDENT DIFFERENTIAL INTRACELLULAR NANOPARTICLE TRAFFICKING

3.1 Introduction

Cancer disease progression to the aggressive metastatic state is a result of the accumulation of various genetic changes. Malignant cells undergo significant differences in their cellular phenotype as a consequence of these genetic changes; characteristic of these include, alterations in intra- and extra-cellular protein expression, cell polarity and cell survival. While the polarized phenotype of non-malignant epithelial cells result in different trafficking mechanisms at their apical and basolateral regions (126), malignant cells are typically characterized by loss in polarity which influences intracellular sorting and trafficking of cargo in these cells (127). In addition, due to the heterogeneous nature of epithelial tumors, phenotypic differences in cancer cells play a significant role in the uptake, intracellular sorting, trafficking, and localization of internalized cargo (128).

Nanoscale therapeutics, diagnostics, and imaging agents hold great promise in the detection and treatment of advanced cancer disease (129-131). An understanding of the processing and fate of targeted and untargeted nanoparticles in cancer cells can facilitate the design and engineering of novel nanoscale agents that possess high efficacies and selectivity. Receptor expression profiles on cancer cells influence the intracellular trafficking of targeted nanoparticles.(132-134) While some reports describe cellular uptake of unconjugated nanoparticles (135), it is largely presumed that cationic molecules such as polymers (136), cell

penetrating peptides (137-139) and / or serum proteins (140) are indispensible for receptor-independent (untargeted) uptake of nanoparticles in cancer cells. Recent reports have described the role of nanoparticle size and surface chemistry on their uptake and intracellular fate in cancer cells. For example, 25-50nm Herceptin-conjugated gold nanoparticles demonstrated the highest uptake in SK-BR-3 breast cancer cells among nanoparticles ranging from 2-100 nm in size (141). Similarly particles of 50nm demonstrated the greatest uptake in HeLa cells among unconjugated gold particles ranging from 14-100 nm in diameter; adsorption of serum-containing proteins on the surface of the anionic nanoparticles was thought to promote the non-specific uptake of the nanoparticles by cancer cells.(140) Polymeric particles less than 25 nm in diameter were reported to be taken up by a non-degradative, cholesterol independent, and non-clathrin and non-caveolae dependent endocytosis leading to their transport as punctate structures in the perinuclear region of HeLa cells; larger sized (40 nm) nanoparticles did not demonstrate this behavior (142).

Prostate cancer (PCa) is the most frequently diagnosed malignancy in men in the United States with 217,730 cases diagnosed and 32,050 estimated deaths in 2010 (143). Lowering androgen levels results in tumor shrinkage or decelerated tumor growth in approximately 90% of treated cases (144). Unfortunately, these results are usually transient and a large number of patients subsequently undergo disease progression to aggressive, androgen-independent, and chemo- and radiation- therapy resistant PCa disease. Consequently, in addition to the

discovery of novel molecular therapeutics, nanoparticle-mediated ablation of PCa cells is currently investigated (145-147).

The role of cancer cell phenotype on the uptake and intracellular routing of unconjugated anionic nanoparticles in bone metastasis-derived PC3, PC3-flu (113) and PC3-PSMA(113) human PCa cells is investigated in this chapter. The differences in these three closely related cell lines can be indicative of phenotypic differences that occur during disease progression and different cancer cell populations existing in tumors. These cells were employed to investigate the role of cellular heterogeneity on nanoparticle fate in cancer cells. Quantum dots (QDs) are of interest in biomedical imaging applications due to their greater photostability, broader excitation and narrower, symmetric emission wavelengths, compared to traditional organic dyes (148, 149). Therefore, unconjugated anionic QDs were chosen in this investigation demonstrating their spontaneous uptake by PCa cells and cell type dependent intracellular fate.

3.2 Materials and Methods

3.2.1 Cell Culture

The PC3 human PCa cell line was obtained from the American Type Culture Collection (ATCC, VA). PC3-PSMA and PC3-flu cells, derived from PC3 cells, were generous gifts from Dr. Michael Sadelain, Memorial Sloan Kettering Cancer Center, New York, NY. The PC3-PSMA cell line is a sub-clone of PC3 cells retrovirally transduced to stably express the PSMA receptor (113); PC-3 flu cells are obtained by retrovirally transducing PC3 cells with the flu peptide (113). All cells were grown in RPMI-1640 medium (HyClone®, UT)

containing 10% fetal bovine serum (HyClone®, UT) and 1% penicillin / streptomycin (HyClone®, UT) in 5% CO_2 at 37°C incubator.

3.2.2 Quantum Dot Treatment

Qdot® 655 nanocrystals (ZnS-capped CdSe quantum dots; 8.2μM) were purchased from Invitrogen, CA. The particle size of quantum dots in PBS was determined as 27 nm using Dynamic Light Scattering (data not shown). PC3, PC3-PSMA, and PC3-flu cells were plated in 24-well cell culture plates (Corning Inc., NY) with or without glass coverslips (12 mm circle diameter; Fisher) at a density of 50,000 cells per well and allowed to attach overnight. For uptake experiments, cells were treated with 0.2nM QDs in serum-free medium for 5h, fixed with 4% paraformaldehyde, and imaged using fluorescence microscopy (AxioObserver D1, Carl Zeiss MicroImaging Inc., Germany). The fluorescence excitation of the Zeiss inverted microscope was equipped with an objective of 40X / 0.6 numerical aperture (NA) (without immersion) incorporating a cover glass correction ring with it. Fluorescence images of QDs were captured using a 605/70 emission filter and a CCD camera. For kinetics experiments, cells were treated with QDs at different time, fixed and imaged as described above.

3.2.3 Uptake, Trafficking and Intracellular Localization of Quantum Dots

Cells (50,000/well) were treated with the lipid raft extracting agent methyl-β-cyclodextrin (mβCD; 1mM for 1h) or clathrin disrupting agent chlorpromazine (10μg/ml for 1h) following which cells were washed with PBS and treated with 0.2nM QDs for 5h. The microtubule depolymerizing agent, nocodazole (Sigma-Aldrich) was employed in order to investigate the role of

microtubule-mediated transport of QDs in cells. Cells grown on glass coverslips placed in 24-well plates were treated with 40µM nocodazole for 1 h at 37 °C. Nocodazole-containing medium was then removed and cells were washed with PBS, and incubated with QDs for 5h. Cells were treated with 10µg/ml FITC-transferrin (Invitrogen, CA) for the last 1h of the incubation in order to investigate the role of microtubule disruption on localization in recycling endosomes.

In order to visualize localization of QDs with respect to the nucleus, cells were treated with QDs for 5h, following which, cells were fixed with 4% paraformaldehyde, and stained with 3µg/ml of the nucleic acid stain, 4',6-diamidino-2-phenylindole (DAPI; Invitrogen, CA), in 500µL PBS for 15min at room temperature (R.T.; 22°C). The cells were then washed three times with PBS and visualized using fluorescence microscopy (Zeiss AxioObserver D1 microscope).

For co-localization experiments, cells were settled on coverslips placed in 24-well plates for 24h following which QDs (0.2nM final concentration in 500µL) were added. After 4 h, the cells were incubated with 10µg/ml FITC-labeled transferrin (Invitrogen, CA), 4µg/ml LysoTracker® Green DND-26 (Invitrogen, CA), or 1.5 µg/ml FITC labeled anti- PSMA antibody (Ab) (Marine Biological Laboratory, MA) for 1h in order to visualize recycling endosomes/perinuclear recycling compartment (PNRC), lysosomes, and the internalized Prostate-Specific Membrane Antigen (PSMA), respectively. After 5h total treatment with QDs, cells were washed twice with PBS and fixed with 4% paraformaldehyde for 10min at R.T. Cells were then gently washed with PBS 3x.

The coverslips were removed from the 24-well plates and mounted in permount mounting medium (Fisher) on glass slides for confocal fluorescence microscopy.

Laser scanning confocal microscopy was carried out with a Leica SP2 microscope (Leica Microsystems, Heidelberg, Germany) in the W. M. Keck Bioimaging Laboratory, Arizona State University, AZ in order to determine the intracellular localization of QDs. Confocal images were obtained in a z-series using an upright microscope equipped with 40X/1.25 NA oil immersion objective lens, Argon laser (488 nm) and a transmitted light detector photomultiplier (PMT). Light emitted at 525nm and 650nm was recorded for the green channel (FITC and Green DND-26) and red channel (QDs), respectively. Images were acquired with dual-channel scanning at 512x512 pixels using PMTs along with image acquisition and analysis software (Leica confocal software, version 2.61, Leica Microsystems, Mannheim, Germany). Images were then stacked in RGB color using Image Processing and Analysis in Java (ImageJ) 1.38X software (150); the average intensity was used to compare different images.

3.3 Results and Discussion

Quantum dots (0.2 nM) demonstrated punctated intracellular localization throughout the cytoplasm in PC3 cells (Figure 3.1a) characteristic of lysozomal localization (151). In contrast, QDs localized mainly at a single juxtanuclear location (‘dot-of-dots’) inside PC3-PSMA cells (Figures 3.1c and 3.1d). Kinetic experiments indicated that the dot-of-dots formation was complete in 5h in a concentration-dependent fashion in PC3-PSMA cells (Figures 3.2 and 3.3) and the structure remained intact for at least 72h (not shown).

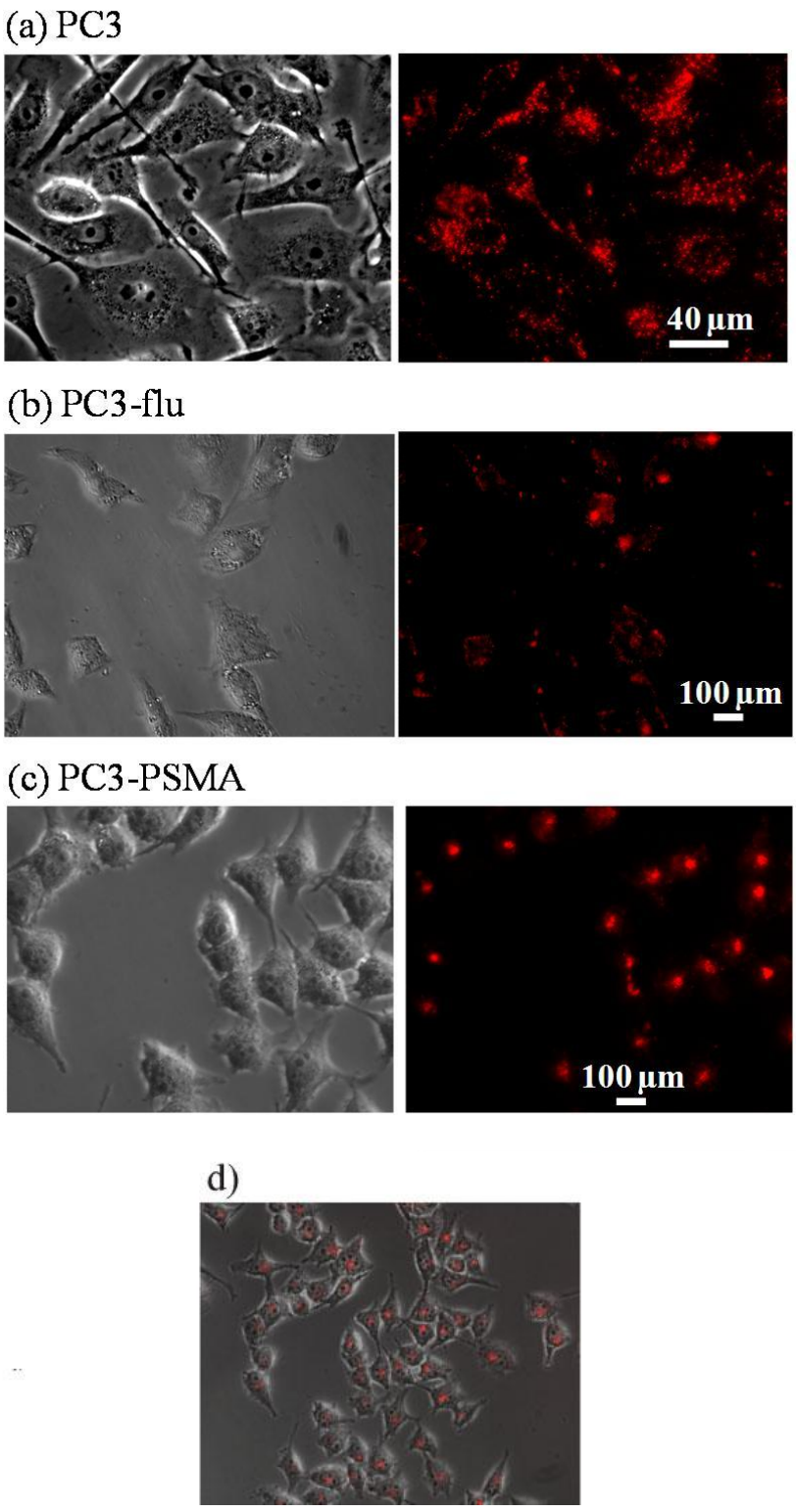

Figure 3.1 Differential intracellular localization of QDs in human prostate cancer cells. (a) PC3, (b) PC3-flu, (c) PC3-PSMA, (d) overlay of phase contrast and fluorescence microscopy image of 'dot-of-dots' formation in PC3-PSMA cells.

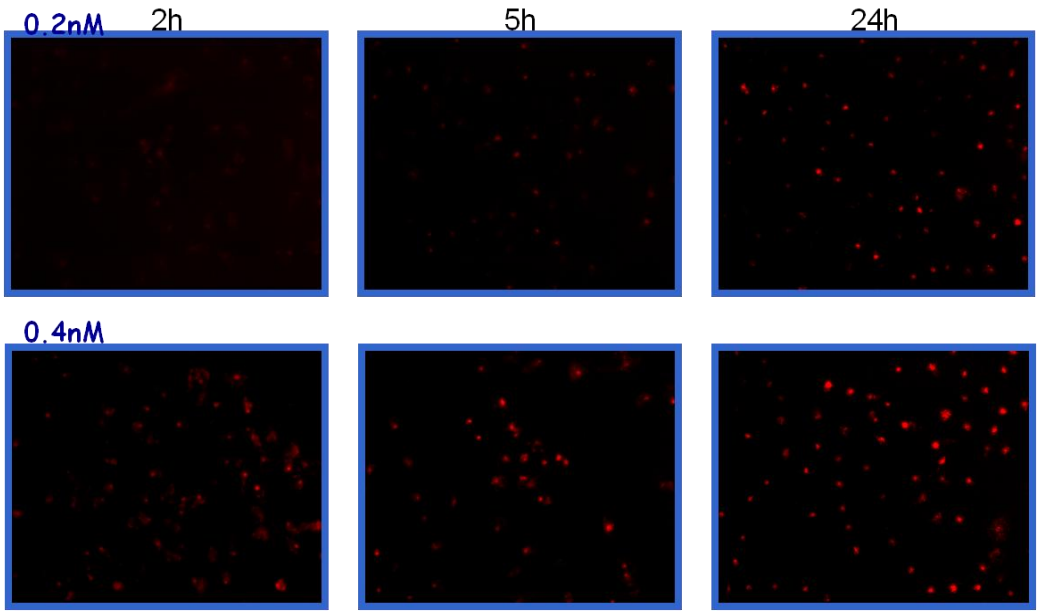

Figure 3.2. Kinetics of 'dot of dots' formation in PC3-PSMA PCa cells. The formation was complete in 5h and was invariant for 72h (not shown)

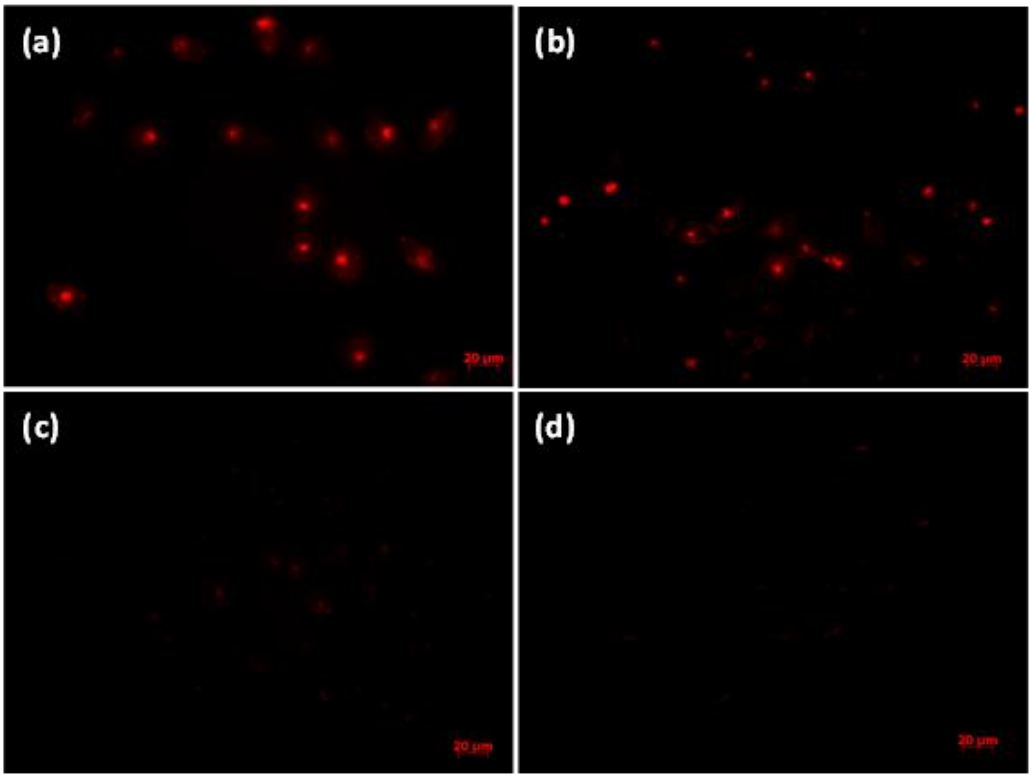

Figure 3.3. Formation of the dot-of-dots structure in PC3-PSMA cells as a function of quantum dot concentration. The formation was seen for concentrations as low as 2picomolar. All

subsequent experiments were carried out with 200picomolar (0.2 nM) concentration of QDs. (a) 9.6 *10^{10} QD particles/ml (= 200pM or 0.2nM); (b) 9.6*10^{9} QD particles/ml (= 20pM); (c) 9.6*10^{8} QD particles/ml (= 2pM); (d) 9.6*10^{7} QD particles/ml (= 0.2pM). Scale bar = 20 µm.

Higher concentrations of the QDs (1nM) were required for the formation of the 'dot-of-dots' structure in the presence of serum under similar conditions (Figure 3.4) indicating that the presence of serum proteins inhibited nanoparticle uptake at lower concentrations. PC3-flu cells demonstrated trafficking profiles similar to both, PC3 and PC3-PSMA cells (Figure 3.1b); while QDs formed the 'dot-of-dots' structure as seen in PC3-PSMA cells, they also localized throughout the cytoplasm similar to PC3 cells, and along the cellular periphery.

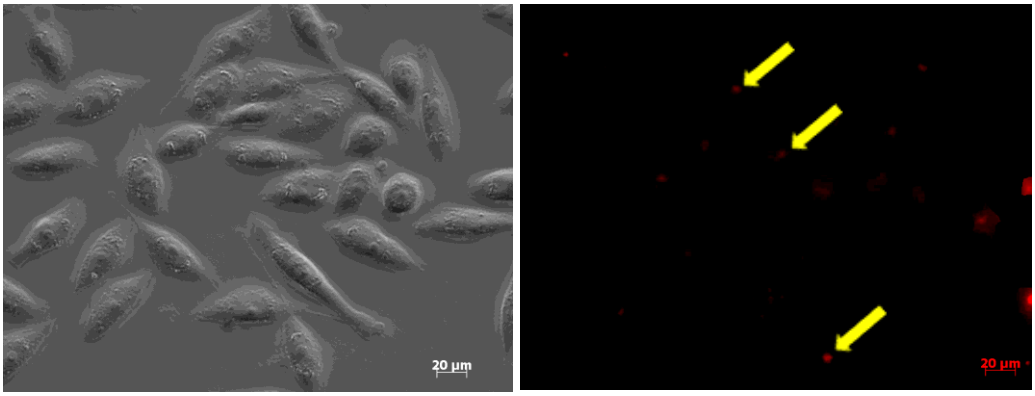

Figure 3.4. Quantum dot (concentration of 1nM) trafficking in PC3-PSMA cells in the presence of serum (10% FBS). Higher concentrations of unconjugated QDs (1nM) were required for uptake and formation of the 'dot-of-dots' structure in PC3-PSMA cells in the presence of serum compared to the absence of serum (0.2nM). Left: Phase contrast image of PC3-PSMA cells, Right: corresponding fluorescence image. Scale Bar = 20 µm

Following the above observations, factors that influenced the uptake of nanoparticles leading to the formation of the dot-of-dots structure in PC3-PSMA cells were investigated. Different mechanisms including, lipid raft-mediated, clathrin-mediated, and adsorptive endocytosis, play a role in the cellular entry of

exogenous material. Lipid rafts are cholesterol-rich membrane platforms that have been implicated in the entry of viruses in mammalian cells.

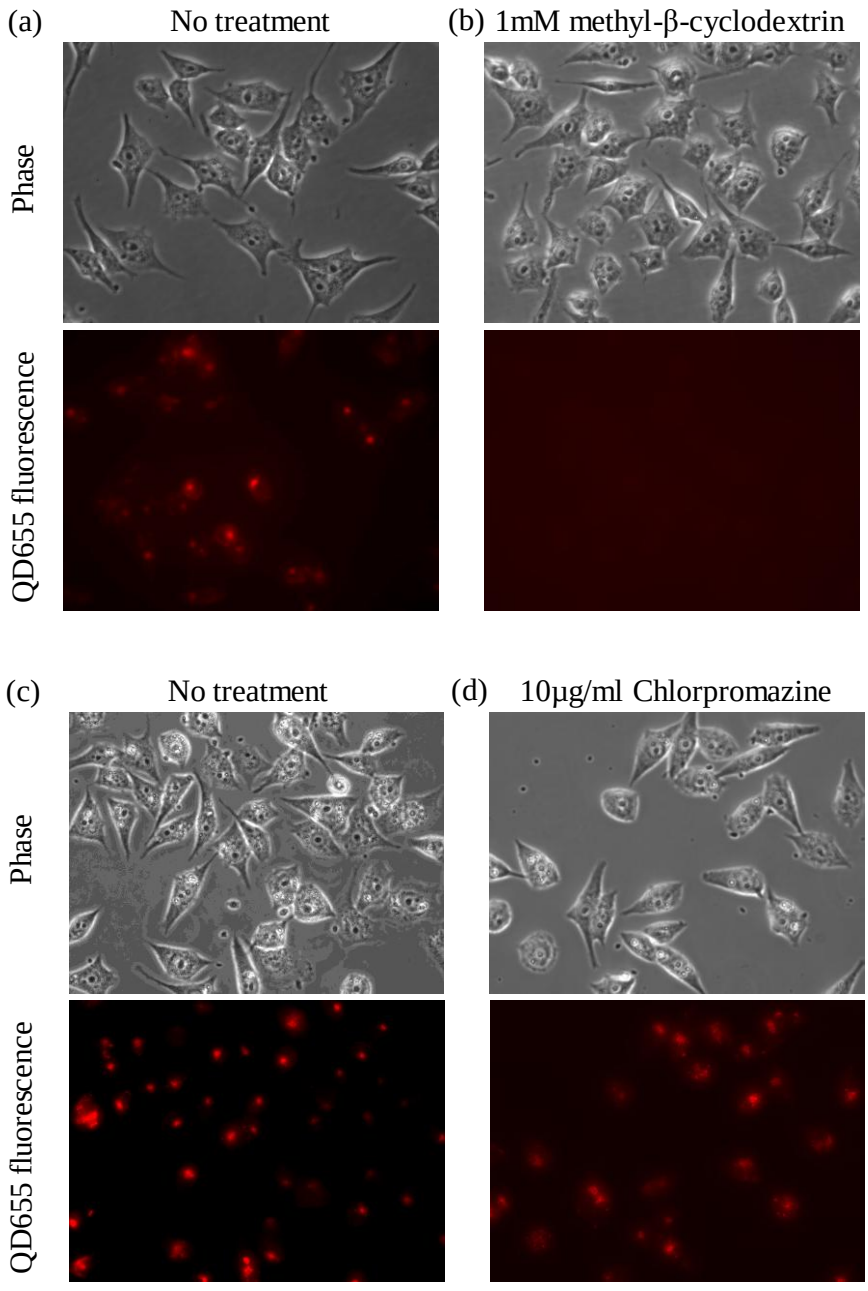

Figure 3.5. Role of lipid rafts and clathrin on quantum dot internalization and 'dot-of-dots' formation in PC3-PSMA cells. PC3-PSMA cells were treated (a) without or (b) with the cholesterol extracting agent, methyl-β-cyclodextrin for evaluating the role of lipid rafts and (c)

without or (d) with the clathrin inhibiting agent, chlorpromazine for evaluating the role of clathrin on the uptake of QDs.

Extraction of cholesterol using mβCD from the surface of PC3-PSMA cells resulted in significant decrease in the uptake and trafficking of QDs (Figures 3.5a and 3.5b), which indicated lipid raft dependent internalization of QDs. Treatment with the clathrin inhibitor chlorpromazine did not affect the QD uptake in PC3-PSMA cells (Figures 3.5c and 3.5d) indicating that clathrin-mediated endocytosis was not responsible for the entry of QDs in these cells. The results are consistent with the report described by Zhang et al.(152). The carboxylated QD655 nanoparticles have been shown to be internalized via lipid-raft mediated endocytosis but not by clathrin or caveolae in human epidermal keratinocytes(152).

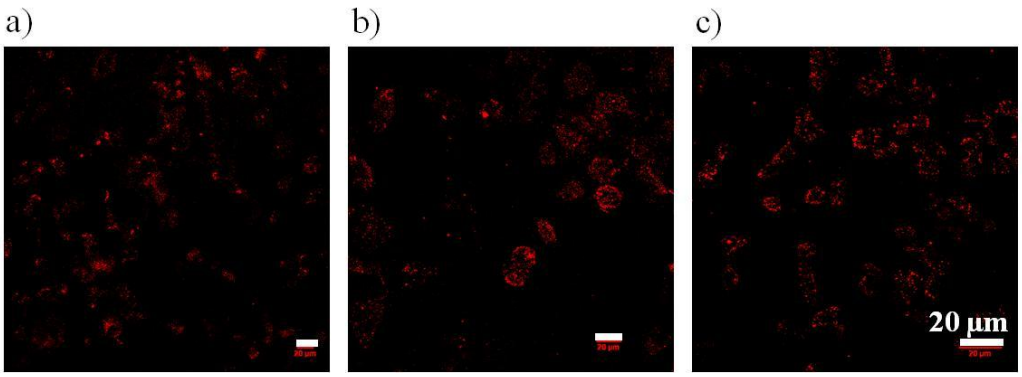

Figure 3.6. Effect of microtubule disruption on quantum dot trafficking in (a) PC3, (b) PC3-flu, and (c) PC3-PSMA cells. Cells were treated with the microtubule depolymerizing agent, nocodazole, for 1h prior to treatment with QDs for 5h. In the figure, scale bar = 20µm.

Motor proteins, kinesin and dynein, transport cargo-containing vesicles to the plus (cell periphery) and minus (microtubule organizing center) ends of

microtubules, respectively. In order to investigate the role of microtubules on the formation of dot-of-dots structure following clathrin-mediated endocytosis, microtubule transport was disrupted by treating cells with the microtubule depolymerizing agent, nocodazole. Microtubule disruption in PC3 cells (Figure 3.6a) resulted in reduced intracellular uptake and trafficking of QDs in these cells; however, the nanoparticles still localized as punctated dots throughout the cytoplasm. Nocodazole treatment resulted in complete disruption of the dot-of-dots formation in both, PC3-flu (Figure 3.6b) and PC3-PSMA (Figure 3.6c) cells, indicating that a functional microtubule network is necessary for the intracellular trafficking of nanoparticles in these cells. Interestingly, QDs were transported closer to the cell periphery and away from the nucleus in PC3-PSMA cells indicating that microtubule disruption results in mis-sorting and altered trafficking, a phenomenon previously observed in both, malignant and untransformed primary cells (153, 154). The punctated nanoparticle distribution in the cytoplasm of PC3-PSMA cells (Figure 3.6c) after nocodazole treatment was qualitatively similar to the nanoparticle distribution observed in PC3 cells without microtubule disruption.

Following uptake by lipid-raft mediated endocytosis, molecular and/or nanoscale cargo are sorted in sorting endosomal complexes and are trafficked on microtubules along one of three different pathways: degradative lysozomal pathway, retrograde transport, or to the perinuclear recycling compartment (PNRC) (155). The intracellular fate of QDs in all three PCa cell lines using confocal fluorescence microscopy was therefore investigated.

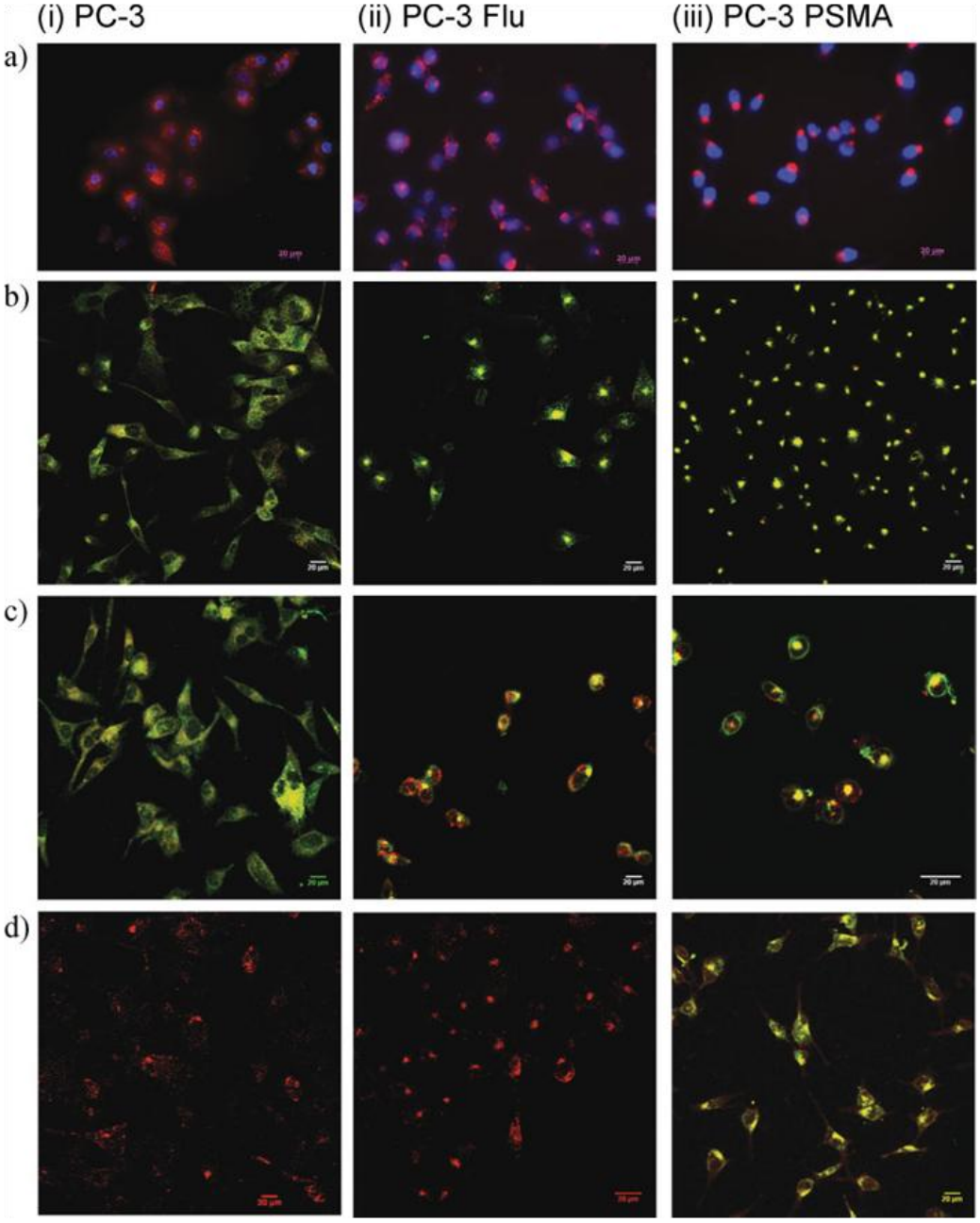

Figure 3.7. Intracellular localization of QDs in (i) PC3, (ii) PC3-flu, and (iii) PC3-PSMA cells determined by colocalization for organelle / vesicle specific markers and QDs using confocal fluorescence microscopy. Confocal microscopy images show colocalization of QDs with: (a) Cell nuclei using DAPI (blue stain); (b) Recycling endosomes using FITC-transferrin; (c) Acidic vesicles (late endosomes & lysosomes) using LysoTracker Green DND-26; (d) PSMA using FITC labeled anti-PSMA antibody. Colocalization of green-fluorescent markers (dyes) and red-fluorescent QDs is shown in yellow color in the images. Scale bars = 20μm

Figure 3.7 shows intracellular colocalization of QDs with DAPI, FITC-transferrin, Lysotracker® Green DND-26, and FITC-labeled antibody against the Prostate-Specific Membrane Antigen (PSMA) which are markers for cell nuclei, recycling endosomes, acidic compartments (late endosomes / lysozomes), and PSMA, respectively. In case of PC3 (Figure 3.7a. i) and PC3-flu (Figure 3.7a.ii) cells, punctated dots were observed throughout the cytoplasmic space around the nuclei (shown in blue). Figure 3.7a. iii shows that the dot-of-dots formation (red) was found at a juxtanuclear location inside PC3-PSMA cells (nuclei shown in blue) which indicates that following uptake from the entire cell surface, QDs were trafficked along microtubules to a centralized juxtanuclear location, the microtubule organizing center (MTOC), in these cells. This behavior was also observed in some PC3-flu cells (Figure 3.7a ii). It was possible that viral transduction of PC3-PSMA and PC3-flu cells stabilized the microtubules in these cells by decreasing depolymerization rates compared to PC3 cells. Endocytic vesicles after being uptaken can therefore be transported along the stable microtubules close to the nucleus and accumulated at one single location in PC3-PSMA and PC3-flu cells. Relatively higher depolymerization rates of microtubules in PC3 cells than PC3-PSMA and PC3-flu cells might carry the endocytic vesicles at different locations in the cytoplasm.

The dot-of-dots structure colocalized with FITC-transferrin in PC3-PSMA (Figure 3.7b. iii) and PC3-flu (Figure 3.7b. ii) cells as seen from the yellow color (shown in blue). Figure 3.7a. iii, however, shows that the dot-of-dots formation (red) was found at a juxtanuclear location inside PC3-PSMA cells (nuclei shown

in blue) which indicates that following uptake from the entire cell surface, QDs were trafficked along microtubules to a centralized juxtanuclear location, the microtubule organizing center (MTOC), in these cells. This behavior was also observed in some PC3-flu cells (Figure 3.7a ii). from an overlay of the red fluorescent QDs and green-fluorescent FITC-transferrin. Transferrin is a known marker for the perinuclear recycling endosomal compartment (PNRC) which, in non-polarized cells, is a long-lived structure found close to the nucleus and near the MTOC (153-155). Near-complete colocalization of transferrin and QDs indicated that the nanoparticles localized almost exclusively as 'dot-of dots' in the PNRC in PC3-PSMA cells. As in the case of QDs, microtubule disruption in PC3-PSMA cells led to disruption of the PNRC and mis-sorting of transferrin. Following microtubule disruption, transferrin was trafficked to cytoplasmic compartments where only partial colocalization of the protein with QDs was seen (Figure 3.8). These results are in agreement with literature reports (153, 154) and were qualitatively similar to those observed with PC3 cells that had not been treated with nocodazole leading to the observation that microtubule disruption reverted trafficking in PC3-PSMA back to that observed in the parental PC3 cells. While some QDs colocalized with transferrin in cytoplasmic recycling endosomes in PC3 cells (Figure 3.7b. i), a significant number of QDs did not colocalize with transferrin indicating their localization in early / sorting endosomes in addition to cytoplasmic recycling endosomes (153). In the case of PC3-flu cells, vesicles containing both transferrin and QDs were seen in the cytoplasm in PC3-flu cells, in addition to the PNRC.

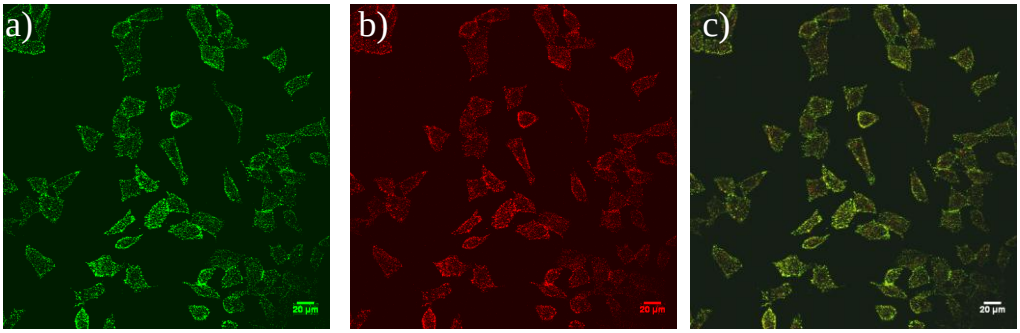

Figure 3.8. Missorting of transferrin and QDs in PC3-PSMA cells following microtubule disruption. Disruption of microtubules in PC3-PSMA cells using nocodazole treatment led to missorting of both, transferrin and QDs, and resulted in profiles similar to those observed in PC3 cells without microtubule disruption (Figure 3.4b i). In the figure: a: FITC-labeled transferrin for labeling recycling endosomes; b: 655 nm QDs; and c: merged image of transferrin and QDs. Scale bar = 20 µm.

Colocalization analyses were also carried out with LysoTracker® Green DND-26 and all three PCa cell lines; LysoTracker® stains acidic vesicles (e.g. late endosomes and lysozomes) inside cells. As with transferrin, a portion of intracellular QDs colocalized with acidic vesicles in PC3 cells (Figure 3.7c. i) further indicating the presence of these nanoparticles in different cytoplasmic compartments. Colocalization experiments also revealed the acidic nature of the QD-containing PNRC in both, PC3-PSMA (Figure 3.7c. ii) and PC3-flu cells (Figure 3.7c. iii). While some reports indicate that the PNRC is only mildly acidic with a pH range of 6.0-6.5 (155), other reports indicate that the compartment has a pH value of 5.6 (153). The latter is in agreement with LysoTracker® staining of the compartment; however, it is possible that the acidic nature of the cargo present in these vesicles, i.e. carboxylated QDs, also contributes to the acidification of these vesicles which in turn, results in strong staining with the reagent. Interestingly, a significant fraction of QDs was also

observed in non-acidic vesicles in PC3-flu cells (Figure 3.7c. ii); the nature of these compartments is not known at this point. In contrast, while QDs were observed in the PNRC in PC3-PSMA cells, acidic compartments without QDs were observed all along the periphery of these cells.

The Prostate-Specific Membrane Antigen (PSMA) is a 750-amino acid type II membrane glycoprotein which is abundantly expressed in all stages of PCa disease. The expression of the protein increases in cases of hormone-refractory and metastatic diseases. The receptor is over-expressed in approximately 70% of the aggressive metastatic diseases and is a reliable marker of disease progression. PSMA overexpression correlates with poor prognosis (156, 157) and has been employed for the targeted ablation of PCa cells (158-162). The extracellular region of the PSMA receptor possesses 26% and 28% homology with transferrin receptors (TfR), TfR1 and TfR2, respectively (163-165). Following both constitutive and antibody binding-induced internalization from clathrin-coated pits, PSMA is known to co-localize with transferrin in the PNRC mediated by a cytoplasmic internalization sequence and filamin (166). Given that QDs colocalized with transferrin in PC3-PSMA cells, colocalization of nanoparticles with PSMA was also investigated in these cells. Colocalization of QDs with the FITC-labeled PSMA antibody was indeed seen in PC3-PSMA cells (Figure 3.7d. iii) further indicating that the nanoparticles reside in the PNRC in PC3-PSMA cells. It is unclear at this point if PSMA has any role to play in the uptake and subsequently, trafficking of QDs. It is more likely that PSMA undergoes the clathrin-mediated uptake, microtubule-mediated transport, and localization in the

perinuclear recycling compartment (167) independent of the nanoparticles. In addition, the partial localization of QDs in the PNRC of PSMA non-expressing PC3-flu cells further indicates that QD trafficking to the PNRC may occur independently of the PSMA. PC3 (Figure 3.7d. i) and PC3-flu (Figure 3.7d. ii) cells did not show staining for the anti-PSMA antibody, which is consistent with the lack of receptor expression in these cells.

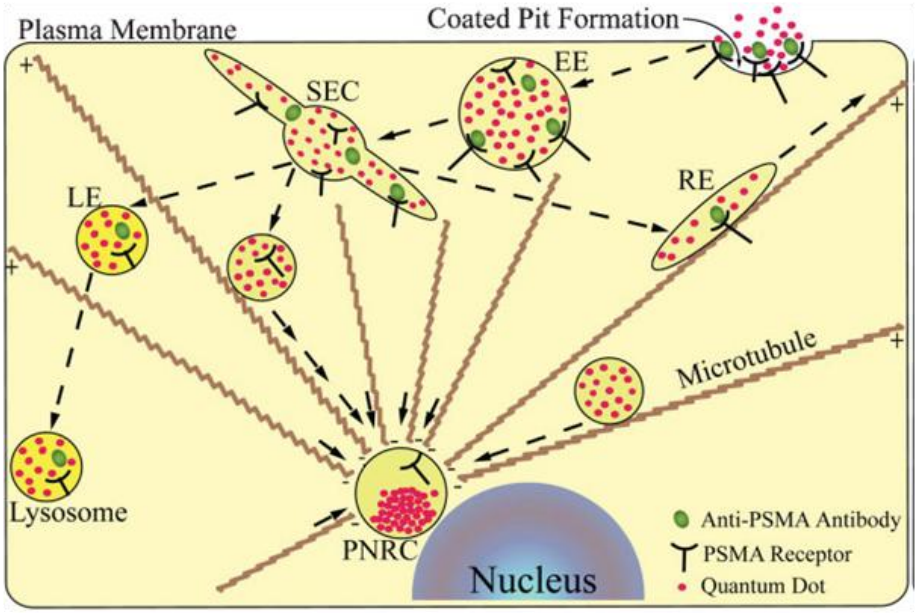

Figure 3.9. Schematic of uptake, sorting, trafficking, and intracellular localization of QDs in cancer cells. Following clathrin-mediated uptake into early endosomes (EE), QDs are trafficked to the sorting endosomal complex (SEC). At this stage, vesicles are either sent back to the cell surface via recycling endosomes (RE), trafficked towards degradative late endosomes (LE) and lysozomes, or are trafficked to the perinuclear recycling compartment (PNRC) near the microtubule organizing center (MTOC).

3.4 Conclusions

In summary, the results in this chapter demonstrate that unconjugated anionic QDs are spontaneously taken up by closely related cancer cells which then sort and traffic these to dramatically different fates (Figure 3.9). Serum

proteins and conjugated molecules such as targeting antibodies or cell penetrating peptides are not necessary for the uptake and trafficking of nanoparticles in these cells. Following internalization via lipid-raft mediated endocytosis, nanoparticles are trafficked in vesicles along microtubules to the sorting endosomal complex in these non-polarized cells. At this stage, nanoparticles are destined for different fates depending on the cell phenotype. Nanoparticles can be either trafficked in vesicles along the default lysozomal degradation pathway as in PC3 cells or they can be sorted and transported along microtubules to the perinuclear recycling compartment (PNRC) as observed in PC3-PSMA cells. These results underscore the importance of investigating intracellular mechanisms for delivered nanoparticles, both as therapeutics and diagnostics. Elucidation of molecular mechanisms underlying cellular decisions that lead to differential sorting of nanoparticles in cancer cells which is anticipated to lead to information that can be exploited to manipulate the delivery of nansocale cargo to predetermined locations inside cells.

Chapter 4

ENHANCEMENT OF POLYMER-MEDIATED TRANSGENE EXPRESSION USING MODULATORS OF INTRACELLULAR TRAFFICKING AND TRANSCRIPTION

4.1 Introduction

Cancer is a molecularly heterogeneous disease that evolves and escapes from all therapeutic agents (168). When most conventional single agent therapies are rarely curative, combination of gene therapy with conventional modalities have shown convincing benefits to cancer patients of phase I and phase II clinical trials (169, 170). However, the poor transfection efficiency, toxicity and lack of targeting of non-viral gene therapy rule out the use of non-viral vectors, including polymers for cancer gene therapy. This chapter analyzes the polymer-mediated gene expression levels in two closely related prostate cancer cell lines and proposes to enhance transgene expression by altering intracellular trafficking and transcription regulation using histone deacetylase (HDAC) inhibitors (HDACi), a new class of chemotherapeutic drugs.

Histone deacetylase (HDAC) enzymes primarily target the histone proteins wrapped around condensed chromosomes inside the nucleus (87). They are involved in cell cycle regulation, transcriptional repressor, cell migration, protein folding, mis-folded protein degradation and several important biological processes (82, 90). In many cancer cells including prostate cancer, HDAC levels are elevated resulting in increased proliferation of cancer cells, tight binding of histones around DNA and transcription inhibition (88). Non-histone proteins like

several transcription factors (p53, E2F, sp1, TFIIB, TFIIF etc.) (88, 171, 172) and non-nuclear proteins (tubulin and HSP90) are also the substrates of HDAC (88). The cytoplasmic HDAC, histone deacetylase 6 (HDAC6) is associated with dynein motor proteins of microtubules and plays an important role in the cytoplasmic transport (173, 174).

Inhibition of HDAC enzymes using HDACi cause accumulation of acetylated histones, increase cytoplasmic movement, activate transcription of selected genes and induce apoptosis (173, 175-178). Therefore, we hypothesize that use of HDACi enhance transgene expression by altering cytoplasmic transport of polyplexes and regulating transcription of transgene, and thus overcome the low efficacies typically associated with polymer-mediated gene delivery. We propose the use of HDAC6 selective inhibitor, tubacin (179) and a pan-HDACi, trichostatin-A to enhance the efficacy of polymer-mediated transgene expression.

4.2 Materials and Methods

4.2.1.Cell Culture

PC3 human prostate cancer cells were obtained from the American Type Culture Collection (ATCC, VA). The PC3-PSMA cell line (113), derived by transducing PC3 cells for stable expression of the Prostate Specific Membrane Antigen (PSMA) receptor, was a generous gift from Dr. Michel Sadelain (Memorial Sloan Kettering Cancer Center, New York, NY). Cells were cultured in RPMI 1640 medium (HyClone®, UT) containing 10% heat-inactivated fetal

bovine serum (FBS; HyClone®, UT) and 1% antibiotics (100units /mL penicillin and 100µg/mL streptomycin; HyClone®, UT).

4.2.2 Transgene Expression in PC3 and PC3-PSMA Cells

Transfection of PC3 and PC3-PSMA cells using polyplexes of pGL3 control vector (Promega Corp., Madison, WI) and 1,4 C-1,4 Bis or pEI-25 (25kDa polyethyleneimine) polymers, were carried out as described previously (180) . The 1,4 C-1,4 Bis polymer was synthesized from the addition polymerization of 1,4-cyclohexanedimethanol diglycidyl ether and 1,4-bis(3-aminopropyl) piperazine) monomers (180) . Cells were seeded at a density of 50,000cells/well in 500µl growth medium (RPMI-1640 medium with 10% FBS) in a 24-well plate and allowed to attach overnight. Polyplexes were prepared by incubating different amounts of polymers and 200ng pGL3 pDNA for 20min at room temperature (approximately 22-25°C) resulting in polymer:pDNA polyplex weight ratios of 1:1, 5:1, 10:1, 20:1, and 25:1. Cells were treated with polyplexes in antibiotics-containing RPMI-1640 medium for 6h, following which the medium was replaced with fresh serum-containing medium. Luciferase protein expression (relative light units or RLU) was determined using a plate reader (Bio-Tek Synergy 2) using the luciferase activity assay (Promega) 48h after transfection. The protein content in each well was determined using the Pierce® BCA Protein Assay Kit (Pierce Biotechnology, Rockford, IL). Transgene expression in PC3 and PC3-PSMA cells was calculated as RLU per milligram (mg) protein (RLU/mg). Cytotoxicity of the polyplexes was determined by measuring cell viability using MTT assay (ATCC, Manassas, VA) at a wavelength of 570nm using the Bio-Tek plate reader (180) .

4.2.3 Characterization of Perinuclear Compartments

Characteristic aggresomal proteins, heat shock protein 70 (HSP 70), ubiquitin (Ub) and vimentin (Vim), were visualized in both PC3 and PC3-PSMA cells by immunofluorescence staining using anti-HSP70 rabbit mAb (Cell Signaling, Beverly, MA), anti-ubiquitin mouse mAb (Cell signaling, Beverly, MA) and anti-vimentin mouse mAb (Millipore Corporation, Temecula, CA), respectively. Co-localization of these proteins with Quantum Dots (QDs) was visualized using confocal microscopy. FITC conjugated goat anti-rabbit and goat anti-mouse secondary antibodies were obtained from the Millipore. PC3 and PC3-PSMA cells were grown overnight at a density of 50,000cells/well on glass coverslips (12 mm circle diameter; Ted Pella) placed in 24-well cell culture plates (Corning Inc., NY). Cells were treated with 0.2nM QDs at 37 °C in serum-free medium for 5h, washed three times (3x) with 1X PBS, fixed with 4% paraformaldehyde at room temperature, following which, cells were washed three times with PBS and blocked with 10% FBS containing 1X PBS (PBS/FBS) for 20min. Primary antibodies were diluted in 0.1% (w/v) saponin containing PBS/FBS at concentrations recommended by the vendor. The PBS/FBS solution containing saponin and no primary antibodies were used as controls. Cells were incubated with the primary antibodies for 1h at R.T. and then were then washed 3x for 5min each in PBS/FBS. The fluorophore-conjugated secondary antibodies were added to the cells at 1:100 dilution in 0.1% saponin/PBS/FBS for an additional hour. Nuclei were stained with 4’-6-diamidino- 2-phenylindole (DAPI; Invitrogen) in PBS for 15min at R.T. Finally, the cells were washed again using

PBS/FBS, mounted on slides in fluoro-gel mounting media (Electron Microscopy Sciences, PA), and viewed at 100x/1.4 numerical aperture (NA) oil objective with laser scanning Nikon C1 confocal microscope (Nikon Instruments Inc., Melville, NY). Confocal images were obtained in a z-series with the excitation by Ar laser (488 nm) for FITC-conjugated antibodies, 402 and 445nm lasers for DAPI and QDs respectively. Light emitted at 470, 525 and 655nms were recorded for the DAPI (blue channel), antibodies (green channel) and QDs (red channel), respectively. Images were acquired, stacked in RGB color using ImageJ software and analyzed to determine the intracellular co-localization of QDs and the antibodies. Immunostaining of cells was carried out for at least n=3.

4.2.4 Size and ζ-potential Measurements

Size and zeta (ζ)-potential of polymer:plasmid DNA (pDNA) polyplexes were determined by dynamic light scattering (DLS) using Malvern Zetasizer Nano Series (Malvern Instruments Inc., Westborough, MA). Polyplexes were incubated for 20min at R.T. at a final concentration of 0.4μg/ml pDNA at various polymer:pDNA weight ratios in 1X phosphate buffered saline (PBS:10mM Na_2HPO_4, 140mM NaCl, pH 7.4). The size and ζ -potentials of the polyplexes are reported as the average values ± standard deviation of n=3 measurements.

4.2.5 Intracellular Trafficking of Nanoscale Cargo (Polyplexes and Quantum Dots) in PC3 and PC3-PSMA Cells

Fluorescein labeled *Label*IT® plasmid delivery control DNA (Mirus Bio Corporation, Madison, WI) was employed in order to visualize the intracellular localization of polyplexes. Two thousand nanograms of *Label*IT® pDNA were

complexed with an equivalent amount of the 1,4C-1,4Bis polymer and incubated for 20min at R.T. in order to form polyplexes; higher amounts of the fluorescently labeled plasmid DNA were required in order to visualize localization inside cells. Red-fluorescent quantum dots (655nm QDs, 0.2nM) were added to cells along with polyplexes in order to facilitate co-localization studies as described previously.(94) Following co-incubation with polyplexes and QDs for 6h, serum-free medium was replaced by serum containing medium for 48h, in order to mimic transfection experiments. Cells were then washed with 1X PBS, mounted in fluoro-gel media (Electron Microscopy Sciences, PA), and analyzed using a laser scanning Nikon C1 confocal microscope (Nikon Instruments Inc., Melville, NY). The *Label*IT® pDNA was excited with a 488nm Ar laser for fluorescein emission at 515nm, while QDs were excited at 445nm and emission was recorded at 655nm. Images were acquired using EZ-C1 FreeViewer analysis software (Gold Version 3.20 build 615, Nikon Corporation) at 100x objective with a z-step of 0.4μm/slice and with dual-channel scanning at 512x512 pixels using PMTs. Images were then stacked in RGB color using Image Processing and Analysis in Java (ImageJ) 1.38X software; the average fluorescence intensity was used in image analyses for visualizing the intracellular co-localization of QDs and fluorescently labeled DNA-polymer polyplexes. Reported images are representative of at least three independent experiments.

4.2.6 Microtubule Involvement in Intracellular Polyplex Transport in PC3-PSMA Cells

PC3-PSMA cells were incubated with or without the microtubule disruption agent nocodazole (40μM; Sigma-Aldrich) for 1h followed by 6h incubation with the polyplexes of *Label*IT pDNA in serum free medium. Live cells were post-stained with 10μg/ml of the nuclear dye 4′,6-diamidino-2-phenylindole (DAPI; Invitrogen) for 1h and washed with 1X PBS. Cells were then fixed in 4% para-formaldehyde for 15min at R.T., washed again with 1X PBS, and mounted in fluoro-gel media. Intracellular localization of the polyplexes was examined as described above.

4.2.7 Role of Histone Deacetylase Inhibitors (HDACi) on Intracellular Trafficking of Nanoscale Cargo

Tubacin,(179, 181) a known inhibitor of HDAC6, a cytoplasmic histone deacetylase, and its inactive analog, niltubacin (179, 181) were gifts from Professor Stuart Schreiber at the Broad Institute in Boston, MA. PC3 and PC3-PSMA cells (50,000/well) were co-incubated with QD655 (Invitrogen) and varying concentrations of tubacin (0-6μM) for 48h at 37 ˚C in order to investigate the effects of tubacin on trafficking of nanoscale cargo. PC3-PSMA cells were also incubated with QDs in presence of 4μM niltubacin which was used as a negative control. QDs were used in the trafficking experiments due to the ease of imaging with these nanoparticles. Following incubation, cell nuclei were stained with DAPI for 1h and cells were washed with 1X PBS. Intracellular localization and redistribution of QDs in the perinuclear region were visualized at 48h using

Zeiss AxioObserver D1 inverted microscope (Carl Zeiss MicroImaging Inc., Germany). Phase contrast images of the cells and the corresponding fluorescence images were captured with an AxioCamMR3 camera (Zeiss Inc.) connected to the microscope with a LD Plan-Neofluor 40X/0.6 (N.A.) objective and exported in TIFF format using AxioVision software (Zeiss Inc.).

PC3-PSMA cells (50,000 /well) were incubated with 2000ng of *Label*IT® pDNA polyplexes using 1,4C-1,4 bis polymer:pDNA for 48h in presence or absence of 4µM tubacin or niltubacin. Cell nuclei were stained with 10µg/ml DAPI for 1h. The cells were then washed, mounted and imaged using confocal microscopy as described previously. Differential interference contrast (DIC) images were captured concurrently using a transmitted light detector.

Quantitative analysis of confocal microscopy images was carried out in order to calculate the percentage of total cell area occupied by QDs and polyplexes in presence or absence of tubacin and niltubacin using the ImageJ software. The tracing tool in ImageJ was used to map a) cellular boundary from phase contrast and DIC images and b) the endocytosed QDs and polyplexes from the fluorescence images. The pixel areas and intensities of the mapped regions were determined, and percentage of total cell area occupied by the QDs and polyplexes was calculated.

4.2.8 Enhancement of Polymer-mediated Transgene Expression using Histone Deacetylase Inhibitors (HDACi)

PC3 and PC3-PSMA cells were co-incubated with 10:1 and 25:1 weight ratios of 1,4C-1,4Bis polymer and pGL3 pDNA polyplexes and different doses of

the HDAC6 inhibitor tubacin (0-6μM) or niltubacin as described in the previous section. Luciferase protein expression in presence of tubacin and niltubacin was determined (RLU/mg) and compared with protein expression in case of cells treated with pGL3 plasmid alone, polymers alone and vehicle (DMSO alone). Transgene expression was reported as fold increase in RLU/mg relative to cells treated with the polyplex alone but not with tubacin or niltubacin.

PC3 and PC3-PSMA cells were treated with polyplexes in the presence and absence of different concentrations (0-1μM) of trichostatin A (TSA; Sigma) a class I and class II HDAC inhibitor. Following incubation with 10:1 and 25:1 polyplex ratios for 48h in presence of TSA, cells were trypsinized, re-suspended in medium and luciferase expression was determined as described previously. Transgene expression was reported as fold increase in RLU/mg relative to cells treated with polyplexes but not with TSA.

4.2.9 Statistical Analyses

Values are expressed as the mean ± one standard deviation (S.D.). All experiments were carried out at least in triplicate. The significance of the difference between the control and each experimental test condition was analyzed by two-tailed, paired Student's t-test.

4.3 Results and Discussion

4.3.1 Differential Intracellular Trafficking of Polyplexes and Transgene Expression in Closely Related Prostate Cancer Cells

Previous studies on the parallel synthesis and screening of a library of cationic polymers resulted in the identification of a polymer, 1,4C-1,4Bis, which

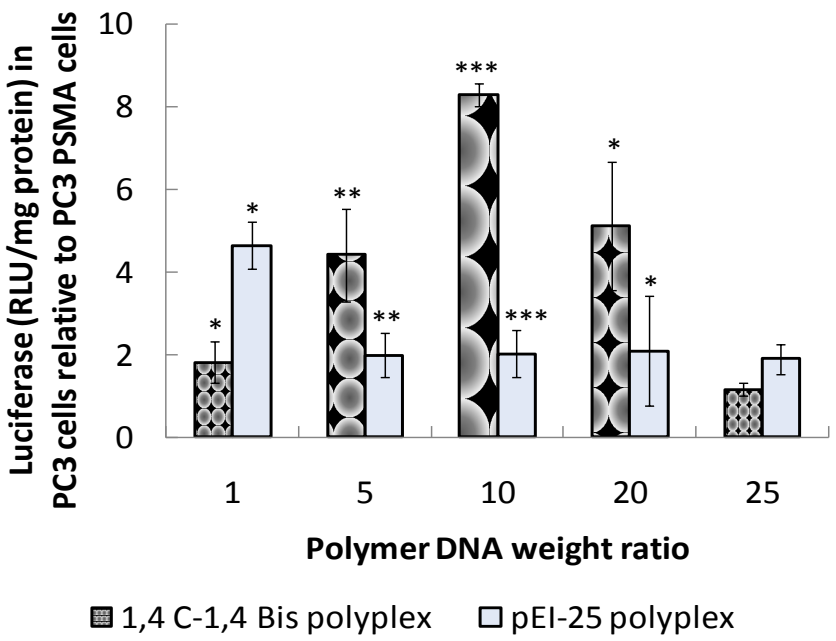

Figures 4.1. Relative transgene expression of luciferase protein encoded by pGL3 DNA vector in PC3 cells compared to those for PC3-PSMA cells. Cells (50,000/well) were transfected using polyplexes of 200ng pGL3 DNA and 1,4C-1,4Bis and pEI-25 polymers at varying polymer:DNA weight ratios of 1:1, 5:1, 10:1, 20:1 and 25:1. Transfection was carried out in serum-free medium (RPMI 1640 medium+1% Penicillin-Streptomycin) for 6h followed by 48h incubation in serum-containing growth medium. Normalized luciferase expressions were found to be higher in PC3 cells than that of PC3-PSMA cells. Luciferase activity was measured as relative RLU/mg protein using means ± standard deviation (n=6). Statistical significance of *, ** and *** indicated $p<0.05$, 0.02 and 0.005 respectively between the two cell lines using two-tailed, paired Student's t-test.

demonstrated significantly higher transgene expression compared to pEI-25 (180). Figure 4.1 compares luciferase expression in the two human prostate cancer cell lines, PC3 and PC3-PSMA, using polymer:pGL3 control vector (pDNA) weight ratios ranging from 1:1 to 25:1. Luciferase expression (RLU/mg) was consistently higher in PC3 cells compared to PC3-PSMA cells at equivalent polymer:pDNA weight ratios for transfections using the 1,4C-1,4Bis polymer. Polyplexes based on pEI-25 did not demonstrate significant differences in luciferase expression between the two cell lines; only up to two-fold higher transfection of PC3 cells over PC3-PSMA cells was observed for most polymer:DNA weight ratios

investigated. Highest transgene expression levels were obtained for a polymer:pDNA weight ratio of 10:1 in both cell lines (Table 4.1). Transgene efficacy correlates with size of the polyplexes; polyplexes formed at 10:1 ratio (150-200 nm) are well within the limit. However, use of 25:1 ratio resulted in larger polyplexes ranging from 240-260 nm which possibly decreased uptake efficiency and subsequent transgene expression at these ratios. The 1,4C-1,4Bis polymer was chosen for all subsequent analyses due to a combination of higher transgene expression and lower cytotoxicity compared to pEI-25 (Table 4.1).

Table 4.1. Absolute Light Units per milligram proteins (RLU/mg) as measured by the luciferase protein expression

Polymer: pDNA weight ratio	PC3-PSMA cells		PC3 cells	
	RLU/mg protein ± S.D. for 1,4C-1,4Bis polymer $\times 10^{-3}$	RLU/mg protein ± S.D. for pEI-25 polymer $\times 10^{-3}$	RLU/mg protein ± S.D. for 1,4C-1,4Bis polymer $\times 10^{-3}$	RLU/mg protein ± S.D. for pEI-25 polymer $\times 10^{-3}$
1	4.5 ± 0.2	0.2 ± 0.07	8.0 ± 0.2	0.8 ±0.03
5	6.5 ± 0.3	0.3 ± 0.03	29.0 ± 0.7	0.7 ± 0.2
10	9.0 ± 0.1	0.7 ± 0.05	69.0 ± 1.1	0.9 ± 0.2
20	5.0 ± 0.3	0.3 ± 0.06	26.0 ± 0.4	0.6 ± 0.4
25	4.4 ± 0.03	0.1 ± 0.08	5.1 ±0.7	0.3 ± 0.02

It has been recently demonstrated that cellular phenotypic differences had a dramatic consequence on the intracellular transport and localization of While QDs localized as punctate structures in vesicles throughout the cytoplasm of PC3 cells, they were trafficked along microtubules primarily to a single perinuclear location, the perinuclear recycling compartment (PNRC), which is close to the microtubule

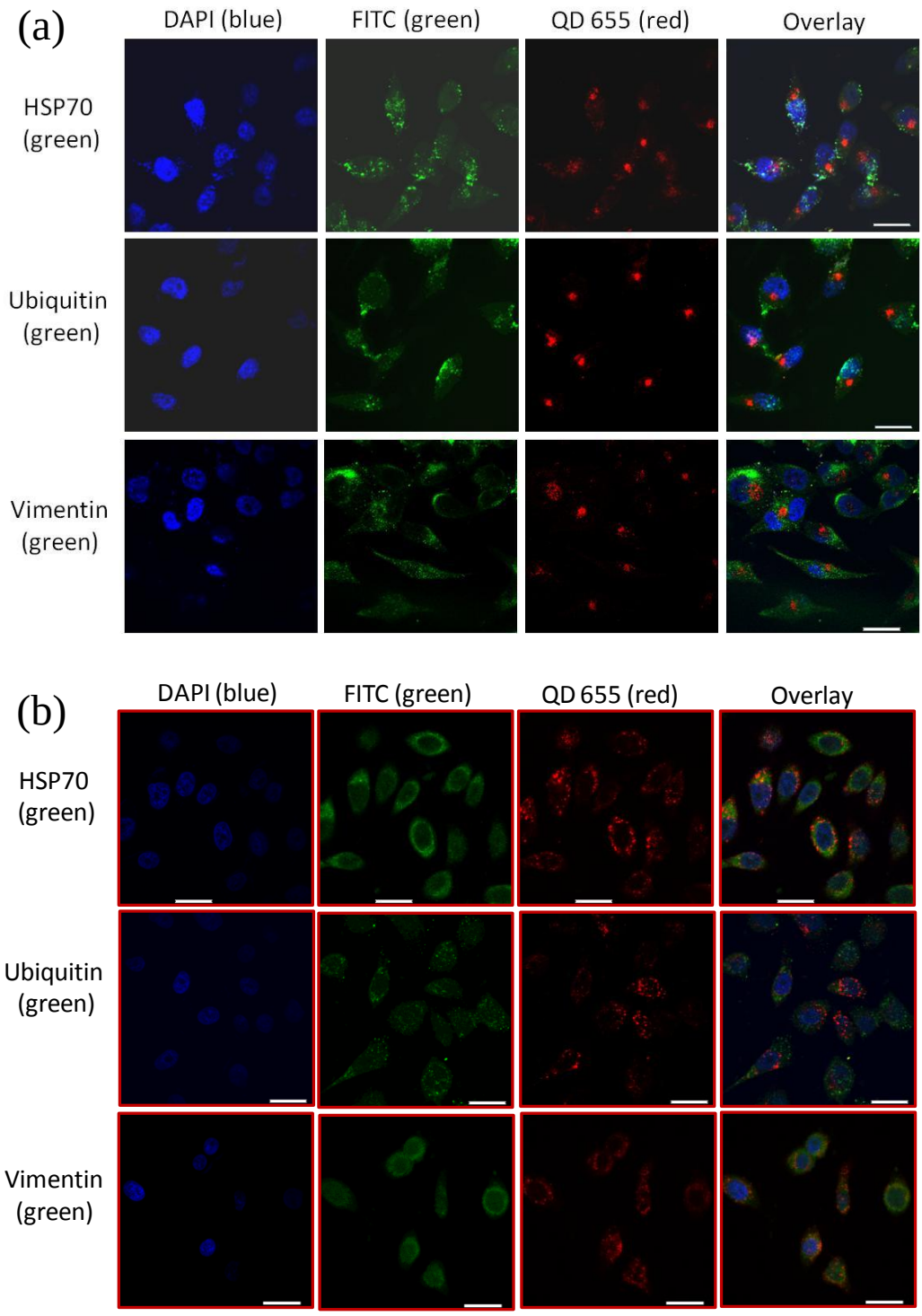

Figure 4.2. Immunofluorescence staining of aggresomal proteins e.g. heat shock protein 70 (HSP70), ubiquitin (Ub) and vimentin (Vim) using FITC-labeled secondary antibodies (green) in (a) PC3-PSMA and (b) PC3 cells. Quantum dots (QDs; red), because of their fluorescence optical properties, were used to visualize the aggregates of nanoparticles at the perinuclear regions of the prostate cancer cells. Cell nuclei were stained with DAPI (blue). It was found that the QDs form a

single cluster at the PNRC/MTOC in distinct clusters close to the nucleus in PC3-PSMA cells but did not co-localize with aggresomal proteins. Scale bar: 100μm.

organizing center (MTOC) in PC3-PSMA cells. Further characterization indicated no presence of aggresome-specific proteins, ubiquitin, HSP70 or vimentin (182-184) at the PNRC/MTOC, indicating that this perinuclear compartment was most likely not an aggresome (Figure 4.2).

An investigation into the intracellular fate of polyplexes indicated high colocalization of QDs (red-fluorescent) and polyplexes (green fluorescent) at the perinuclear location in PC3-PSMA cells as seen from the single yellow-colored spot in Figure 4.3 top row, indicating that the delivered plasmid was largely sequestered as aggregates in the PNRC/MTOC. Diverse cargo including anti-PSMA antibodies,(94) transferrin,(94) 27nm diameter QDs (94) and 150-250nm polyplexes, meet a similar intracellular fate in PC3-PSMA cells, despite the differences in size (polyplex and QD size was determined using DLS; Table 4.2), indicating that PC3-PSMA cells employed this as a default trafficking pathway. Polyplexes, but not QDs, were found around the cell periphery in both cells, presumably due to cationic polymer-cell membrane binding. It was verified that localization of polyplexes at the PNRC/MTOC was dependent on microtubule-based transport; disruption of microtubules using nocodazole led to an arrest of polyplexes at the cell surface (Figure 4.4) which was consistent with our previous observations with QD trafficking (94).

Correlation of intracellular trafficking profiles with transgene expression indicated that sequestration of polyplexes as aggregates in the PNRC/MTOC may

be partly responsible for the lower luciferase expression in PC3-PSMA cells compared to PC3 cells, particularly in case of the 1,4C-1,4Bis polymer. In contrast, polyplexes, like QDs, were seen localized in vesicles throughout the cytoplasm of PC3 cells (Figure 4.2 bottom row). It is possible that distribution of polyplexes in smaller vesicles throughout the cytoplasm, as opposed to aggregation at a single large perinuclear location, can allow for greater endosomal escape, which in turn can enhance transgene expression.

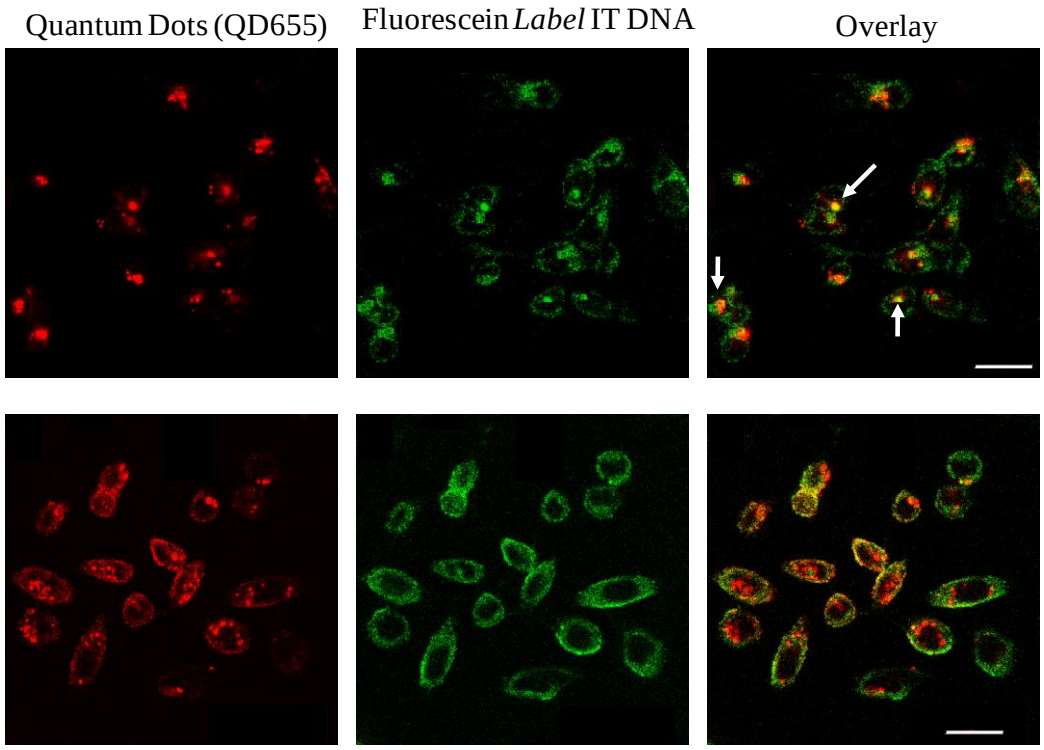

Figure 4.3. Intracellular localization of Quantum Dots (QDs; red) and fluorescein labeled *Label*IT DNA polyplexes using 1,4C-1,4Bis polymer (green) in PC3-PSMA (top row) and PC3 cells (bottom row). Cells were co-incubated with QDs and polyplexes for 6h and visualized after 48h by laser scanning confocal microscopy. The overlay images in the third column show co-localization of the QDs and polyplexes at the PNRC / MTOC in PC3-PSMA cells while they are distributed in vesicles in the cytoplasm of PC3 cells. Scale bar: 20 µm.

Table 4.2. Size and zeta potential measurements of the polyplexes

Polymer:DNA weight ratio	Polyplexes with 1,4C-1,4Bis polymer		Polyplexes with pEI-25 polymer	
	Size (nm)	Zeta Potential (mV)	Size (nm)	Zeta Potential (mV)
10:1	154.5 ± 13	22.8 ± 2.7	190.7 ± 6.3	20.7 ± 2.2
25:1	244.8 ± 17	27 ± 4.3	261.7 ± 9.3	25.7 ± 1.6

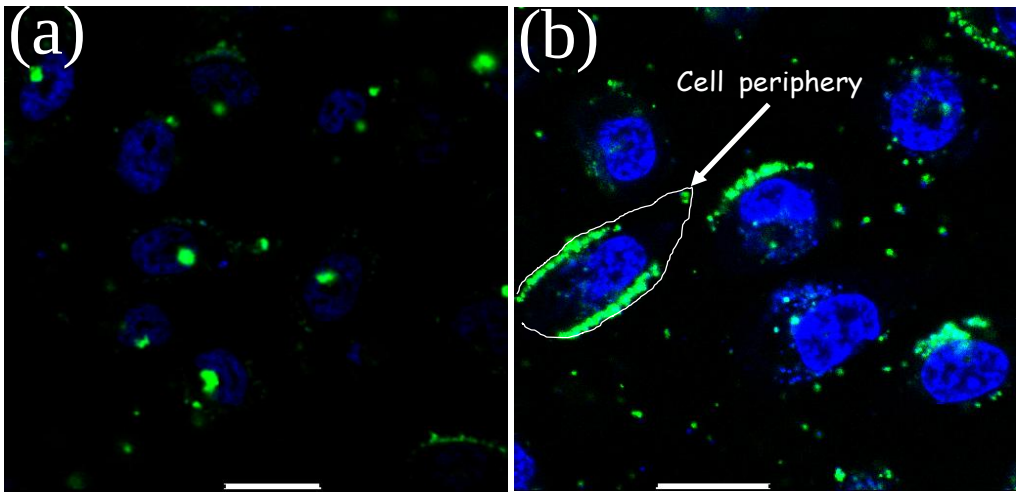

Figure 4.4. Microtubule disruption using the drug, nocodazole reduced perinuclear accumulation of polyplexes in PC3-PSMA cells and arrested them close to the cell periphery. Confocal laser scanning microscopic images of fixed PC3-PSMA cells were captured (a) without or (b) with nocodazole (40μM) treatment for an hour followed by 6h incubation with polyplexes of 1,4C-1,4Bis polymer and fluorescein labeled *Label*It pDNA. Nocodazole treatment dispersed the polyplexes in the perinuclear region in contrast to the untreated control. Scale bar represent 20 μm.

4.3.2 HDAC Inhibitors alter Intracellular Trafficking of Nanoscale Cargo

In light of the hypothesis that polyplex localization in the PNRC near the MTOC correlated with lower transgene expression in PC3-PSMA cells, it was asked if altering the intercellular localization of nanoscale cargo, away from the MTOC in these cells can increase transgene expression levels. HDACs, that are mostly nuclear in their location, cleave acetyl groups from ε-N-acetyl-lysines in target proteins and regulate transcription, angiogenesis, cell motility, and a variety of other functions in cancer cells (82, 88, 171). Cytoplasmic HDACs, in particular

HDAC6, mediate intracellular trafficking of cargo to the MTOC by deacetylating α-tubulin and regulating dynein motor transport on microtubules (Figure 4. 5) (173, 183). Tubacin is a recently discovered small-molecule HDAC6 inhibitor (HDAC6i) which acts as an inhibitor of α-tubulin deacetylation (179). Increased tubulin acetylation (or reduced deacetylation) results in microtubule stabilization and enhances intracellular transport due to greater recruitment of dynein and kinesin motors to microtubules (173).

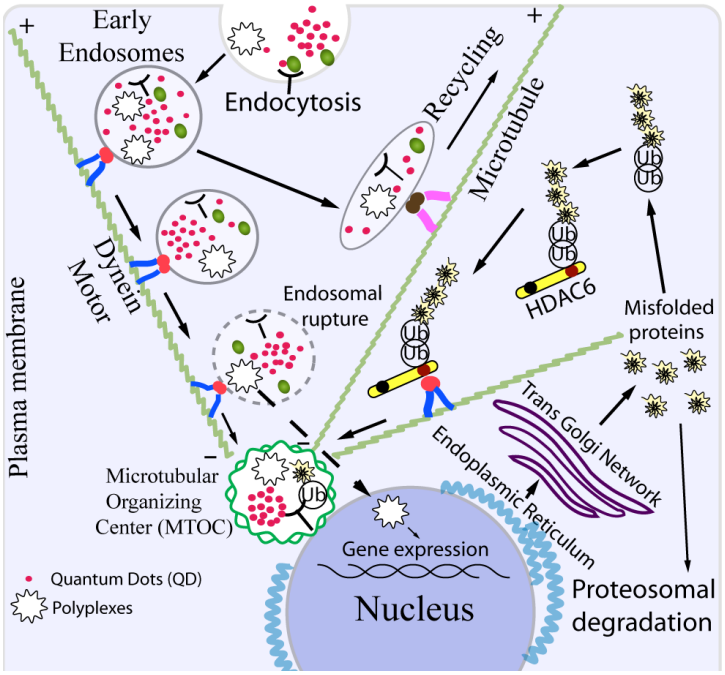

Figure 4.5. Schematic of polyplexes and quantum dot nanoparticle uptake, sorting and localization in cells. Transfection was correlated with aggregations of particles at the perinuclear recycling compartment (PNRC)/ microtubule organizing center (MTOC) in PC3-PSMA cells.

PC3-PSMA cells treated with tubacin concentrations of 0-4μM did not demonstrate any obvious changes in trafficking or localization of internalized QDs (Figure 4.6). However, at tubacin concentrations ≥ 4μM, internalized QDs

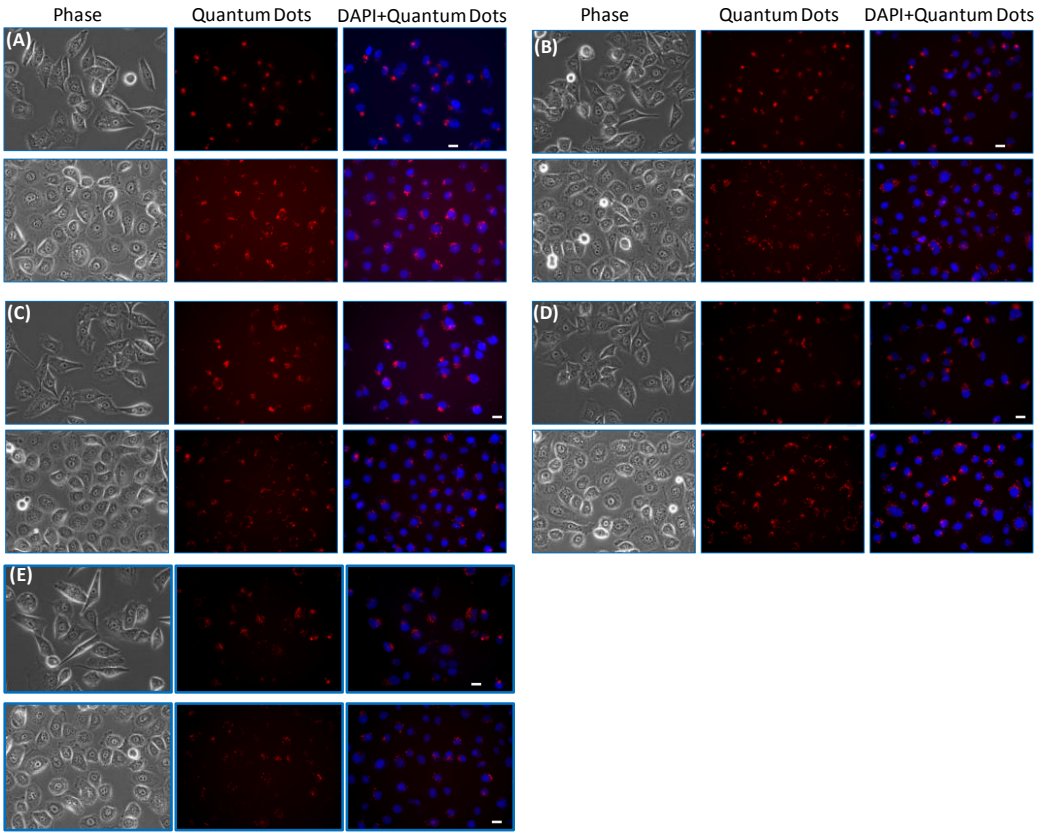

Figure 4.6: Dose-dependent effects of HDAC6i (tubacin) on Quantum Dot (QD) trafficking in PC3-PSMA (top row in each panel) and PC3 (bottom row in each panel) cells. In each panel: left column: phase contrast images; middle: cell nuclei stained with DAPI (blue-fluorescent); and right column: QDs (red-fluorescent). Tubacin concentrations (μM) used were: (A) 0 (untreated cells); (B) 2; (C) 4; (D) 5; and (E) 6. Tubacin concentrations ≥ 4μM caused diffused QD localization from the perinuclear region of the PC3-PSMA cells. Uniform distributions of QDs in the cytoplasm were seen in PC3 cells. Scale bar = 20 μm.

showed a diffused profile around the PNRC, indicating that the nanoscale cargo was delivered over a larger area in the cytoplasm with the possibility that some cargo was delivered outside of the PNRC (Figure 4.7a). This concentration range is consistent with previous reports which indicate that the half-maximum effective concentration (EC_{50}) of tubacin-inhibited tubulin deacetylation was 2.5μM (185). Niltubacin, which lacks HDAC6i activity (179), did not alter (179, 186) QD trafficking behavior under similar conditions, indicating that the altered

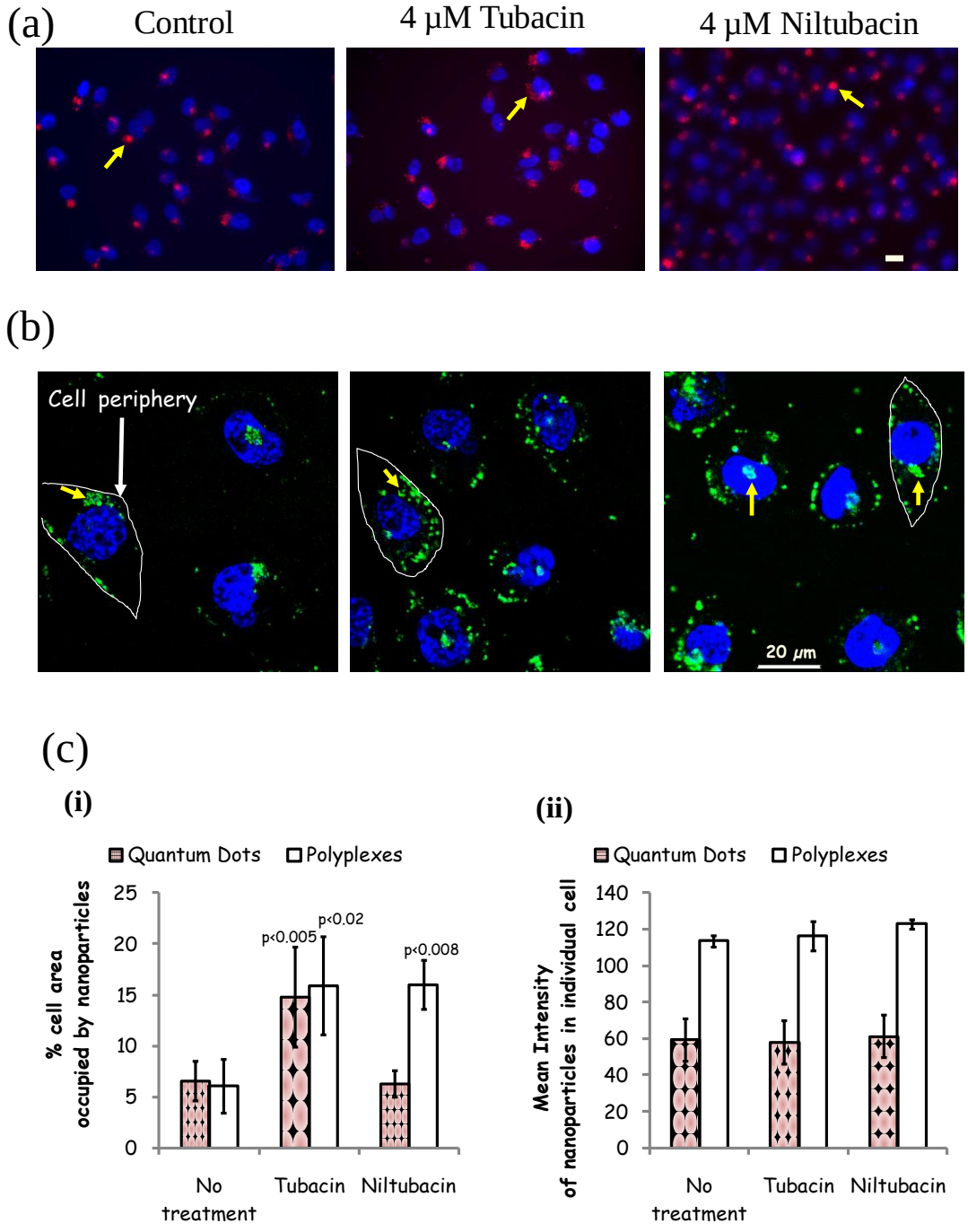

Figure 4.7. Effect of histone deacetylase 6 inhibitor (HDAC6i), tubacin on (a) Quantum Dot (QD) and (b) polyplex trafficking in PC3-PSMA cells. Cells were incubated with QDs or polyplexes of fluorescein labeled *Label*IT pDNA in the absence of tubacin (left; control), in presence of 4µM tubacin (middle) and 4µM niltubacin (right). Cell nuclei were stained with DAPI (blue). Tubacin concentrations ≥ 4µM redistributed the accumulation of QDs and polyplexes from the PNRC/MTOC into the peri-nuclear region in the cells. Scale bar=20µm. (c) Quantification of nanoparticle dispersion in the presence or absence of 4µM tubacin and niltubacin in PC3-PSMA cells. (i) percentage of QD and polyplex in the total cytoplasmic area and (ii) mean intensities of

the nanoparticles were quantified using ImageJ software. At least 15 cells were counted and scored for the analysis. Columns: mean of n=15 cells, error bars: standard deviation.

trafficking depended on HDAC6 inhibition activity (Figure 4.7a). The effect of tubacin on QD trafficking in PC3 cells was not obviously different from untreated cells under the microscopy resolution employed (Figure 4.6).

Remarkable differences were also seen in polyplex trafficking following tubacin treatment in PC3-PSMA cells. Polyplexes by themselves were largely found localized at the PNRC/MTOC or at the cell periphery (Figure 4.7b). Tubacin treatment (4μM), however, completely abolished the sequestration of polyplexes in the PNRC/MTOC; polyplexes were found distributed in vesicles throughout the cytoplasm in these cells, much similar to the intracellular localization profile observed in PC3 cells. On the other hand, polyplexes were largely seen at the cell periphery and at the PNRC/MTOC in cells treated with 4μM niltubacin, indicating that the HDAC6 inhibition activity was necessary for abolishing polyplex transport to the PNRC/MTOC. It is not clear why niltubacin promotes arrest of polyplexes at the cell periphery; it is possible that the molecule possesses hitherto unexplored activity that may be responsible for this behavior. Tubacin concentrations above 6μM were toxic to cells (Figure 4.8) and were therefore not employed.

Quantitative image analyses indicated that the cell surface area covered by QDs was 2-3 fold higher in case of tubacin-treated cells compared to untreated cells and niltubacin treated cells (Figure 4.7c), which indicated the distribution of

the nanoparticles over a larger cytoplasmic area. The average fluorescence intensity remained invariant in all three cases (Figure 4.7c).

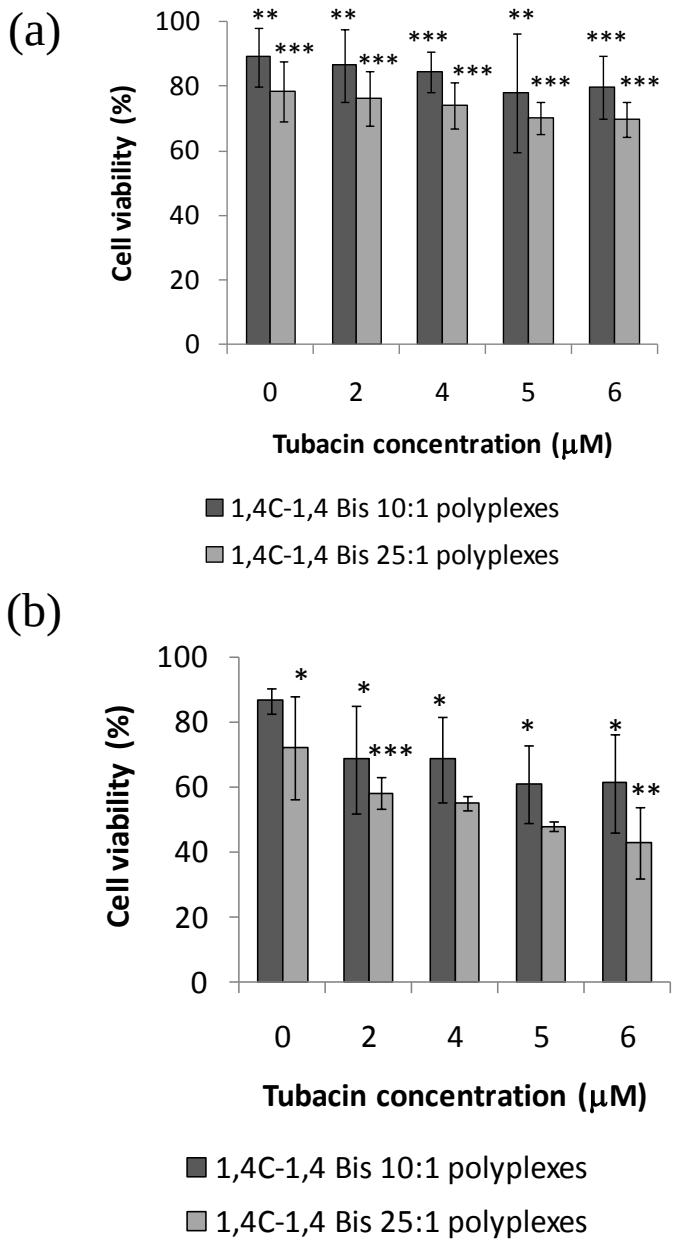

Figure 4.8. Cytotoxicity of tubacin in (a) PC3-PSMA and (b) PC3 transfected cells using MTT cell viability assay. Tubacin doses up to 6μM (48h) did not cause any cell death over and above any cell death caused by the polyplexes themselves. Percentage cell viability was expressed as mean number of viable cells for treated relative to untreated cells. Each point represents a mean ± S.D. (bar) for n = 6 independent experiments. p-values were *<0.05, ** <0.02, and *** < 0.005.

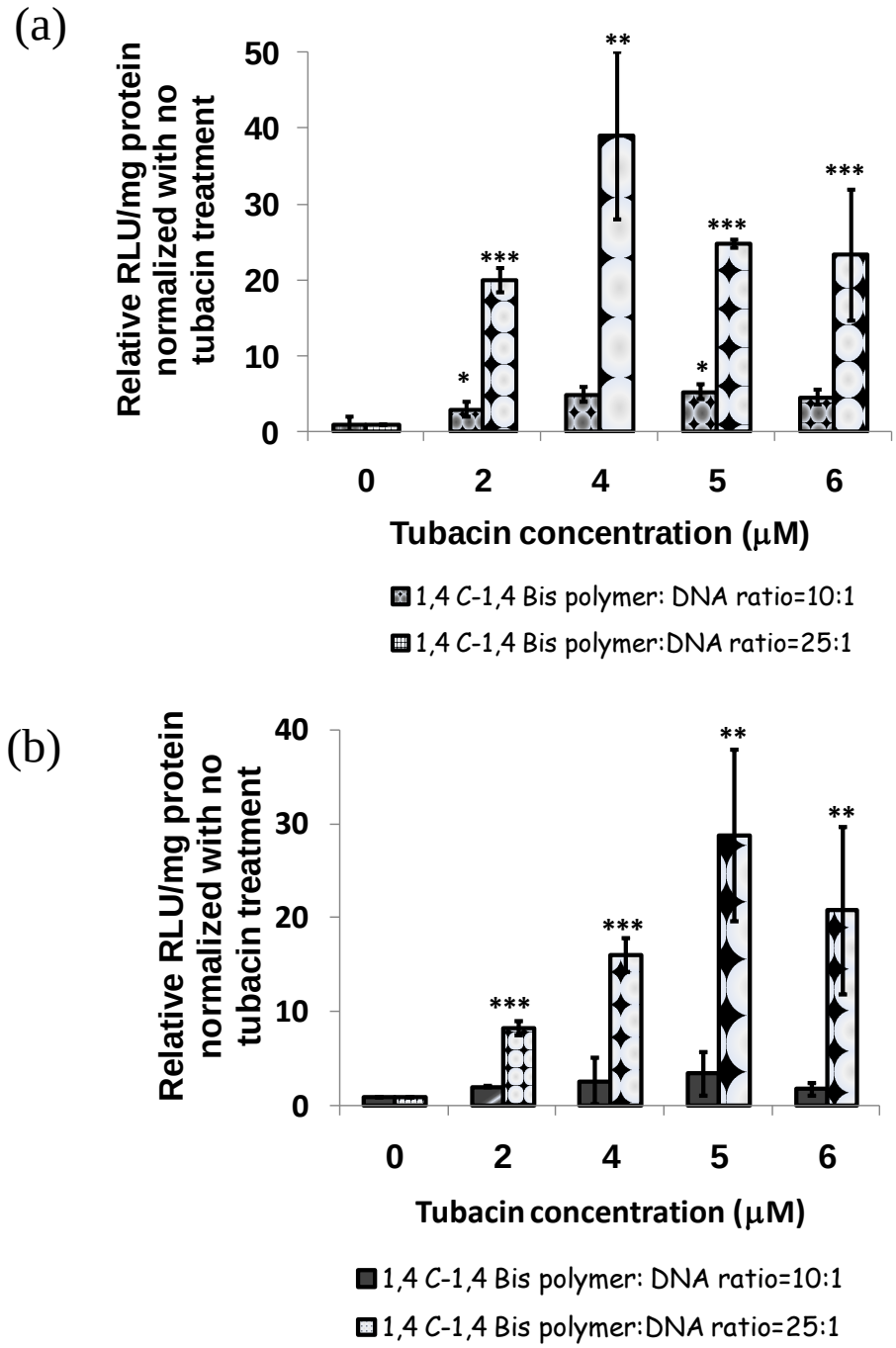

Figure 4.9. Enhancement of transgene expression using histone deacetylase 6 (HDAC6) inhibitor, tubacin in (a) PC3-PSMA & (b) PC3 cells. Cells were transfected with pGL3 DNA encoding for luciferase gene in presence of tubacin for 6h followed by 48h incubation with tubacin, after which luciferase activity and the corresponding protein content in the lysate were measured. The relative luminescence units (RLU) / mg protein ± standard deviation (n= 6) were normalized to the values for cells not treated with tubcain (control). Two-tailed, paired student's t-test between tubacin treated and untreated transfected cells showed $p < 0.05$, 0.02 and 0.005 as indicated by *, ** and *** respectively

Interestingly, both tubacin and niltubacin treatment enhanced the cytoplasmic coverage of polyplexes in PC3-PSMA cells compared to untreated cells; however, tubacin alone was able to abolish polyplex localization at the PNRC/MTOC. The current analysis cannot rule out the intriguing possibility that more nanoscale cargo (QDs or polyplexes) is delivered to the perinuclear region following increased molecular motor-mediated transport as a consequence of tubulin acetylation with tubacin (173, 179).

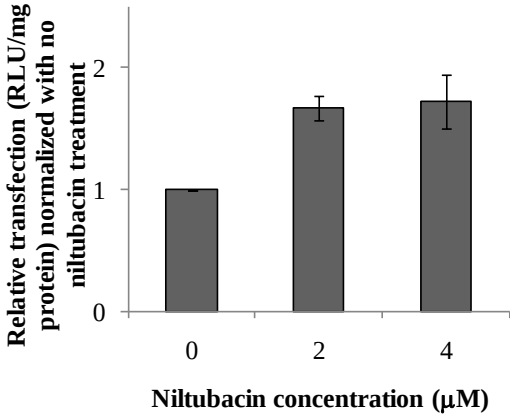

Figure 4.10. Transgene expression was not greatly enhanced by niltubacin treatment. PC3-PSMA cells were co-incubated with polyplexes of 25:1 1,4C-1,4Bis polymer:DNA weight ratio and different concentrations of niltubacin for 6h. The luciferase activity was measured 48h later and compared to that of no niltubacin control cells. Mean luciferase activities ± S.D. were calculated for triplicates.

4.3.3 HDAC Inhibitors enhance Polymer-Mediated Transgene Expression in Cells

PC3-PSMA cells were treated with different concentrations of tubacin (0-6μM) along with 10:1 and 25:1 weight ratios of 1,4C-1,4Bis polymer and pGL3 plasmid-based polyplexes in order to investigate if tubacin-mediated differences in intracellular trafficking also influenced transgene expression. A forty-fold

increase in transfection efficacy in PC3-PSMA cells was observed when polyplexes were employed at 25:1 polymer:pDNA weight ratio along with 4μM tubacin compared to cells not treated with tubacin (Figure 4.9a). Other tubacin concentrations showed up to twenty-fold ($p<0.005$) higher transgene expression in PC3-PSMA cells compared to cells not treated with the HDAC6i. Treatment with similar concentrations of niltubacin resulted in a statistically insignificant 1.5-fold enhancement of transgene expression (Figure 4.10) compared to untreated cells. This increase was negligible compared to that observed with tubacin, and therefore, implicated HDAC6 inhibition and tubulin deacetylation in enhancing transgene expression. Interestingly, only a two-fold enhancement in transgene expression was observed with tubacin when 10:1 polyplex ratio was used, indicating that the tubacin activity was dependent on basal levels of transgene expression, polyplex dose and composition, and possibly, size. Taken together, these results indicate that tubacin concentrations which result in inhibition of tubulin deacetylation and alter nanoparticle trafficking in PC3-PSMA cells, also resulted in high (40-80 fold) increase in transfection efficacies. It is important to point out that 1,4C-1,4Bis polymer demonstrated a forty-fold higher transgene expression than pEI-25 in PC3-PSMA cells at a polyplex ratio of 25:1. This was further enhanced up to 40-80 fold by using tubacin, indicating that transgene expression could be enhanced by 1600-fold in PC3-PSMA cells by using a synergistic combination of more effective polymeric transfection agent (1,4C-1,4Bis) and the HDAC6 inhibitor, tubacin. The efficacy of this combination treatment is significantly higher than what has been traditionally possible with

pEI-25, a standard for polymeric gene delivery. Tubacin treatment (5 µM) resulted in a thirty-fold increase in transfection of PC3 cells compared to cells not treated with the HDAC6i for the 25:1 polyplex ratio. Significant levels of transfection enhancement, approximately 8-,16- and 20-fold, were observed in case of 2, 4, and 6µM tubacin, respectively (Figure 4.9b), similar to what was observed with PC3 cells.

Trichostatin A (TSA), is a class I and II HDAC inhibitor that has both nuclear and cytoplasmic activity, and was also employed in order to determine if the enhancement in transgene expression was specific to tubacin or HDAC6 inhibition alone. As shown in Figure 4.11a, approximately 35-fold increase in luciferase expression was observed in PC3-PSMA cells treated with 250nM TSA and 25:1 polyplex ratio of 1,4C-1,4Bis:pGL3 plasmid, compared to cells treated with in the absence of the HDACi. Enhancement of transfection efficiency in PC3 cells was also dependent on TSA dose (Figure 4.11b); maximum relative luciferase expression in PC3 cells was found with 100nM TSA for 25:1 polyplex ratio. However, TSA treatment led to only up to ten-fold enhancement of transgene expression in PC3 cells. The reasons for the differential enhancement between PC3 and PC3-PSMA cells with TSA are unclear at this point.

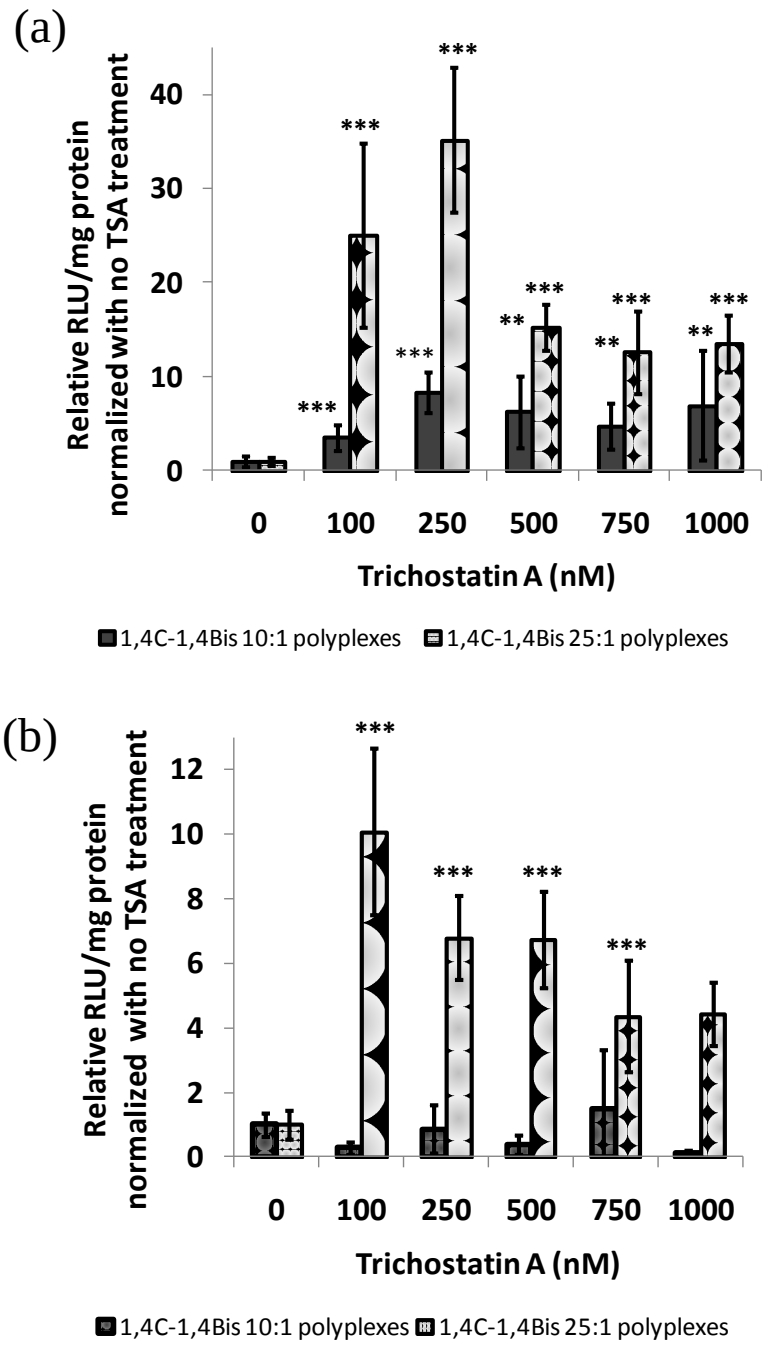

Figure 4.11. Transgene expression of luciferase protein was enhanced by Trichostatin A (TSA), a known cytoplasmic and nuclear histone deacetylase inhibitor in (a) PC3-PSMA and (b) PC3 cells. The relative light units (RLU) per milligram (mg) proteins were normalized in each cell line to that of no TSA treatment. Data is represented as mean values ± one standard deviation of three independent experiments (n=3). TSA increased the luciferase expression in a concentration dependent manner. The highest TSA activity was found at 100 and 250nM in PC3-PSMA and PC3 cells respectively. Asterisks ** and *** indicate p values < 0.02 and 0.005 respectively.

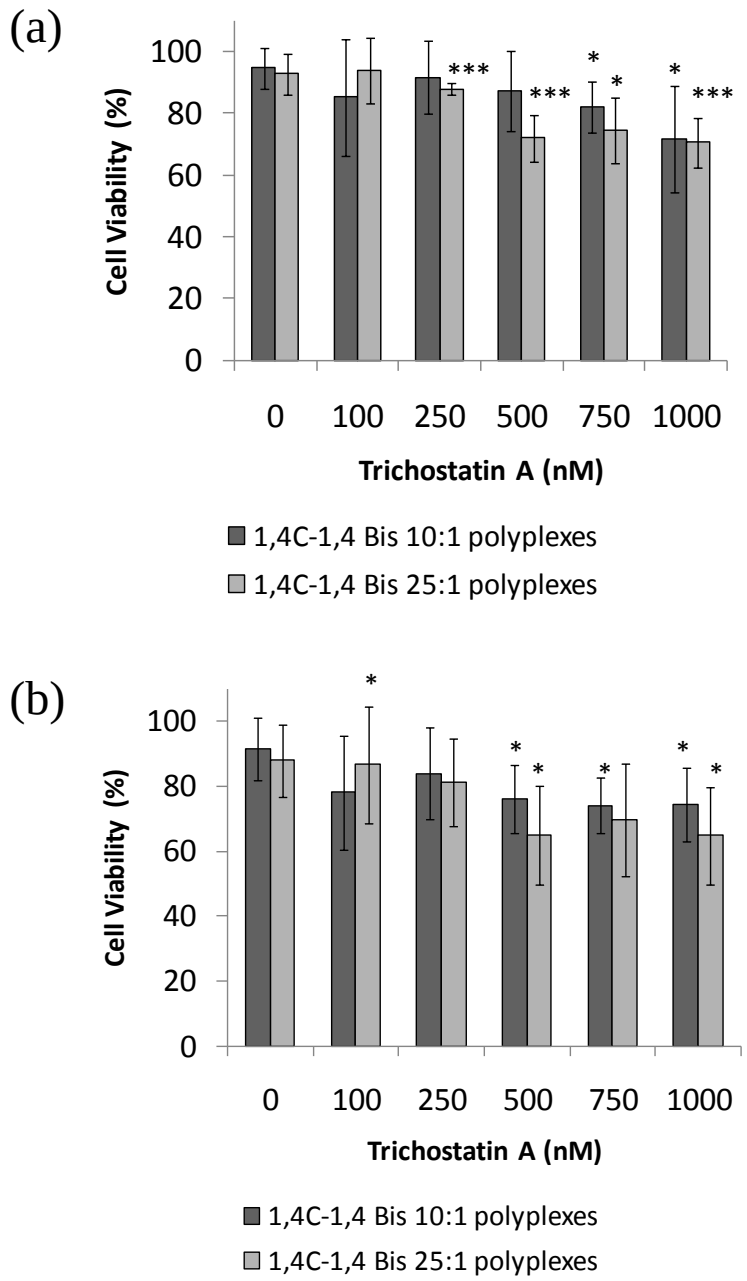

Figure 4.12. Dose dependent toxicity of Trichostatin A (TSA) in (a) PC3-PSMA and (b) PC3 transfected cells using 1,4C-1,4Bis: pGL3 DNA polyplexes. Polymer:pDNA weight ratios of 10:1 and 25:1 were used. Values are the mean ± S.D. of three independent experiments with duplicates. Statistical significance: * $p<0.05$, *** $p< 0.005$ as compared with no TSA treatment.

Co-treatment of TSA and polyplexes resulted in negligible loss of PC3-PSMA cell viability, while PC3 cell viability was found to be between 60-70%;

similar results were seen in case of tubacin (Figures 4.12 (a) and 4.12 (b)). Taken together, the above results indicate that both cytoplasmic and nuclear HDACi, tubacin and TSA were able to enhance transgene expression in the two human prostate cancer cell lines employed in the current investigation. Importantly, not just relative levels but also absolute levels of transgene expression (RLU /mg) were highest with tubacin treatment in both cell types investigated (Table 4.3). The level of enhancement was dependent on the polymer:pDNA ratio, the HDAC inhibitor, and the cell line employed.

Following uptake, nanoscale cargo, including polyplexes, is trafficked along the default degradative lysozomal pathway in most cells. After being escaped from the lysosomes or endosomes, polyplexes must traffic through dense cytoplasm to the nucleus and at some point the plasmid must be accessible to the nuclear machinery for transcription of the delivered transgene. While passive diffusion of plasmid DNA is negligible through the cytoplasm, the current results and those of others demonstrate that cytoplasmic trafficking of polyplexes / pDNA is dependent on microtubules and is mediated by molecular motors (187). Furthermore, only a small fraction of pDNA in the cytoplasm is imported into the nucleus; cytoplasmic proteins that bind to specific sequences on the DNA sequence mediate active nuclear import (188). The distribution and localization of pDNA inside the nucleus also greatly influences transcription and transgene expression.(189) The efficacy of non-viral gene delivery can be greatly enhanced by strategies that enhance both cytoplasmic trafficking and nuclear import and transcription machineries.

Tubacin selectively inhibits HDAC6 and is therefore largely cytoplasmic in its action. It is important to note that the 1,4C-1,4Bis polymer resulted in approximately 40-fold enhancement over pEI-mediated transgene expression. In addition, use of tubacin led to an additional 40-fold increase of transgene expression using the 1,4C-1,4Bis polymer, indicating that a combination of increased polymer efficacy and HDAC6 inhibition using tubacin resulted in approximately 1600-fold improvement over conventionally used pEI-mediated transgene expression.

Tubacin treatment resulted in significant changes in intracellular trafficking of nanoscale cargo in PC3-PSMA cells and also led to increase in transgene expression in these cells. In the absence of tubacin, transgene expression was higher using 10:1 polyplex ratio than 25:1 polyplex ratio in PC3-PSMA cells. Tubacin treatment, however, resulted in highest transgene expression levels in case of the 25:1 polyplex ratio, but did not lead to similar levels of enhancements in case of transfection using 10:1 polyplex ratio (Table 4.3). It is possible that a combined effect of higher polyplex size (approximately 250nm for 25:1 polyplex ratio compared to 150nm for 10:1 polyplex ratio) and the effect of tubacin on polyplex /pDNA trafficking resulted in high transgene expression in this case.

Table 4.3. Transgene expression (RLU/mg) in PC3 and PC3-PSMA cells using different concentrations of (a) tubacin and (b) trichostatin A and 10:1 and 25:1 (w/w) 1,4C-1,4Bis:pGL3 plasmid DNA polyplexes

(a)

Tubacin(μM)	PC3-PSMA cells		PC3 cells	
	RLU/mg protein ± S.D. for 10:1 polyplexes $\times 10^{-4}$	RLU/mg protein ± S.D. for 25:1 polyplexes $\times 10^{-4}$	RLU/mg protein ± S.D. for 10:1 polyplexes $\times 10^{-4}$	RLU/mg protein ± S.D. for 25:1 polyplexes $\times 10^{-4}$
0	0.9 ± 0.13	0.44 ± 0.03	6.9 ± 1.1	0.53 ± 0.03
2	2.7 ± 0.9	9.3 ± 3.3	14.3 ± 2.5	4.7 ± 1.7
4	4.4 ± 1.1	16.72 ± 3.8	17.8 ± 2.2	13.2 ± 3.2
5	5.0 ± 1.3	9.5 ± 2.8	23.8 ± 3.3	14.3 ± 2.4
6	4.7 ±1.3	8.5 ± 1.8	12.6 ± 3.5	11.9 ±1.7

(b)

Trichostatin (TSA) (nM)	PC3-PSMA cells		PC3 cells	
	RLU/mg protein ± S.D. for 10:1 polyplexes $\times 10^{-4}$	RLU/mg protein ± S.D. for 25:1 polyplexes $\times 10^{-4}$	RLU/mg protein ± S.D. for 10:1 polyplexes $\times 10^{-4}$	RLU/mg protein ± S.D. for 25:1 polyplexes $\times 10^{-4}$
0	0.83 ± 0.07	0.45 ± 0.14	6.1 ± 2.6	0.55 ± 0.23
100	2.7 ± 0.81	9.4 ± 3.2	2 ± 0.2	6.1 ± 2.1
250	6.3 ± 2.5	13.6 ± 4.5	5.9 ± 2.2	4.0 ± 1.2
500	5.2 ± 2.2	6.5 ± 2.2	2.0 ± 0.14	3.9 ± 2.1
750	3.7 ±1.2	5.2 ± 1.9	5.7 ± 2.9	2.0 ± 0.8
1000	7.0±3.9	5.7 ± 1.9	1.4 ± 0.83	2.5 ± 0.71

Results in PC3 cells were different in that while tubacin enhanced transgene expression in all cases, obvious differences in pDNA localization were not apparent in these cells. Although, single-molecule level changes cannot be detected using our current methods. Transgene expression remained highest in the

case of 10:1 polyplexes even after tubacin treatment, in contrast to PC3-PSMA cells. These results indicate that uniform distribution of polyplexes throughout the cytoplasm may be required for high basal levels of polymer-mediated transgene expression as seen in PC3 cells. On the other hand, sequestration of polyplexes in a single compartment compromises transfection efficacy as in the case of PC3-PSMA cells leading to low basal levels of transgene expression. Although mediators of intracellular trafficking such as tubacin can enhance transgene expression in both cases, polyplex size, intracellular localization profiles, and corresponding basal levels of transgene expression affect the overall enhancement observed. Similar trends were observed with TSA treatments (Table 4.3).

The HDAC6i activity of tubacin is responsible for enhanced acetylation of microtubules in cells. Enhanced recruitment of dynein and kinesin motor proteins by acetylated microtubules (173, 190) following tubacin treatment can increase the transport of pDNA towards the nucleus and therefore increase transgene expression. It is thought that increased stability of microtubules following acetylation is partly responsible for increased affinity for molecular motors, which increases transport (191). Additionally, faster minus-end transport can also reduce degradation of pDNA in the cytoplasm, which can contribute to increased transgene expression. An intriguing but hitherto unexplored possibility is that tubacin modulates the ‘tug-of-war’ dynamics (192) between both plus-end (kinesin) and minus-end (dynein) on microtubules by activating both molecular motors. Tug-of-war between vesicles containing nanoscale cargo (QDs or polyplexes) due to opposing motor activity may provide enough time for escape

of additional polyplexes or dissociated pDNA into the cytoplasm from endosomal compartments, leading to higher transgene expression. It is possible that some of these processes were visualized in case of PC3-PSMA cells due to the sequestration of polyplexes in a relatively large, micron-sized juxtanuclear location. However, single-molecule studies may be necessary to further elucidate the role of tubacin in intracellular pDNA transport and nuclear uptake in cells.

HDACi promote the relaxation of DNA wrapped around core histones following acetylation of histones and enhance transgene expression by allowing the transcription apparatus to access DNA promoter regions (82, 193, 194). TSA possesses both, class I and II HDAC inhibition activity, and therefore can act in the cytoplasm and nucleus. In the cytoplasm, TSA can inhibit HDAC6 and therefore has similar activity to that described for tubacin. In the nucleus, TSA is known to enhance transcription and transgene expression by acetylating histones. Acetylation of core histones reduces interactions with DNA and is associated with increased transcriptional activation. Recent studies have shown that TSA plays a role in repositioning pDNA towards transcriptionally active sites (e.g. acetylated histones) in the nucleus and therefore enhances transgene expression(189, 195). Other mechanisms, including promoter activation (171), may contribute towards the observed enhancement in transgene expression by HDACi.

4.4 Conclusions

In this work, mediators of intracellular trafficking for enhancing polymer-mediated transgene expression were investigated. The histone deacetylase 6-inhibitor (HDAC6i), tubacin was able to enhance transgene expression in both

PC3 and PC3-PSMA cells, indicating that microtubule stabilization and /or enhanced recruitment of molecular motors to microtubules can enhance the efficacy of polymer-mediated gene delivery. The use of tubacin, which is cytoplasmic in its action, unequivocally implicates microtubule acetylation in enhancing polymer-mediated transgene expression. The use of trichostatin A indicated that HDAC inhibitors with both nuclear and cytoplasmic activity could also be employed as enhancers of transgene expression. A synergistic approach that involves novel materials chemistry (polymer design) along with mediators of intracellular trafficking can therefore result in high transgene expressions using polymers. These approaches can have significant implications for polymer gene delivery in clinical applications, which has traditionally lagged behind viral vectors and other non-viral methods, including lipofection and hydrodynamic injection, due to poorer transgene expression levels and toxicity concerns. Finally, these results with nanoparticles, both quantum dots and polyplexes, indicate that tubacin might be a promising molecule for enhancing the delivery of nanoscale therapeutics and imaging agents to a variety of cells.

Chapter 5

ENHANCEMENT OF POLYMER-MEDIATED TRANSGENE EXPRESSION USING MODULATORS OF CELL-CYCLE PROGRESSION

5.1 Introduction

Gene therapy using non-viral vectors have demonstrated limited clinical translation, primarily due to inefficiency of transgene delivery and expression. Although development of efficient delivery vectors is a critical aspect and still demands improvement, there is a new therapeutic window of combination treatments of gene therapy with chemotherapeutic agents that act as transgene expression inducers. Here we propose delivery of polymer-DNA complexes (polyplexes) in combination with a chemotherapeutic drug that modulates intracellular transport and cell cycle progression. We have found that the inhibitor (VX-680) of a serine-threonine kinase member- known as Aurora kinases, enhanced polyplex localization inside prostate cancer cells, amplified polymer-mediated gene expression, delayed cell-cycle progression and arrested the cells in S and G2-M phases. Disassembled nuclear membrane openings were found in the cells treated with VX-680 alone with polyplex accumulation at the openings indicating their free access inside the nucleus. Combination treatments of polymer-p53 gene delivery with VX-680 suppressed the percentage of live-cell growth by 80% and induced synergistic apoptotic cell death in 60% of the growth inhibited PC3-PSMA cells *in vitro*. This strategy of gene therapy with Aurora kinase inhibitors (AKI) may offer an important direction in non-viral gene therapy of cancer disease.

Despite the emergence of gene therapy in the early 1990s, substantial translation of this therapy from 'bench to bedside' has remained a challenging task. Both, viral and non-viral methods of transgene delivery have been used in clinical trials for cancer, cardiovascular, and monogenic diseases. (9, 10, 196). Cationic polymers are attractive non-viral alternatives to viral vectors, due to favorable properties regarding cost, immunogenicity, size of genetic materials to carry and flexibility in design (104, 197-202). However, the efficacy of cationic polymers is offset by cellular level barriers such as ineffective endosomal escape, cytoplasmic transport, and nuclear entry of delivered DNA. In particular, nuclear entry has been identified as a key rate-limiting factor for efficient polymer-mediated gene transfer. Poor translocation of plasmid DNA (pDNA) or its non-viral complexes (100-200 nm in diameter) through 45nm diameter pores in nuclear membranes limits the efficacy of polymer-mediated transgene delivery (203-206).

A eukaryotic cell duplicates and distributes its genetic material equally to two daughter cells following four distinct phases, G1, S, G2 and M, of a cell cycle. DNA synthesis, replication, and mitotic segregation occur in the S and M phases, respectively. The events are checked and regulated during the G1 and G2 phases, which precede S and M phases, respectively. The nuclear pores dilate during these different stages of the cell cycle. For example, the diameter of nuclear pores are approximately 90 nm during the early G1 phase, and 120-180nm during the late G1 and early S phase in over 99% of cultured HeLa cervical cancer cells (207). In addition, the number of nuclear pore complexes

(NPC) have been shown to increase from 4.57±0.49 to 5.10±0.39 per μm^2 of the nuclear surface during the early G1/S phase and reach 5.43±0.39 NPC per μm^2 in the G2 phase (207). Following these changes in the nuclear membrane, cells, just before entering the M phase, undergo a temporary nuclear envelope breakdown (NEBD) at the transition from G2 to M phase (208). NEBD can facilitate import of exogenous DNA into the nucleus during this stage of mitotic cell division (209). We hypothesized that delivery of pDNA would be most efficient in the S phase of the cell cycle in cancer cells due to the significantly larger pore sizes observed at this stage, compared to the G1 (resting) phase. We further hypothesized that clinically relevant chemotherapeutics can be employed for modulating the cancer cell cycle in order to synergistically enhance transgene delivery and cell death.

Aurora kinases are serine-threonine kinases that regulate centrosome duplication and separation, mitotic spindle pole formation, mitotic spindle assembly, and chromosome alignment and segregation during cytokinesis in the cell cycle (210, 211). Two different kinds of Aurora kinases (Aurora kinase-A and -B) are overexpressed in cancer cells, and contribute to tumor progression due to defects in spindle-assembly checkpoint and chromosomal alignment(210, 212, 213). Inhibition of Aurora kinase-A and -B using chemotherapeutics or siRNA activities overrides the checkpoint-triggered mitotic arrest, arrests cells in the G1/S or G2/M phases, and delays entry to mitosis and cytokinesis (210).

In this study, we report a combination treatment strategy in which polymer-mediated transgene expression is enhanced by arresting or prolonging

the residence of cells in S or G2/M phases. A chemotherapeutic inhibitor of Aurora kinases (AKI), VX-680 was employed to induce the cell cycle arrest. We further demonstrate that a combination treatment of AKI and polymer-mediated p53 gene delivery induce apoptosis in prostate cancer cells *in vitro*.

5.2 Materials and Methods

5.2.1 Cell Culture

The PC3 human prostate cancer cells were purchased from the American Type Culture Collection (ATCC, VA). The PC3-PSMA cell line, a derivative of PC3 cells by stably transducing Prostate Specific Membrane Antigen (PSMA) receptor, was a generous gift from Dr. Michel Sadelain, director of the Center for Cell Engineering, and principal investigator of the Gene Transfer and Somatic Cell Engineering Laboratory, at Memorial Sloan-Kettering Cancer Center, New York, NY (113). Cell lines were grown in RPMI-1640 medium (HyClone®, UT) containing 10% heat-inactivated fetal bovine serum (FBS; HyClone®, UT) and 1% antibiotics (100 units /mL penicillin and 100µg/mL streptomycin; HyClone).

5.2.2 Plasmid DNA and Polyplex Formation

Fluorescein labeled *Label*IT® plasmid delivery control (empty vector) DNA was purchased from Mirus Bio Corporation in Madison, WI. The 4.7kbp reporter vector pEGFP-C1 containing the cytomegalovirus (CMV) promoter driven enhanced green fluorescent protein (EGFP) gene was a generous gift from Dr. Christina Voelkel-Johnson, Assistant Professor of Microbiology and Immunology, Medical University of South Carolina in Charleston, SC. The pCEP4 vector (10.2kbp) control and CMV driven human p53 gene containing

pCEP4p53 DNA were kindly provided by Dr. Blanka Sharma and Professor Vinod Labhasetwar of Department of Biomedical Engineering, Cleveland Clinic in Cleveland, OH (214). The reporter gene containing pDNAs were grown in DH5α *E. coli* cells at 37°C and 200rpm in a shaker incubator (New Brunswick Scientific), and purified between 12-14 h of the growth using the QIAGEN mega DNA purification kit. The DNA concentration and purity were determined by measuring the ratio of absorbance at 260 and 280nm using a Nanodrop 2000 (Thermo Scientific).

The polymer 1,4C-1,4Bis was synthesized by mixing 1:1 molar ratio of 1,4-Cyclohexanedimethanoldiglycidyl ether (1,4C) (Sigma) with 1,4-Bis(3-aminopropyl)-piperazine (1,4Bis) (Sigma) at room temperature (R.T.; 22-25°C) as described previously (180) and dissolved in 1X phosphate buffered saline (PBS; 140mM NaCl) after 16 h of the polymerization reaction (180). A stock solution of (20µg/ml) of 25kDa polyethylene imine (pEI-25; Sigma) was prepared in 1X PBS and stored at R.T. Polyplexes were prepared by adding 10µl of either 1,4C-1,4Bis solution (500µg/ml) or pEI-25 to 200ng DNA at a predetermined optimum polymer:DNA weight ratio of 25:1 or 1:1, respectively (95, 180). Polyplexes were incubated at R.T. for 20min prior to transfection.

5.2.3 Intracellular Localization of Polyplexes

PC3-PSMA cells were seeded as 50,000/well in glass-bottomed 24-well plates (MatTek Corp., Ashland, MA) and transfected using polyplexes of *Label*IT DNA and 1,4C-1,4Bis polymer in presence or absence of VX-680 (a generous gift from Dr. Haiyong Han and Professor Daniel Von Hoff, TGEN, Phoenix, AZ) as

described previously (95). Briefly, two thousand nanograms of the DNA was complexed with 1,4C-1,4Bis polymer at a polymer:DNA weight ratio of 1:1. Polyplexes were added to the cells with or without 100nM VX-680 in serum-free medium for 6 h followed by additional 24 h incubation in serum-containing medium and VX-680. The cells were then washed with 1X PBS, fixed in 4% para-formaldehyde for 20 min at R.T., washed 5X using PBS and then permeabilized using 0.1% Triton X-100 containing PBS for 2 min at R.T. Cell nuclei were stained by incubating the cells using DAPI (10µg/ml; Invitrogen) for 30 min at R.T. The subcellular localization of polyplexes was observed using a Nikon C1 confocal microscope (Nikon Instruments Inc., Melville, NY) (95). Fluorescence intensities per cell were quantified using a Cell Lab Quanta SC MPL flow cytometer and the accompanying Cell Lab Quanta analysis software (Beckman Coulter Inc., Fullerton, CA). Relative fluorescence intensities/cell in the VX-680 treated cells were normalized to those in the untreated cells.

5.2.4 *In Vitro* Transfection

Cells (50,000/well) were plated in 500µl growth medium in Costar 24-well polystyrene plates (Corning) and allowed to adhere overnight. When the cells were 75-90% confluence, the medium was replaced with antibiotics containing serum-free medium followed by the addition of different VX-680 doses (0-10µM) and polyplexes of pEGFP-C1. After 6 h co-incubation of the cells with VX-680 and polyplexes, the medium was replaced with fresh serum-containing medium and VX-680 in which the cells were let to grow for 72 h and then analyzed for EGFP expression. The EGFP expressing cells were imaged

using a Zeiss AxioObserver D1 inverted microscope (Carl Zeiss MicroImaging Inc., Germany) equipped with a 10x/0.3 objective lens and AxioVision software (Zeiss Inc.). To quantify the EGFP expression, cells were washed using 1X PBS, removed from the plates by trypsinization, centrifuged, re-suspended in 250µl of 1X PBS and, assayed using the Cell Lab Quanta flow cytometer. The percentage of EGFP positive cells (EGFP+) were measured for 10,000 cells. The PMT voltage and gain settings were adjusted for untreated control (EGFP non-expressing) cells to exclude any autofluorescence. Gating and analysis were performed using the software. Data presented was obtained from three independent experiments performed in duplicate.

5.2.5 Cell Cycle Arrest

To monitor cell cycle arresting, cells were transfected using EGFP DNA and 1,4C-1,4Bis polymer, and co-incubated with varying VX-680 concentrations of 0-10µM for 72h. The cells were then washed with PBS, trypsinized, centrifuged and resuspended in 120µl of 5% FBS containing PBS (PBS-FBS). Fixation of the cells was carried out by adding 280µl of cold (-20°C) absolute ethanol (Sigma) slowly after which cells were stored overnight at -20°C.
The fixed cells were centrifuged, washed with 0.01% Triton X-100 (Sigma) containing PBS-FBS followed by 2X washing with PBS-FBS, and re-suspended in PBS-FBS containing 50µg/ml propidium iodide (PI) and 200µg/ml RNaseA (Sigma). The cell suspension was incubated at 37°C for 30min and run in the flow cytometer to measure the PI emission at 610nm. Cells in the G0/G1 phase showed a peak at PI intensity of 200, G2/M phase cells showed the peak at 400 and S

phase cells emerged peaks in between these two phases. The histograms of number of cells versus PI intensity were analyzed quantitatively to determine the percentage of cells in each of the G0/G1, S and G2/M phases.

5.2.6 Immunostaining and Confocal Microscopy

To investigate if VX-680 treatment induced NEBD, PC3-PSMA cells were transfected using the polyplexes of *Label*IT DNA and 1,4C-1,4Bis polymer with or without the VX-680 incubation for 24h, washed with 1X PBS, fixed and then permeabilized using 0.1% Triton X-100. Non-specific binding sites of the cells were blocked by immersing the cells in 5% BSA containing PBS for 1h at R.T. following which cells were incubated with mouse anti-lamin A/C antibody (Santa Cruz Biotechnology, Inc.; 1:50 dilution in PBS-FBS) overnight at 4°C. After additional washing using PBS-FBS, the cells were incubated with rhodamine conjugated mouse IgG for 1h, washed 5x for 5min and stained with 10µg/ml of DAPI (Invitrogen) for 30 min. Stained parts of the cells were imaged in a z-series using a laser-scanning Nikon C1 confocal microscope (Nikon Instruments Inc., Melville, NY) and EZ-C1 FreeViewer analysis software (Gold Version 3.20 build 615, Nikon Corporation). DAPI, fluorescein conjugated *label*IT pDNA, and rhodamine labeled lamin were excited using a 402, 488 and 561 laser, respectively and the corresponding emissions were recorded at 450/35, 515/30 and 605/75nm, respectively. The z-stacks of an image were captured at every 0.2µm step using a 60x objective with either 240x or 720x zooming. The stacks of images were imported in Image Processing and Analysis in Java

(ImageJ) 1.38X software where the average intensity of the stacked images was chosen. Imaging was carried out for n=3.

5.2.7 Cell Proliferation and Viability

Cell counts and viability measurements were performed using the standard trypan blue dead cell staining technique and a Countess Automated Cell Counter (Invitrogen) imaging and counting system. PC3-PSMA cells after transfecting using EGFP were trypsinized, collected in culture medium and mixed with 10µl trypan blue stain (Invitrogen) in a 1:1 v/v ratio from which 10µl of the mixture was loaded on a Countess cell counting chamber slide. The cells were imaged and analyzed automatically in the cell counter to obtain the total, live and dead cell concentrations, and cell viability. Percentage inhibition in cell growth was calculated as follows: 100*(total cell concentrations of (untreated control-cells treated with VX-680))/(total cell concentrations of untreated control). Cell doubling time was calculated using the equation: $t_d = (t_2-t_1)*Ln2/(Lnq_2-Lnq_1)$, where $t_1=0$, $t_2=72h$, $q_1=50,000$ cells and q_2=cells at different VX-680 doses.

5.2.8 p53 Gene Delivery and Apoptosis Analysis

The programmed cell death or apoptosis as induced by the combination treatments of p53 gene delivery with VX-680 was determined by annexinV-PI staining of transfected cells. Transfection was carried out in PC3-PSMA cells grown in 24-well plates. Polyplexes of pCEP4 vector and p53 DNA were incubated with the cells in 500µl serum-free medium for 6h in presence or absence of 100nM VX-680. After 72h additional incubation of the cells in serum-containing medium and VX-680, the cells were trypsinized, collected in 1.5ml

microcentrifuge tubes (Costar), centrifuged and washed using 1X PBS. The cells were resuspended in 1X binding buffer containing FITC annexin V (1:100 dilution; Invitrogen) and 50µg/ml PI (Invitrogen) and incubated at 37°C for 30min in dark. The number of viable, early apoptotic, late apoptotic and dead cells were quantified by the Cell Lab Quanta SC MPL flow cytometer (Beckman Coulter), and analyzed for at least 10,000 cells using the Cell Lab Quanta analysis software (Beckman Coulter).

5.2.9 Western Blot Analysis

Following 72h transfection of PC3-PSMA cells using pCEP4 and p53 polyplexes in presence or absence of VX-680, the cells were washed using PBS and lysed using RIPA buffer containing 150mM sodium chloride, 1% IGEPAL® CA-630 (Sigma), 0.1% sodium azide, protease inhibitor cocktail (Boehringer Mannheim), 1mM sodium vanadium oxide (Sigma) and 1mM sodium fluoride (Sigma). The cell lysates were centrifuged to measure the protein concentrations in the supernatant using BCA protein assay kit (Pierce Biotechnology, Rockford, IL) and stored at -80°C until the gel run. Twenty microgram proteins were separated on 4-20% precast gel (Bio-Rad) and transferred to nitrocellulose for an hour at 20V. Membranes were blocked in 5% milk in TBS-0.2%Tween for 1h and incubated overnight with primary antibody in 5% milk containing PBS-Tween at 4°C. The primary antibodies and dilutions used were as follows: monoclonal anti-p53 clone DO-1 (1:1000; Sigma), cytochrome-C (1:1000; Cell Signaling) and caspase-3 (1:1000; Cell Signaling). Following five washes in every 5min using PBS-Tween, the membranes were incubated with HRP-

conjugated anti-mouse (1:1000; Cell Signaling) or anti-rabbit (1:1000; Cell Signaling) for 1h at R.T. The membranes were washed 5x for 5min in PBS-Tween, incubated with Supersignal West Dura Substrate (Pierce; Thermo Scientific) and imaged using the Alpha Innotech Corporation ChemiImager.

5.2.10 Statistical Analyses

All experiments were carried out at least in triplicate. Values were expressed as the mean ± standard deviation (S.D.). The significance of the difference between the control and each experimental test condition was analyzed by two-tailed, paired Student's t-test.

5.3 Results and Discussion

5.3.1 The Aurora kinase inhibitor VX-680 increases cellular uptake of polyplexes and enhances polymer-mediated transgene expression

Fluorescein-conjugated *Label*It pDNA (empty vector) was delivered to PC3-PSMA human prostate cancer cells using a polymer, 1,4C-1,4Bis in presence or absence of an AKI (VX-680). VX-680 is a pan-AKI which is known to inhibit all three Aurora kinases at nanomolar concentrations (215). The polymer was synthesized in our laboratory as described previously (180). In the absence of VX-680, pDNA following trafficking on microtubules (94, 95) accumulated largely at a single location in the perinuclear recycling compartment (PNRC) of PC3-PSMA cells (Figure 5.1(a)) (94, 95). It is likely that sequestration of pDNA at the PNRC, close to the microtubule organizing center (MTOC) decreased the availability of pDNA to enter inside the nucleus and thus resulted in low levels of transgene expression in PC3-PSMA cells (95).

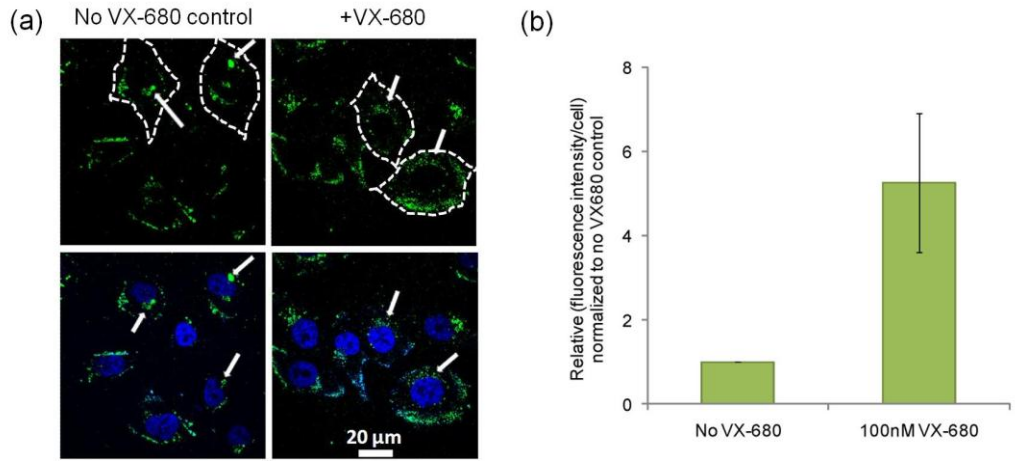

Figure 5.1. Perinuclear localization of polyplexes in PC3-PSMA cells with or without VX-680 treatments. (a) Cells were transfected in presence or absence of 100nM VX-680 using an empty vector control DNA (fluorescein conjugated *Label*It DNA; Mirus) and 1,4-C-1,4Bis polymer that was synthesized in our laboratory [19]. Subcellular localization of the polyplexes was examined at 24h post-transfection using a confocal microscope. The white dotted lines are representing cellular peripheries. The images are representative of three independent experiments. Polyplexes were concentrated in distinct single spots in the untreated control cells while they were spread in the cytoplasm around the nucleus with VX-680 treatments. Scale bar=20 µm. (b) Fluorescence intensities of the fluorescein labeled DNA polyplexes in each cell were quantified (FACS analysis) five times higher after VX-680 treatments than the untreated control cells.

Co-treatment with VX-680 altered intracellular localization of pDNA (Figure 5.1(a); right column) and enhanced the uptake of pDNA by five-fold compared to the cells treated with polyplexes without VX-680 (Figure 5.1(b)). Increased levels of pDNA were observed distributed throughout the cytoplasm following VX-680 treatment. Recent studies have demonstrated the association of Aurora kinase-A with the microtubule organizing center (MTOC) and microtubules (216). Aurora kinase-A also decreases the affinity of dynein-dynactin motor complexes towards microtubules by phosphorylating the microtubule binding domain of dynactin sub-unit $p150^{glued}$ both *in vitro* and *in vivo* (216). These previous studies indicate that inhibition of Aurora kinases using VX-680 can alter the intracellular transport and localization of nanoscale

complexes, including polyplexes by enhancing the recruitment of motor proteins to the microtubule network (94, 95, 191).

Next, the 1,4C-1,4Bis polymer was employed to deliver pDNA expressing enhanced green fluorescent protein (EGFP) in the presence and absence of VX-680 to PC3-PSMA and PC3 cells. Analysis of microscopic images indicated that VX-680 enhanced the number of EGFP expressing cells as well as the fluorescence intensities in both, PC3-PSMA (Figure 5.2(a)) and PC3 cells (Figure 5.3). Polyplex delivery in the absence of VX-680 resulted in only 1-2% EGFP positive (EGFP+) PC3-PSMA cells. However, treatment with 100nM VX-680 resulted in approximately 23% EGFP+ cells, which was a significant increase over cells treated with the polyplexes alone (Figure 5.2(b)). VX-680 concentrations of 250nM and 500nM also enhanced EGFP expression in PC3-PSMA cells to similar levels. Further increase in VX-680 concentrations decreased the percentage of EGFP+ cells presumably because of inhibition of cell growth and toxicity. VX-680 treatment resulted in only moderate enhancement of EGFP expression in PC3 cells from 1.7% to ~9% (Figure 5.2(b)), indicating that the activity of VX-680 was dependent on the cell type (Figure 5.4). VX-680 also enhanced the number of EGFP+ in PC3-PSMA cells from 6% in untreated cells to 20% in 100nM VX-680 treated cells following delivery with 25kDa poly(ethylene imine), indicating that this strategy can be used with different polymers (Figure 5.4). Collectively, these results demonstrate that treatment with VX-680 modulates intracellular distribution of polyplexes and significantly enhances

transgene expression following delivery with different polymers to prostate cancer cells.

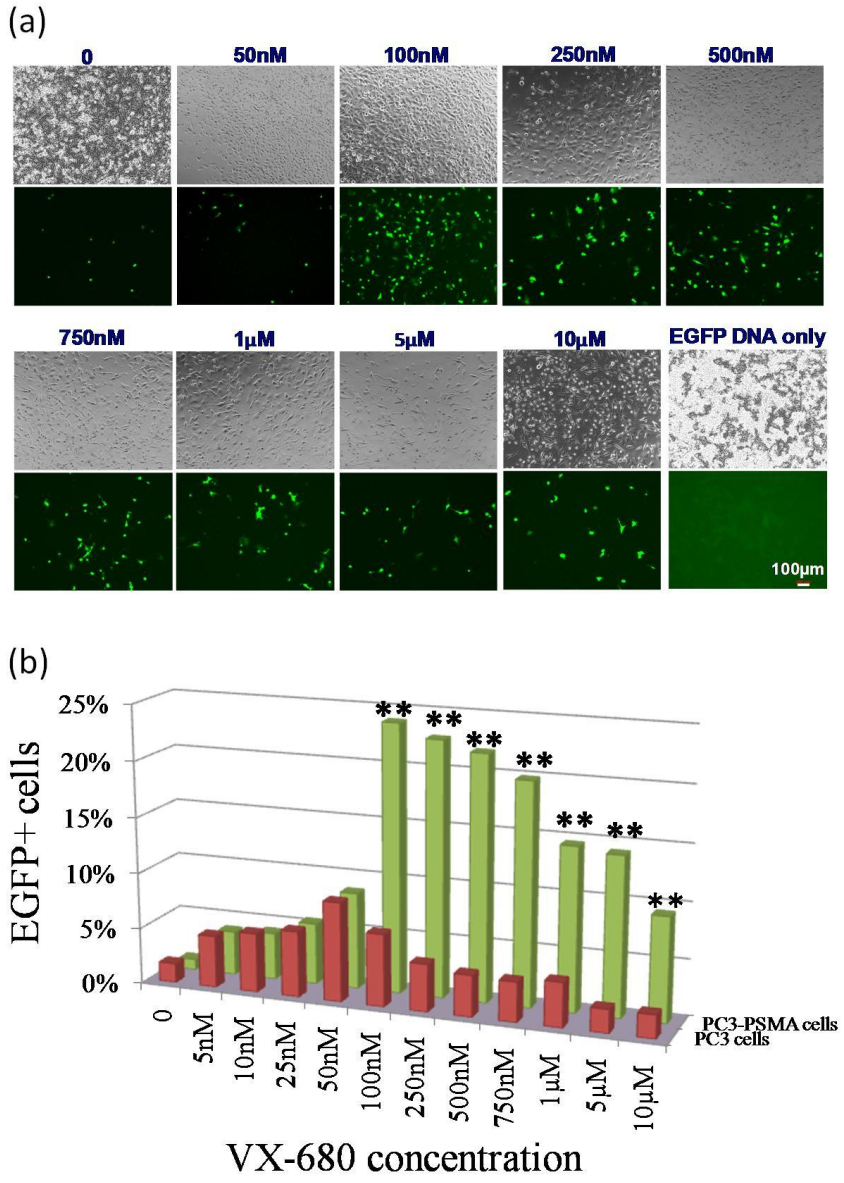

Figure 5.2 Enhanced green fluorescent protein (EGFP) expression in PC3-PSMA cells following treatments with different VX-680 concentrations (0-10µM). The cells were incubated with 1,4C-1,4Bis polymer and EGFP DNA weight ratio of 25:1 for 6h and the transgene expression were observed at 72h after the transfection. EGFP expressing cells were (a) imaged using a fluorescence microscope and (b) counted in 10,000 cells using a flow cytometer. Scale bar=100µm. Data represent mean±standard deviation for n=6. Statistical significance was calculated by two-tailed Student's t-test where p-values were <0.05 and <0.005 for * and **, respectively.

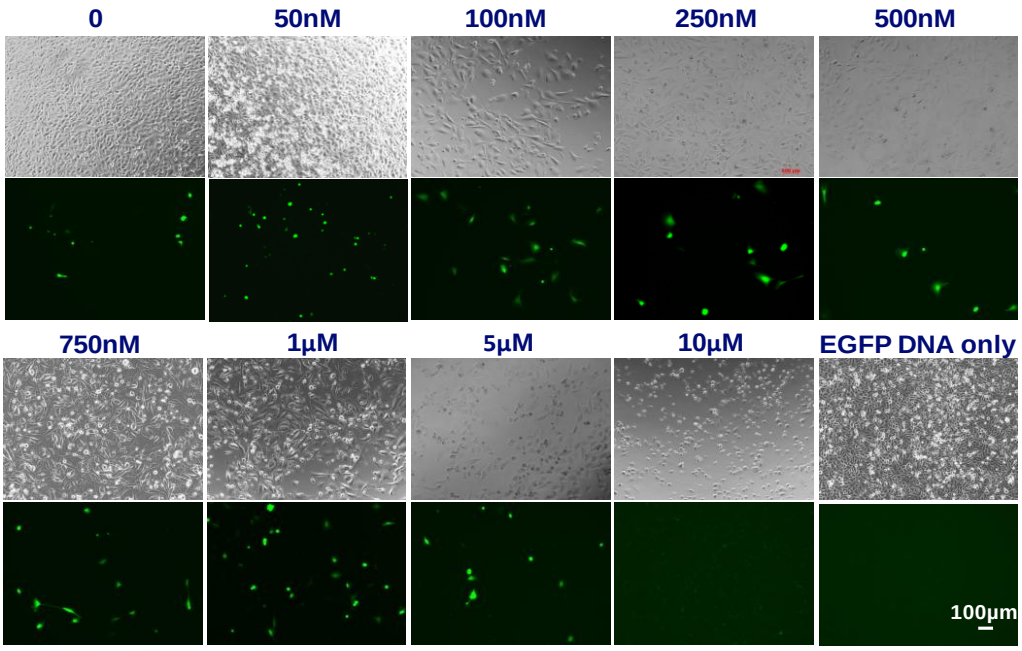

Figure 5.3. The increase in the number of EGFP expressing PC3 prostate cancer cells after VX-680 treatments in a dose-dependent manner. Following 6 h transfection using 1,4C-1,4Bis polymer and EGFP pDNA and 72 h of incubation in presence of VX-680, cells were imaged using the Zeiss Axiovision fluorescence microscope. Images are representative of n=3 experiments.

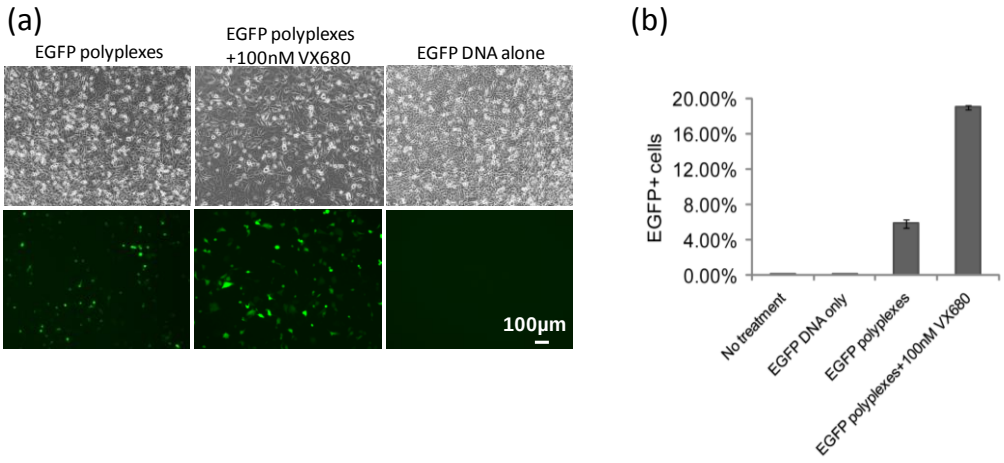

Figure 5.4. VX-680 enhanced EGFP expression in PC3 PSMA cells by transfecting with 25kDa polyethylene imine (pEI-25) polymer standard. Polymer:EGFP DNA weight ratio of 1:1 was used. (a) Fluorescence microscopic images of the cells at 72h after transfection and incubation in presence or absence of 100nM VX-680. (b) Quantitative analysis using FACS showed 5 and 20% EGFP+ cells without and with 100nM VX-680 treatments, respectively.

5.3.2 Aurora kinase inhibition using VX-680 induces cell cycle arrest in S and G2/M phases resulting in enhancement of transgene expression

In the absence of Aurora kinase inhibition, PC3-PSMA cells were found primarily in the G0/G1 (56%) and S (35%) phases of the cell cycle; only 9% cells were in the G2/M phase (Figure 5.5). Polymer-mediated delivery of the EGFP DNA did not result in a significant change in these numbers, indicating that polyplex delivery did not alter cell cycle dynamics. However, 100nM, 250nM and ≥500nM VX-680 resulted in the shift of significant fractions of PC3-PSMA cells (42%, 66%, and 80%, respectively) to the S and G2/M phases of the cell cycle (Figure 5.5(b) and Figure 5.6).

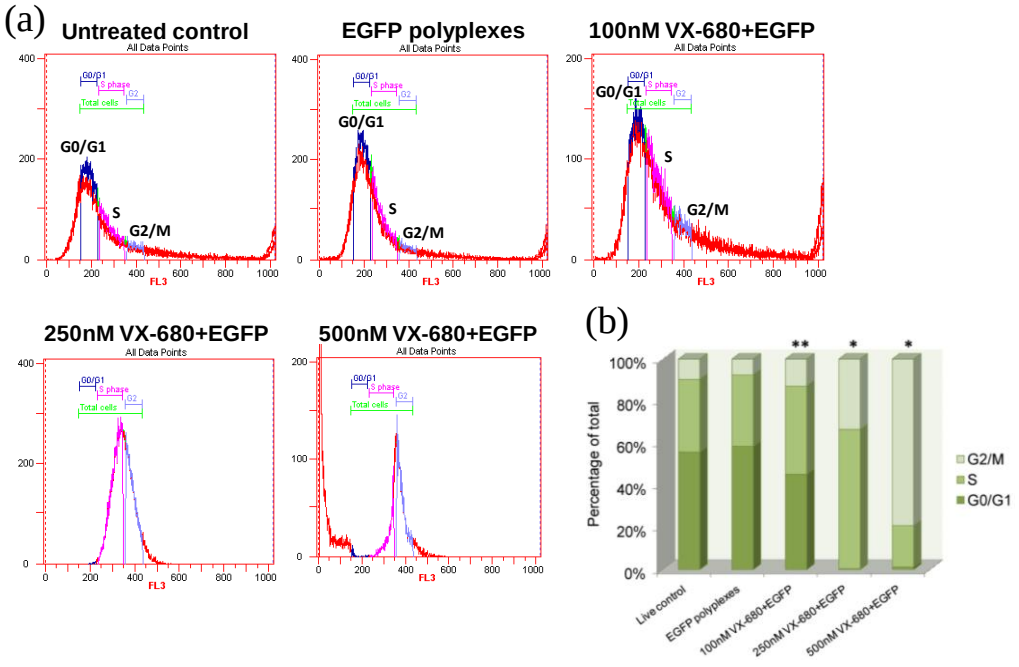

Figure 5.5. VX-680 caused accumulation of PC3-PSMA cells in the S (DNA synthesis) and G2/M (mitotic check point) phases after 72 h incubation. Cells were washed, fixed, permeabilized, stained with propidium iodide (PI) and analyzed by flow cytometry. (a) The PI intensities for each cell cycle phases were expressed and (b) quantified as shown. Correlating the cell cycle data with EGFP expression it was revealed that maximum transgene expression was found when majority of

the cells were arrested in the S and G2/M phases. * and ** indicate p<0.05 and <0.005, respectively.

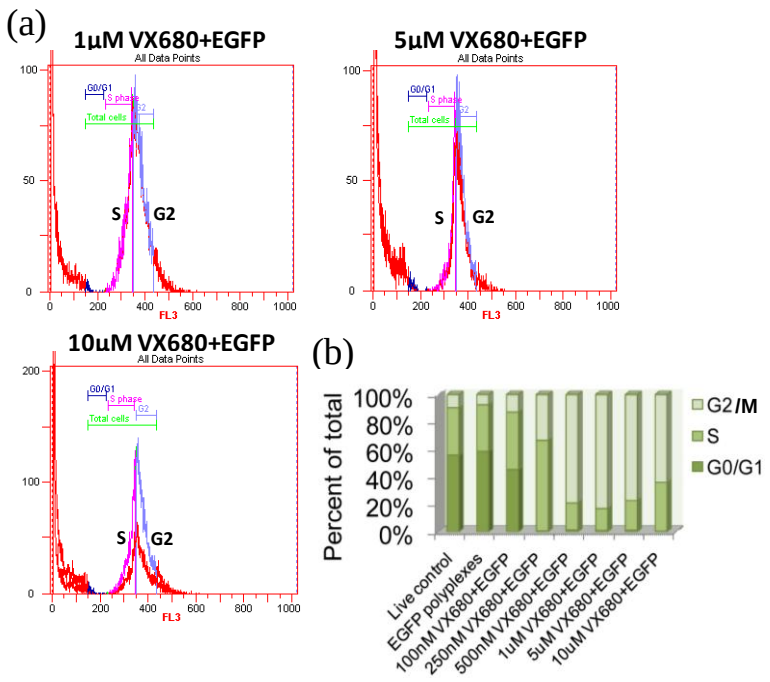

Figure 5.6. (a) Histograms of propidium iodide (PI) fluorescence intensities in EGFP transfected PC3-PSMA cells in presence of VX-680. Most of the cells were arrested in the late S and G2/M phases at high VX-680 concentrations. (b) Quantitative analysis of the histograms using the Cell Lab Quanta Analysis software (Beckman Coulter) represented 80% cells in the G2/M phase at VX-680 concentrations ≥500nM. Data were collected for n=4.

These results indicated that the doses of VX-680 treatments which led to highest increases in transgene expression correlated with arresting of PC3-PSMA cells in the S and G2/M phases. This is consistent with previous reports, which indicate that lipid and polymer-mediated transgene expression was highest in late S or G2/M phases than G1 phase (209, 217, 218). For example, Brunner et al. elutriated K562 leukemia cells in different stages of the cell cycle by centrifugation. Following this fractionation, 200,000 cells in each phase were transfected using Lipofectamine and transferrin (Tf)-conjugated polylysine and

polyethylene imine (pEI) (217). Luciferase expression using polylysine and pEI ranged from $4x10^4$ to $1x10^5$ RLU for cells in the G1 phase, while it was $6x10^6$ RLU for cells in the late S and S/G2 phases. Lipofectamine-mediated luciferase expression was enhanced from $2x10^5$ to $3x10^6$ RLU under similar conditions. Tf-pEI mediated transgene delivery, using 200 mM chloroquine as an enhancer, resulted in GFP expression in only 4% cells in the G1 phase, while 17% cells in the early S-phase demonstrated expression of GFP. Akita et al. cultured HeLa cervical cancer cells in the G1 phase using 2mg/ml hydroxyurea for 18 h and re-cultivated the cells in hydroxyurea free medium for 24 h (218). The cells were collected and transfected at 0, 3, 6, 9 and 12 h after G1 phase release in order to analyze them for cell cycle and transgene expression. LacZ expression was observed in ~15-17% cells at G2/M phase, while minimal gene expression was reported for the cells at G1 phase. In contrast to these previous studies, our approach of using a chemotherapeutic modulator (AKI) does not require cumbersome cell cycle synchronization protocols. Chemotherapeutic modulation using AKI is a facile approach not only for *in vitro* transfection protocols, but also for eventual cancer gene therapy applications for cancer cell ablation.

5.3.3 VX-680 treatments results in disintegrated nuclear envelope

The number, size and density of nuclear pore complexes (NPC), and surface area of nuclear envelope increase continuously from G1 to G2 phase of the cell cycle and eventually double in the G1/S phase transition (208). The nuclear envelope is discontinuous and contains more nuclear pores in the late G1 phase compared to the early G1 phase (208). Lamin is an important component of

nuclear envelope that undergoes significant reorganization during cell cycle (219). Lamins are rapidly disassembled during the G2/M phases with the help of dynein-dynactin motor complexes, lost during mitosis, and reassembled at the end of mitosis (219, 220). The disassembly of the nuclear envelope in the S (86)and G2/M phases can allow exogenous DNA to access the internal nuclear environment for transcription and translation.

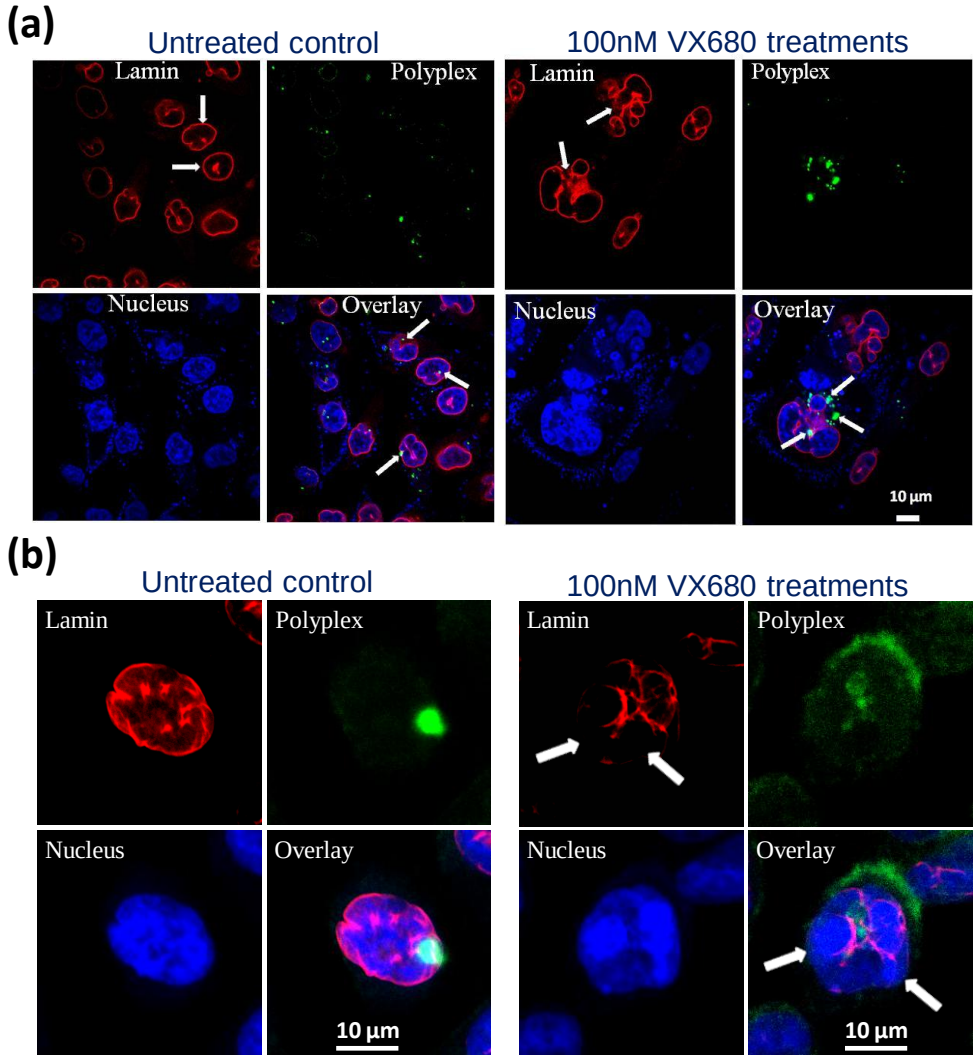

Figure 5.7. Structures of nuclear envelope in polyplex transfected PC3-PSMA cells without or with VX-680 treatments. Nuclear membrane was stained using anti-lamin A/C antibody (red) after

transfecting and incubating the PC3-PSMA cells using *Label*It DNA (Mirus) polyplexes (green). A continuous and intact nuclear membrane was found around the nucleus (blue) in the untreated control cells while disassembly in the nuclear lamins (arrows) were found in the VX-680 treated cells (overlay images). The cells were imaged under a confocal microscope at (a) 240X and (b) 720X zooming. Scale bar=10 µm. Polyplexes were found at the transient local openings in the nuclear envelope suggesting a mechanism for polyplex entry into the nucleus that might help enhancing transgene expression in these cells.

Confocal microscopy analysis showed strong and continuous lamin A/C staining (red) surrounding the cell nuclei (blue) in control cells transfected with the *Label*IT plasmid control vector (Figure 5.7). Consistent with our previous observations (94, 95), polyplexes were sequestered in the PNRC close to the cell nuclei, presumably at the microtubule organizing complex (MTOC). The intact nature of the nuclear membrane is expected since most PC3-PSMA cells were in the G0/G1 phase of the cell cycle (Figure 5.5). VX-680 treatment resulted in breakdown of the nuclear envelope (NEBD) in PC3-PSMA cells. Lamin A/C staining was discontinuous around the nuclear material in VX-680-treated cells and exhibited either weak or undetectable signal in several locations around the genetic materials (Figure 5.7). The discontinuous lamin signal is typically indicative of temporary nuclear envelope disassembly, a characteristic of S and G2/M phases of the cell cycle (220, 221). This is significant since exogenous pDNA, localized at the periphery of the disintegrated nuclear membrane, can access the nuclear space via temporary discontinuities in the nuclear membrane. Taken together, the above results demonstrate that VX-680 treatment induces S and G2/M phase arrest and nuclear membrane breakdown, which allows for higher transcription, translation and transgene expression following polymer-mediated pDNA delivery.

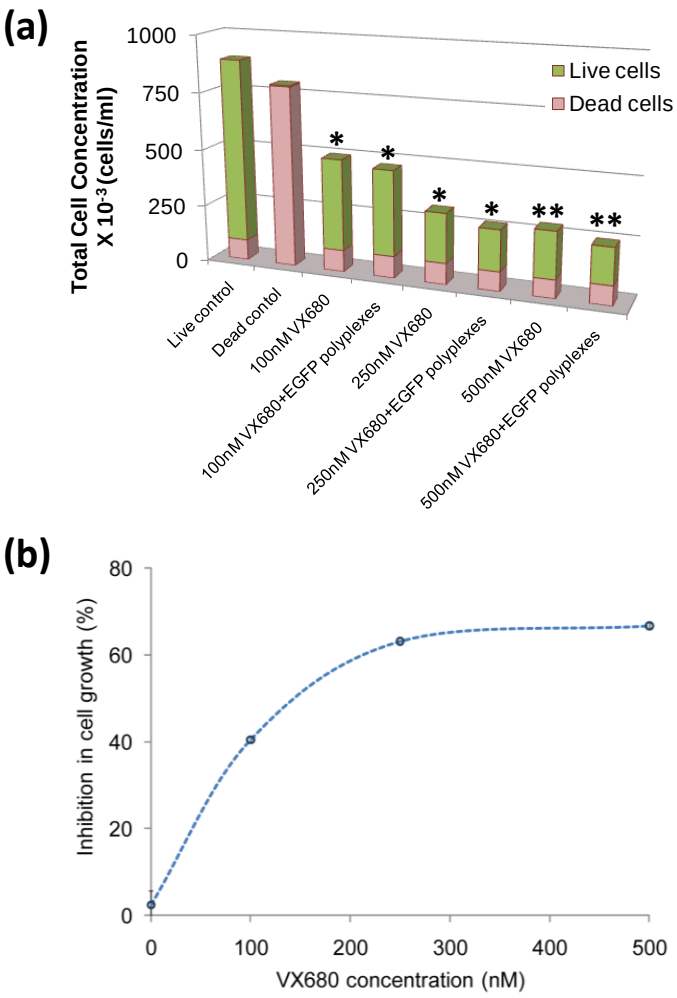

Figure 5.8. Effects of VX-680 on cell growth of PC3-PSMA transfected cells. EGFP transfected PC3-PSMA cells were incubated for 72h with 100, 250 and 500nM VX-680 concentrations, collected and counted using trypan blue stain. (a) Total, live and dead cell concentrations were measured using an automated cell counter. VX-680 was not toxic to the cells as it was revealed by the similar amount of live cell concentrations without or with VX-680 treatments. Rather it inhibited the cell growth by 70% as shown in (b). Statistical significance by Student's t-test: *, $p<0.05$ and **<0.005.

5.3.4 VX-680 treatment slows down kinetics of cell-cycle progression resulting in longer residence of cells in S and G2/M phases

VX-680 inhibits proliferation of a variety of tumor cells, arrests cells in the S and G2/M phases, allows them to go through mitosis without cytokinesis and proceeds into the subsequent S phase.(215). We examined the total number of

cells after 72h of delivery of EGFP polyplexes in order to correlate the consequences of VX-680 on cell proliferation and transgene enhancement in PC3-PSMA cells. Treatment with 100, 250 and 500nM VX-680 resulted in a reduction in the total number of PC3-PSMA cells by 40, 65 and 70% respectively compared to untreated cells (Figure 5.8(a)). The reduction in cell numbers was similar in VX-680 cells with or without polyplex treatment, indicating that polyplex delivery did not affect cell numbers under these conditions. The suppression in cell numbers (Figure 5.8(b)) was not due to VX-680-induced cytotoxicity under these conditions. Conversely, VX-680 increases the cell doubling times and therefore reduces the number of divisions that cells go through in a given time period (Table 5.1). This, in turn, results in reduced proliferation and therefore, lower numbers of PC3-PSMA cells compared to rapidly proliferating prostate cancer cells not treated with VX-680. Thus, VX-680 treatment delays cellular entry to mitosis, resulting in longer cell cycles and reduced proliferation. The combined activity of VX-680, namely, reducing cell proliferation and enhancing polymer-mediated transgene expression, is an attractive combination treatment strategy for the ablation of cancer cells.

Table 5.1 Quantitative analysis of cell doubling time and theoretical number of cell cycles for PC3-PSMA cells after transfecting with EGFP in absence or presence of VX-680

[VX680] μM	0	0.1	0.25	0.5
Cell doubling time, h	17.7±0.3	21.8±2.3	27.4±1.5	28.7±1.3
Theoretical number of cell cycles in 72h	4.07	3.31	2.63	2.51

5.3.5 Inhibition of Aurora kinases enhances cancer cell apoptosis following polymer-mediated p53 transgene delivery

We combined the anti-proliferative activity of VX-680 with its newly identified ability to enhance polymer-mediated transgene expression in order to induce synergistic death of prostate cancer cells. The 1,4C-1,4Bis polymer was employed to deliver pDNA expressing the tumor suppressor p53 protein. The p53 protein functions as a genome guardian by repairing DNA damage in the G1 phase, inhibiting entry of cells to the S phase of the cell cycle, and inducing apoptosis in cases of irreparable DNA damage (222-225). Mutations or functional loss in p53 gene are often seen in malignant cells and contribute to the aggressive cancer cell phenotypes that respond poorly to chemotherapeutic drugs (226, 227). DNA damage in normal cells leads to elevated p53 levels and arrest cells in the G1 phase (222). p53 then triggers either genome repair or apoptosis by activating the transcription of p21 or proapoptotic proteins, respectively. In cells with defective or lost p53 (e.g. cancer cells), DNA damage is irreparable leading to multistage carcinogenesis. Thus, p53 plays a key role in cell cycle, proliferation and genomic stability. Consequences of mutated or lost p53 can be overcome by exogenously introducing wild-type p53 in cancer cells; p53 gene therapy has shown promising results for inducing apoptosis in several tumor cells *in vitro*, *in vivo* and clinical trials (214, 225, 228-230). Specifically for prostate cancer, the p53 gene therapy paradigm has been evaluated with some success in Phase I clinical trials (231).

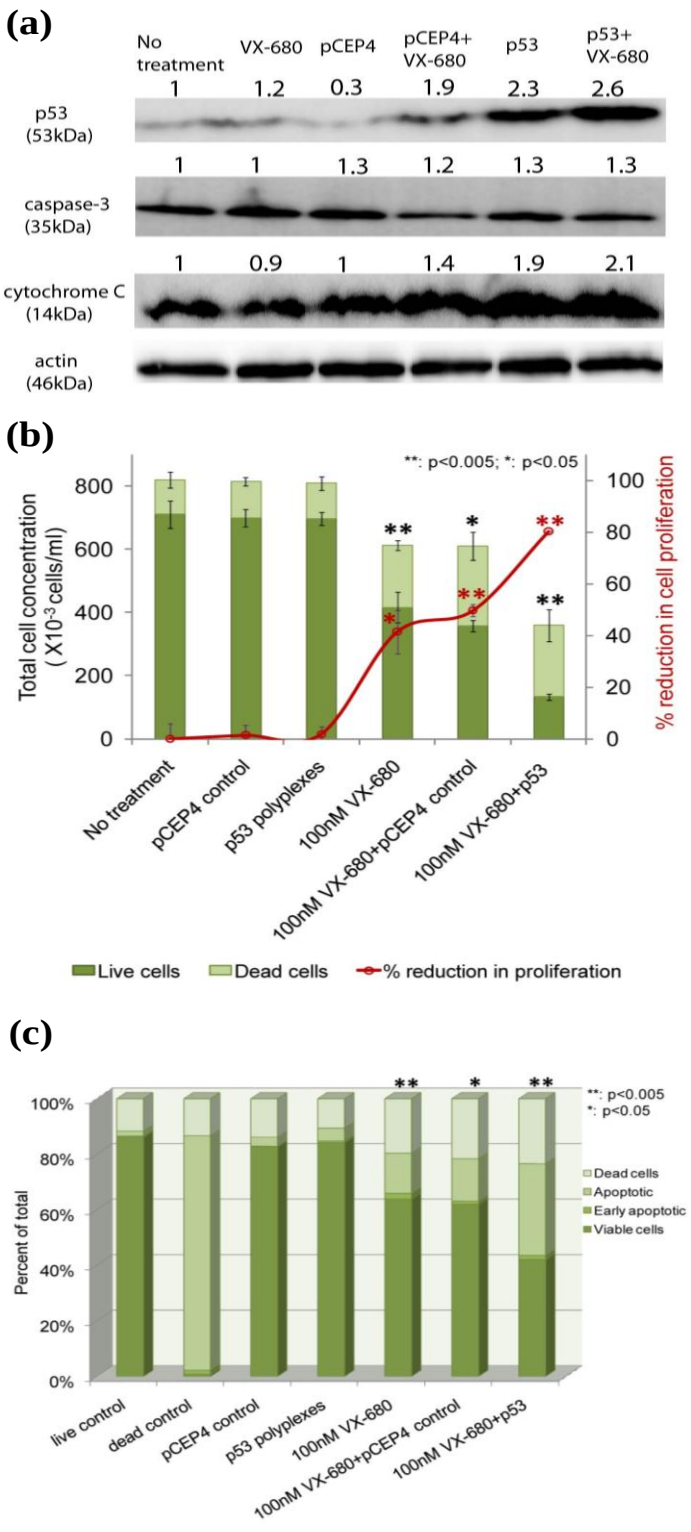

Figure 5.9. VX-680 activated p53 in PC3-PSMA cells and induced apotosis in combination treatments with p53 gene delivery. (a) Cells were transfected with pCEP4 control and p53 expression vectors using 1,4C-1,4Bis polymer and co-incubated with or without 100nM VX-680.

Cell lysates were obtained at 72h after transfection. Expression levels of p53, caspase-3 and cytochrome-C were determined by Western blotting and quantified by densitometry analysis using ImageJ software. Actin was used as loading control. Data are representative of three independent experiments. (b) Total, live and dead cell concentrations of the transfected were measured using trypan blue staining (bar graph). Percentage suppression in live cell growth was calculated compared to the untreated live control cells (line graph). (c) Apoptosis in pCEP4- and p53-transfected PC3-PSMA cells in combination with VX-680 were analyzed by flow cytometry after annexinV-PI staining of cells. Data are expressed as mean values of n=6 (*, $p<0.05$, **, $p<0.005$).

The 1,4C-1,4Bis polymer was used to deliver a plasmid expressing p53 in order to induce apoptosis in PC3-PSMA cells; delivery of the pCEP4 plasmid, which does not result in p53 expression, was employed as a control. Western blot analyses at 72 h indicated that treatment with 100nM VX-680 resulted in ~2.6-fold higher levels of p53 protein expression compared to untreated cells as well as those transfected with the pCEP4 control vector (Figure 5.9(a)). Delivery of the p53 transgene in the absence of VX-680 did not result in growth inhibition and death of PC3-PSMA cells compared to untreated cells or cells treated with the control vector (Figure 5.9(b)). Lack of induction of any cell death response by single agent treatment of p53 gene delivery alone might be due to low efficacies associated with polymer-mediated transgene expression. Treatment with VX-680 alone decreased the cell growth by approximately 40% compared to the no treatment control (line graph in (Figure 5.9(b)), not simply by inhibiting the cell proliferation but also by causing ~35% cell death in the growth-inhibited cells (Figure 5.9(c)). Delivery of the pCEP4 control vector in the presence of VX-680 did not result in increased cell death compared to treatment with VX-680 alone which is in agreement with the lack of p53 expression using this plasmid. Co-treatments of p53 gene delivery with VX-680 suppressed cell growth of live cells by 80% (line graph in Figure 5.9(b)) as well as induced apoptosis in 60% of the

growth-inhibited cells. The results indicated a synergistic effect of p53 and VX-680 to sensitize cells to p53-induced apoptosis, whereas their individual treatment merely sensitized the cells to apoptosis (Figure 5.9(b)).

Transgene expression of p53 protein triggers apoptotic signaling that leads to the activation of caspases, namely caspase-8 and caspase-3, which in turn induce apoptosis (232). The p53 protein can trigger the mitochondria-dependent intrinsic pathway (or transcription-independent pathway) in response to DNA damage, translocate to mitochondria and cause mitochondrial depolarization (232). Cytochrome-c released from inner mitochondrial membrane upon depolarization ultimately results in the activation of caspase-3, 6 and 7. Cytochrome-C and caspase-3 status was investigated in order to confirm the role of apoptosis in the combination treatment induced PC3-PSMA cell death. A moderate increase (1.3-2 fold) in these proteins were found in the cells transfected using p53 compared to the untreated control and pCEP4 transfected cells (Figure 5.9(a)), indicating induction of apoptosis in p53-expressing prostate cancer cells.

Loss of functional activity and stability of p53 is correlated with Aurora kinase-A overexpression in cancer cells (233). . Aurora kinase-A phosphorylates two sites (serine 215 and 315) of p53 protein and thus inhibits p53 activity and promotes degradation of this protein. The observed synergistic enhancement of apoptosis can, in part, be attributed to the fact that inhibition of Aurora kinase-A can enhance p53 stability and lead to a G2/M arrest by preventing its ubiquitin-driven degradation process (233). A recent study with HCT-116 colorectal cancer cells showed that AKI (ZM447439) upregulated p53 expression and induced p53

mediated intrinsic apoptotic pathway (234). It is therefore possible that polymer-mediated p53 gene delivery, in combination with a pan-AKI (VX-680), resulted in a '*dual synergistic effect*': enhancement of VX-680-mediated transgene expression as well as inhibiting degradation of p53 ultimately resulting in enhanced p53-mediated cancer cell apoptosis.

Taken together, the above results demonstrate that single agent treatment of polymer-mediated p53 gene delivery alone or VX-680 alone did not affect PC3-PSMA cell viability. Whereas the combination treatments of VX-680 and polymer-mediated p53 transgene expression demonstrated a synergistic effect in decreasing cancer cell viability due to apoptosis. Thus inhibition of Aurora kinases using VX-680 not only overcomes the poor levels of transgene expression observed with polymer-mediated delivery but also synergizes with higher levels of p53 protein in order to enhance cancer cell apoptosis.

5.4 Conclusions

Polymer-mediated pDNA delivery has traditionally suffered from poor levels of transgene expression. We employed a combination treatment strategy in which chemotherapeutic inhibition of Aurora kinases using VX-680 demonstrated (i) an increase in uptake of polyplexes; (ii) alteration in the intracellular localization of polyplexes that leads to enhancement in perinuclear accumulation around the nucleus; (iii) arresting of cells in the S and G2/M phases of the cell cycle; (iv) a temporary breakdown of nuclear membrane; and (v) delaying in the cell cycle progression with minimal cytotoxicity. VX-680 treatment resulted in higher uptake of the polyplexes of *Label*IT control vector and increased EGFP

expression following polymer-mediated EGFP reporter pDNA delivery compared to cells not treated with VX-680. Following VX-680 incubation, cells were arrested in the S and G2/M phases which demonstrated a temporary opening in nuclear lamin membrane to facilitate greater import of pDNA into the nucleus. VX-680 suppressed cancer cell proliferation due to reduction in the kinetics of cell cycle progression, but did not cause significant cell death. The combination treatment of tumor suppressor gene, p53 delivery along with VX-680 incubation, suppressed the PC3-PSMA cell growth significantly and induced apoptotic cell death. Our results highlight a novel combination therapeutic strategy by which AKI enhances polymer-mediated transgene expression and restores susceptibility to p53 leading to synergistic apoptosis of cancer cells. Future studies will involve investigation of the effects of Aurora kinase inhibition on therapeutic efficacies of lipid- and virus-based transgene delivery systems.

Chapter 6

SUMMARY

In this study, a library of eighty cationic polymers was developed for gene delivery, and combination treatments using chemotherapeutic drugs were evaluated to enhance polymer-mediated transgene expression. The polymers were synthesized by employing ring-opening reactions between diglycidyl ethers and polyamine monomers (180). Five polymers from the library named as 1,4C-1,4Bis; EGDE-3,3'; EGDE-1,4Bis; PPGDE-1,4Bis; and NPGDE-1,4Bis demonstrated higher transgene expression than a current polymer standard, 25kDa polyethylene imine (pEI-25). Polymer 1,4C-1,4Bis (23.5kDa) showed the highest gene expression in two different cell types, PC3-PSMA prostate cancer cells and murine osteoblasts cells. In addition, polyplexes of 1,4C-1,4Bis polymer were less cytotoxic than those of pEI-25.

In subsequent studies, it was found that polymer-mediated transgene expression levels using 1,4C-1,4Bis polymer were eight times higher in PC3 prostate cancer cells than that in its sub-clone PC3-PSMA cells (95). The differential expression levels were in part due to differences in sub-cellular distribution of the polyplexes in these two cell types. Polyplexes were distributed throughout the cytoplasm in PC3 cells, while they were arrested in single perinuclear recycling compartments (PNRC) in PC3-PSMA cells. Intracellular distribution patterns indicated a higher probability of cytoplasmic endosomal escape and gene delivery inside the nucleus in PC3 cells than those in PC3-PSMA cells for efficient transgene expression.

Combination treatments using small molecule chemotherapeutic drugs were evaluated to modulate the subcellular distribution of polyplexes and enhance transgene expression. Transfcetion in presence of histone deacetylase inhibitors (HDACi), such as tubacin and trichostatin (TSA), excluded the accumulation of polyplexes from the PNRC by dispersing them in the cytoplasm around the cell nuclei. Following more cytoplasmic dispersion of polyplexes using tubacin, transgene expression were measured 40 and 30-fold higher in presence of tubacin than no tubacin control in PC3-PSMA and PC3 cells, respectively. TSA enhanced transgene expression up to 35 and 10-fold in PC3-PSMA and PC3 cells, respectively relative to the gene expression in untreated cells.

Aurora kinase inhibitor (AKI), a modulator of cell cycle progression was also evaluated to enhance polymer-mediated transgene expression. AKI, e.g., VX-680 treatments increased the uptake of polyplexes up to 5-fold in PC3-PSMA cells compared to that of untreated cells. The polyplexes were localized dispersedly around the nuclei in presence of VX-680 rather accumulating in single spots in its absence. VX-680 treatments slowed down the progression of a cell cycle in S and G2/M phases in PC3-PSMA cells, and caused temporary local openings in nuclear membranes to allow diffusion of polyplexes inside the nucleus for efficient gene expression. Polymer-mediated enhanced green fluorescent protein (EGFP) expression was found to increase from 1% in untreated PC3-PSMA cells up to 20% after VX-680 treatments. EGFP expression was enhanced moderately from 2% of the untreated PC3 cells to 10% after VX-680 incubation. Combination treatments of polymer-mediated p53 gene delivery

with VX-680 suppressed *in vitro* PC3-PSMA cell proliferation up to 80% compared to the untreated cells and induced apoptosis by moderately increasing pro-apoptotic proteins, cytochrome C and caspase-3. The p53 gene delivery approach in combination with AKI treatments offers a new therapeutic strategy for non-viral gene therapy of cancer diseases.

Chapter 7

FUTURE WORK

This study demonstrated that polymer-mediated transgene expression can be enhanced by combining the effects of small molecule chemotherapeutic drugs. While the results are promising, further investigations are needed to improve the biocompatibility of lead polymer vectors, develop the specificity of delivery, evaluate the effects of various histone deacetylase inhibitors on transgene expression, and identify new chemotherapeutic modulators of intracellular trafficking and cell cycle progression. This chapter focuses on the improvements of lead polymers for prostate cancer target-specific gene delivery, and exploration of new strategies for enhancing polymer-mediated transgene expression.

7.1 Biocompatibility of Lead Polymers

Polyplexes, because of the high cationic charges on their surfaces, interact with serum proteins which lead to aggregation and loss of the polyplexes before reaching their target (235). The common approach to reduce the serum protein-polyplex interactions is to shield them with polyethylene glycol (PEG) (9, 236-239). PEG can be conjugated to the amine groups of the five lead polymers (PPGDE-1,4Bis; EGDE-3,3'; EGDE-1,4Bis; NPGDE-1,4Bis; and 1,4C-1,4Bis) identified from our cationic polymer library. However, PEGylation can alter cellular uptake, modulate intracellular trafficking, inhibit endosomal escape of polyplexes, and decrease transfection efficiency (240). The endosomal escape process of PEG-shielded polymers can be facilitated by introducing a biodegradable disulfide linkage (S-S) (241, 242) that is cleavable in acidic

lysosomal compartments. This can be achieved by employing a three-step reaction. First, amine groups of the lead cationic polymers will be reacted with *N*-hydroxysuccinimide (NHS) esters of an S-S linker, *N*-succinimidyl-3-(2-pyridyldithio) propionate (SPDP) (243, 244). The resulting polymers containing dithiolpyridine linker will be reduced using dithiothreitol (DTT) and conjugated with PEG-orthopyridyl-disulfide (PEG-OPSS) to form reversible disulfide bonds. The cationic polymer-S-S-PEG conjugates will decrease aggregation with serum proteins, increase endosomal escape and transgene expression (243).

7.2 Targeted Gene Delivery

Five lead polymers from the library can be improved in order to bind to target-cells specifically. This can be accomplished by conjugating the lead polymers with antibodies specific to target-cell surface receptors. For example, prostate specific membrane antigen (PSMA) receptors are well-characterized markers for prostate cancer treatment. Targeted delivery using the J591 antibody that recognizes PSMA surface proteins has been shown to deliver the gene effectively to prostate cancer cells both *in vitro* and *in vivo* (245, 246). Conjugation of anti-PSMA monoclonal antibodies J591 (160, 247) to the cationic polymers-S-S-PEG via a SPDP linker will result in prostate cancer target specific gene expression (243, 244). Other antibodies and ligands that have been identified for targeted gene delivery to prostate cancer cells are Herceptin (Her-2 or trastuzumab) (248) and transferrin (Tf) (249). Such attempts of antibody conjugation to the cationic polymers will successfully deliver genes to prostate

cancer cells. Several projects are being undertaken in our laboratory for developing target-specific polymers for gene delivery.

7.3 Expansion of Combination Treatments of Polymer-Mediated Gene Delivery and HDACi

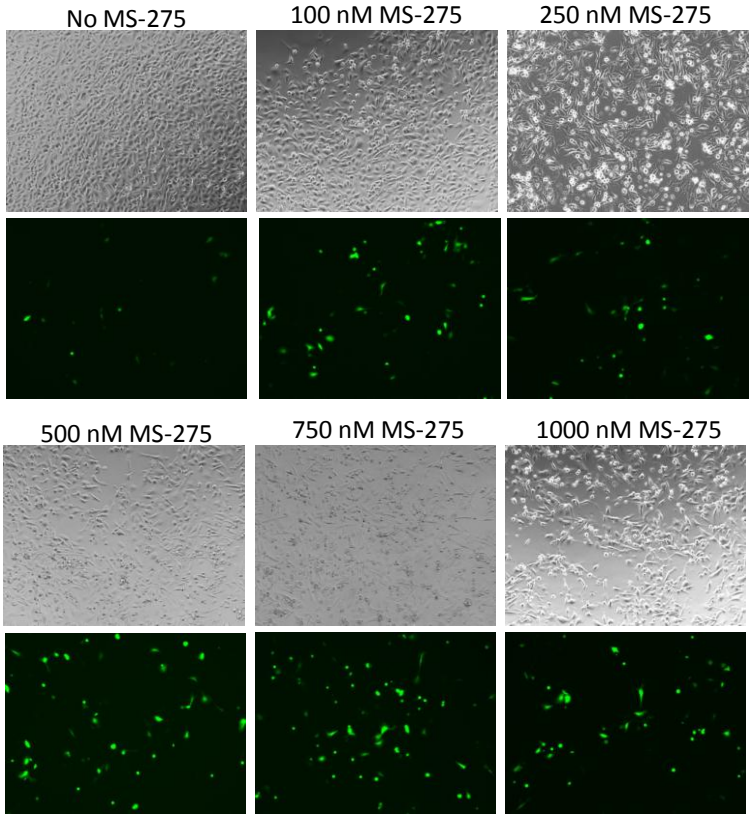

Figure 7.1. Effects of MS-275 on polymer-mediated EGFP expression in PC3 cells. The cells were transfected using a polymer:DNA weight ratio of 25:1 in presence of different doses of MS-275. Fluorescence microscopic images were captured using 10X objective after 72 h of transfection.

Our previous results of enhancement of SV40-luciferase reporter gene expression using tubacin and trichostatin A (TSA) suggest that the exploitation of other HDACi e.g. MS-275, depsipeptide and belinostat on enhancing polymer-mediated transgene expression must be thoroughly investigated using both SV40-

lucirferase and CMV-EGFP pDNA. Previous studies of EGFP polyplex delivery to PC3 cells in combination with MS-275 demonstrated significant enhancement of EGFP expression *in vitro* (Figure 7.1). Detailed studies using combination treatments of gene delivery in the presence of MS-275, depsipeptide, or belinostat will be required in a variety of cancer cell lines e.g. PC3, PC3-PSMA, LNCaP and 22Rv1 prostate cancer cells, Panc-1 and Mia PaCa-2 pancreatic cancer cells, and MCF-7 breast cancer cells.

The enhancement of p53-induced apoptosis using the combination treatments of HDACi and polymer-mediated p53 gene delivery should be investigated. Histone deacetylase 1 (HDAC1) and a class III HDAC, Sirt1 binds to p53 and deacetylates at multiple lysine residues leading to the destruction of p53 or the reduction in its transcriptional ability to activate a cell cycle protein, p21 (250, 251). The activation of p21 arrests cells in G0/G1 phase, translocates Bax proteins in mitochondria and induces apoptosis (252). A class IIb HDACi, TSA has been reported to inhibit HDAC6 and acetylate lysine-40 of α-tubulin (253) that leads to microtubule stabilization. Microtubule stabilization arrests cells in the prometaphase or G2/M phases (254). Combination treatments using polymer-mediated p53 gene delivery and HDACi provide a promising option to induce synergistic apoptotic cancer cell death. It can be hypothesized that polymer-mediated p53 gene delivery in combination with HDACi treatments would enhance p53 expression, and arrest cells in either G0/G1 or G2/M phases leading to apoptosis. A detailed mechanistic study will be required to verify the cell-cycle induction pathway.

7.4 Identification of New Chemotherapeutic Modulators

7.4.1 Sirtuin2 Inhibitors

In this study, we have demonstrated that inhibition of histone deacetylase 6 (HDAC6) is a promising strategy to enhance polymer-mediated transgene expression (Chapter 4). Besides HDAC6, another enzyme that also deacetylates the α-tubulin of microtubules is nicotinamide adenine dinucleotide (NAD^+) dependent histone deacetylase sirtuin 2 (Sirt2) (255). Sirtuins are chromatin-associated enzymes that can modify histones wrapped around the concentrated chromosomes inside the nucleus (256). They also have non-histone substrates, e.g., transcription factors (i.e., GATA1, BCL6, STAT3, NF-κB, MyoD, YY1), tumor suppressors (p21, p53), cell cycle regulators (Rb, E2F), cytoskeletal proteins (α -tubulin) and the chaperone heat shock protein 90 (Hsp90) (175, 257). Like HDAC6, Sirt2 is predominantly a cytoplasmic protein that colocalizes with microtubules and deacetylates α-tubulin (258). Therefore, it can be hypothesized that Sirt2 inhibitors enhance microtubule stability and vesicular transport within the cells. While the HDAC6 selective inhibitor, tubacin, has been shown to enhance polymer-mediated transgene expression in PC3-PSMA and PC3 cells (Chapter 4), inhibition of Sirt2 represents an interesting approach for enhancing transgene expression levels in these two cell lines. Among the small number of Sirt2 inhibitors identified so far, sirtinol is the first molecule showing an IC_{50} of 38μM for human Sirt2 in *in vitro* HeLa cervical cancer cells (259). Recently, salermide has been published as a potent Sirt2 inhibitor with anti-cancerous activity in MDA-MB-231 breast cancer and SW480 colon cancer cells (260). The

most selective Sirt2 inhibitor is AGK2 with an IC_{50} value of 3.5μM (261). AGK2 inhibited the deacetylation activity of Sirt2 and increased the acetylated tubulin relative to the sirtinol treatments in various types of cells including HeLa cells. The results suggest that targeting Sirt2 may be beneficial in enhancing polymer-mediated transgene expression.

7.4.2 Inhibitors of Centromere-associated Protein-E (CENP-E)

Mitosis is a key cell cycle regulator process in which a eukaryotic cell segregates its chromosomes into two daughter cells. In cancer cells, regulation of the cell-cycle process is abolished, resulting in uncontrolled cell proliferation and alterations in genetic materials. Therefore, identification of novel drugs that can target mitotic progression in cancer cells without interrupting the normal cell proliferation has gained much attention for cancer treatments. Wood et al. has reported the discovery of an inhibitor of a mitotic motor protein, centromere-associated protein-E (CENP-E; also known as kinesin-7), that is overexpressed in multiple cancer cells during mitosis and limit cancer cell proliferation upon inhibition (262). CENP-E is a mitotic protein of 312kDa consisting of an N-terminal kinesin motor domain that hydrolyzes ATP to produce mechanical force along microtubules. CENP-E helps proper alignment of chromosomes in the metaphore plate during prometaphase when the nuclear envelope breaks down. The novel CENP-E inhibitor, GSK923295 demonstrated obstruction in ATP hydrolysis by CENP-E, and resulted in tight binding of the protein to microtubules, failure in chromosome alignment, induction in cell cycle arrest, and apoptotic cell death in Colo205 colon cancer cells xenografted in mice. Growth

inhibition (IG_{50}) values of GSK923295 were tested in 237 different cancer cell lines out of which 212 cell lines exhibited IG_{50}<100nM. The phase I clinical trial of this drug is underway.

This drug can be tested at sub-nanomolar concentrations to enhance polymer-mediated transgene expression in rapidly dividing cancer cells. It can be hypothesized that CENP-E inhibition using GSK923295 elongates the time for prometaphase and slows down the process of nuclear membrane break down in cancer cells. This allows more diffusion of exogenous DNA to transcriptional accessories, resulting in enhanced transcription and gene expression. It is noteworthy that CENP-E is overexpressed in pancreatic and breast cancer cells but not in prostate cancer cells (262). It would therefore be interesting to see the effects of GSK923295 in prostate cancer cells.

REFERENCES

1. Kawabata, K., Takakura, Y., and Hashida, M. (1995) The fate of plasmid DNA after intravenous injection in mice-involvement of scavenger receptors in its hepatic upatake *Pharmaceutical Research* **12**, 825-830

2. Bielinska, A., KukowskaLatallo, J. F., Johnson, J., Tomalia, D. A., and Baker, J. R. (1996) Regulation of in vitro gene expression using antisense oligonucleotides or antisense expression plasmids transfected using starburst PAMAM dendrimers. *Nucleic Acids Research* **24**, 2176-2182

3. Branden, L. J., Christensson, B., and Smith, C. I. E. (2001) In vivo nuclear delivery of oligonucleotides via hybridizing bifunctional peptides. *Gene Therapy* **8**, 84-87

4. Boussif, O., Lezoualch, F., Zanta, M. A., Mergny, M. D., Scherman, D., Demeneix, B., and Behr, J. P. (1995) A versatile vector for gene and oligonucleotide transfer into cells in culture and *in vivo* polyethyleneimine. *Proceedings of the National Academy of Sciences of the United States of America* **92**, 7297-7301

5. Scanlon, K. J., Jiao, L., Funato, T., Wang, W., Tone, T., Rossi, J. J., and Kashanisabet, M. (1991) Ribozyme-mediated cleavage of c-fos messenger-RNA reduces gene expression of DNA synthesis enzymes and metallothionein *Proceedings of the National Academy of Sciences of the United States of America* **88**, 10591-10595

6. Sui, G. C., Soohoo, C., Affar, E., Gay, F., Shi, Y. J., Forrester, W. C., and Shi, Y. (2002) A DNA vector-based RNAi technology to suppress gene expression in mammalian cells. *Proceedings of the National Academy of Sciences of the United States of America* **99**, 5515-5520

7. Neumann, B., Held, M., Liebel, U., Erfle, H., Rogers, P., Pepperkok, R., and Ellenberg, J. (2006) High-throughput RNAi screening by time-lapse imaging of live human cells. *Nat Methods* **3**, 385-390

8. Cho, S. W., Goldberg, M., Son, S. M., Xu, Q. B., Yang, F., Mei, Y., Bogatyrev, S., Langer, R., and Anderson, D. G. (2009) Lipid-Like Nanoparticles for Small Interfering RNA Delivery to Endothelial Cells. *Advanced Functional Materials* **19**, 3112-3118

9. Davis, M. E. (2009) The First Targeted Delivery of siRNA in Humans via a Self-Assembling, Cyclodextrin Polymer-Based Nanoparticle: From Concept to Clinic. *Molecular Pharmaceutics* **6**, 659-668

10. Edelstein, M. L. (2010) Gene therapy clinical trials worldwide. website at: http://www.wiley.co.uk/genmed/clinical. *The Journal of Gene Medicine*

11. Friedmann, T., and Roblin, R. (1972) Gene Therapy for Human Genetic Disease? *Science* **175**, 949-955

12. Rosenberg, S. A., Aebersold, P., Cornetta, K., Kasid, A., Morgan, R. A., Moen, R., Karson, E. M., Lotze, M. T., Yang, J. C., Topalian, S. L., Merino, M. J., Culver, K., Miller, A. D., Blaese, R. M., and Anderson, W. F. (1990) Gene-transfer into humans-immunotherapy of patients with advanced melanoma using tumor-infiltrating lymphocytes modified by retroviral gene transduction *New England Journal of Medicine* **323**, 570-578

13. Edelstein, M. L., Abedi, M. R., and Wixon, J. (2007) Gene therapy clinical trials worldwide to 2007 - an update. *Journal of Gene Medicine* **9**, 833-842

14. Bilbao, G., GomezNavarro, J., Contreras, J. L., and Curiel, D. T. (1997) Advances in adenoviral vectors for cancer gene therapy. *Expert Opinion on Therapeutic Patents* **7**, 1427-1446

15. Burton, E. A., Fink, D. J., and Glorioso, J. C. (2002) Gene delivery using herpes simplex virus vectors. *DNA and Cell Biology* **21**, 915-936

16. McTaggart, S., and Al-Rubeai, M. (2002) Retroviral vectors for human gene delivery. *Biotechnology Advances* **20**, 1-31

17. Coura, R. D., and Nardi, N. B. (2008) A role for adeno-associated viral vectors in gene therapy. *Genetics and Molecular Biology* **31**, 1-11

18. Collins, S. A., Guinn, B. A., Harrison, P. T., Scallan, M. F., O'Sullivan, G. C., and Tangney, M. (2008) Viral vectors in cancer immunotherapy: Which vector for which strategy? *Current Gene Therapy* **8**, 66-78

19. Marshall, E. (1999) Clinical trials - Gene therapy death prompts review of adenovirus vector. *Science* **286**, 2244-2245

20. Kohn, D. B., Sadelain, M., and Glorioso, J. C. (2003) Occurrence of leukaemia following gene therapy of X-linked SCID. *Nature Reviews Cancer* **3**, 477-488

21. Wasungu, L., and Hoekstra, D. (2006) Cationic lipids, lipoplexes and intracellular delivery of genes. pp. 255-264

22. Funhoff, A. M., Van Nostrum, C. F., Lok, M. C., Kruijtzer, J. A. W., Crommelin, D. J. A., and Hennink, W. E. (2005) Cationic polymethacrylates with covalently linked membrane destabilizing peptides as gene delivery vectors. *Journal of Controlled Release* **101**, 233-246

23. Pouton, C. W., Lucas, P., Thomas, B. J., Uduehi, A. N., Milroy, D. A., and Moss, S. H. (1998) Polycation-DNA complexes for gene delivery: a comparison of the biopharmaceutical properties of cationic polypeptides and cationic lipids. *Journal of Controlled Release* **53**, 289-299

24. Zeng, J. M., and Wang, S. (2005) Enhanced gene delivery to PC12 cells by a cationic polypeptide. *Biomaterials* **26**, 679-686

25. Fayazpour, F., Lucas, B., Alvarez-Lorenzo, C., Sanders, N. N., Demeester, J., and De Smedt, S. C. (2006) Physicochemical and transfection properties of cationic hydroxyethylcellulose/DNA nanoparticles. *Biomacromolecules* **7**, 2856-2862

26. Borchard, G. (2001) Chitosans for gene delivery. *Advanced Drug Delivery Reviews* **52**, 145-150

27. Huang, M., Fong, C.-W., Khor, E., and Lim, L.-Y. (2005) Transfection efficiency of chitosan vectors: Effect of polymer molecular weight and degree of deacetylation. *Journal of Controlled Release* **106**, 391-406

28. Moreira, C., Oliveira, H., Pires, L. R., Simoes, S., Barbosa, M. A., and Pego, A. P. (2009) Improving chitosan-mediated gene transfer by the introduction of intracellular buffering moieties into the chitosan backbone. *Acta Biomaterialia* **5**, 2995-3006

29. Lee, C. C., MacKay, J. A., Frechet, J. M. J., and Szoka, F. C. (2005) Designing dendrimers for biological applications. *Nature Biotechnology* **23**, 1517-1526

30. Mendiratta, S. K., Quezada, A., Matar, M., Wang, J., Hebel, H. L., Long, S., Nordstrom, J. L., and Pericle, F. (1999) Intratumoral delivery of IL-12 gene by polyvinyl polymeric vector system to murine renal and colon carcinoma results in potent antitumor immunity. *Gene Therapy* **6**, 833-839

31. Lungwitz, U., Breunig, M., Blunk, T., and Gopferich, A. (2005) Polyethylenimine-based non-viral gene delivery systems. *European Journal of Pharmaceutics and Biopharmaceutics* **60**, 247-266

32. Kamiya, H., Fujimura, Y., Matsuoka, I., and Harashima, H. (2002) Visualization of intracellular trafficking of exogenous DNA delivered by cationic liposomes. *Biochemical and Biophysical Research Communications* **298**, 591-597

33. Davis, M. E., and Brewster, M. E. (2004) Cyclodextrin-based pharmaceutics: Past, present and future. *Nature Reviews Drug Discovery* **3**, 1023-1035

34. Heidel, J. D., Yu, Z. P., Liu, J. Y. C., Rele, S. M., Liang, Y. C., Zeidan, R. K., Kornbrust, D. J., and Davis, M. E. (2007) Administration in non-human primates of escalating intravenous doses of targeted nanoparticles containing ribonucleotide reductase subunit M2 siRNA. *Proceedings of the National Academy of Sciences of the United States of America* **104**, 5715-5721

35. Bartlett, D. W., and Davis, M. E. (2008) Impact of tumor-specific targeting and dosing schedule on tumor growth inhibition after intravenous administration of siRNA-containing nanoparticles. *Biotechnology and Bioengineering* **99**, 975-985

36. Eldridge, G. R., Vervoort, H. C., Lee, C. M., Cremin, P. A., Williams, C. T., Hart, S. M., Goering, M. G., O'Neil-Johnson, M., and Zeng, L. (2002) High-throughput method for the production and analysis of large natural product libraries for drug discovery. *Analytical Chemistry* **74**, 3963-3971

37. Harris, D. (2002) Efficient combinatorial chemistry/high throughput screening paradigm for small molecule drug discovery: Maximizing the discovery of drug candidates and minimizing waste. *Abstracts of Papers of the American Chemical Society* **224**, 008-BTEC

38. Seneci, P., and Miertus, S. (2000) Combinatorial chemistry and high-throughput screening in drug discovery: Different strategies and formats. *Molecular Diversity* **5**, 75-89

39. Congreve, M. S., and Jamieson, C. (2002) High-throughput analytical techniques for reaction optimization. *Drug Discovery Today* **7**, 139-142

40. Shoemaker, R. H., Scudiero, D. A., Melillo, G., Currens, M. J., Monks, A. P., Rabow, A. A., Covell, D. G., and Sausville, E. A. (2002) Application of high-throughput, molecular-targeted screening to anticancer drug discovery. *Curr Top Med Chem* **2**, 229-246

41. Khandurina, J., and Guttman, A. (2002) Microchip-based high-throughput screening analysis of combinatorial libraries. *Curr Opin Chem Biol* **6**, 359-366

42. Thomas, M., Lu, J. J., Zhang, C. C., Chen, J. Z., and Klibanov, A. M. (2007) Identification of novel superior polycationic vectors for gene delivery by high-throughput synthesis and screening of a combinatorial library. *Pharmaceutical Research* **24**, 1564-1571

43. Van Vliet, L. D., Chapman, M. R., Avenier, F., Kitson, C. Z., and Hollfelder, F. (2008) Relating chemical and biological diversity space: A tunable system for efficient gene transfection. *Chembiochem* **9**, 1960-1967

44. Anderson, D. G., Lynn, D. M., and Langer, R. (2003) Semi-automated synthesis and screening of a large library of degradable cationic polymers for gene delivery. *Angewandte Chemie-International Edition* **42**, 3153-3158

45. Green, J. J., Shi, J., Chiu, E., Leshchiner, E. S., Langer, R., and Anderson, D. G. (2006) Biodegradable polymeric vectors for gene delivery to human endothelial cells. *Bioconjugate Chemistry* **17**, 1162-1169

46. Zugates, G. T., Peng, W. D., Zumbuehl, A., Jhunjhunwala, S., Huang, Y. H., Langer, R., Sawicki, J. A., and Anderson, D. G. (2007) Rapid optimization of gene delivery by parallel end-modification of poly(beta-amino ester)s. *Molecular Therapy* **15**, 1306-1312

47. Sunshine, J., Green, J. J., Mahon, K. P., Yang, F., Eltoukhy, A. A., Nguyen, D. N., Langer, R., and Anderson, D. G. (2009) Small-Molecule End-Groups of Linear Polymer Determine Cell-Type Gene-Delivery Efficacy. *Advanced Materials* **21**, 4947-4951

48. Green, J. J., Zugates, G. T., Tedford, N. C., Huang, Y. H., Griffith, L. G., Lauffenburger, D. A., Sawicki, J. A., Langer, R., and Anderson, D. G. (2007) Combinatorial modification of degradable polymers enables transfection of human cells comparable to adenovirus. *Advanced Materials* **19**, 2836-2842

49. Jere, D., Yoo, M. K., Arote, R., Kim, T. H., Cho, M. H., Nah, J. W., Choi, Y. J., and Cho, C. S. (2008) Poly (amino ester) composed of poly (ethylene glycol) and aminosilane prepared by combinatorial chemistry as a gene carrier. *Pharmaceutical Research* **25**, 875-885

50. Pun, S. H., Bellocq, N. C., Liu, A. J., Jensen, G., Machemer, T., Quijano, E., Schluep, T., Wen, S. F., Engler, H., Heidel, J., and Davis, M. E. (2004) Cyclodextrin-modified polyethylenimine polymers for gene delivery. *Bioconjugate Chemistry* **15**, 831-840

51. Lu, B., Wang, C. F., Wu, D. Q., Li, C., Zhang, X. Z., and Zhuo, R. X. (2009) Chitosan based oligoamine polymers: Synthesis, characterization, and gene delivery. *Journal of Controlled Release* **137**, 54-62

52. Nagasaki, T., Hojo, M., Uno, A., Satoh, T., Koumoto, K., Mizu, M., Sakurai, K., and Shinkai, S. (2004) Long-term expression with a cationic polymer derived from a natural polysaccharide: Schizophyllan. *Bioconjugate Chemistry* **15**, 249-259

53. Davis, M. E., Zuckerman, J. E., Choi, C. H. J., Seligson, D., Tolcher, A., Alabi, C. A., Yen, Y., Heidel, J. D., and Ribas, A. (2010) Evidence of RNAi in humans from systemically administered siRNA via targeted nanoparticles. *Nature* **464**, 1067-1070

54. Belting, M. (2003) Heparan sulfate proteoglycan as a plasma membrane carrier. *Trends in Biochemical Sciences* **28**, 145-151

55. Mukherjee, S., Ghosh, R. N., and Maxfield, F. R. (1997) Endocytosis. *Physiological Reviews* **77**, 759-803

56. Mellman, I. (1996) Endocytosis and molecular sorting. *Annu Rev Cell Dev Biol.* **12**, 575-625

57. Goldstein, J. L., Anderson, R. G. W., and Brown, M. S. (1979) Coated pits, coated vesicles, and receptor-mediated endocytosis. *Nature* **279**, 679-685

58. Soenen, S. J. H., Vercauteren, D., Braeckmans, K., Noppe, W., De Smedt, S., and De Cuyper, M. (2009) Stable Long-Term Intracellular Labelling with Fluorescently Tagged Cationic Magnetoliposomes. *Chembiochem* **10**, 257-267

59. Day, P. M., Lowy, D. R., and Schiller, J. T. (2003) Papillomaviruses infect cells via a clathrin-dependent pathway. *Virology* **307**, 1-11

60. Sieczkarski, S. B., and Whittaker, G. R. (2002) Influenza virus can enter and infect cells in the absence of clathrin-mediated endocytosis. *J Virol* **76**, 10455-10464

61. Oh, J. M., Choi, S. J., Kim, S. T., and Choy, J. H. (2006) Cellular uptake mechanism of an inorganic nanovehicle and its drug conjugates: Enhanced efficacy due to clathrin-mediated endocytosis. *Bioconjug Chem* **17**, 1411-1417

62. Oh, J. M., Choi, S. J., Kim, S. T., and Choy, J. H. (2006) Cellular uptake mechanism of an inorganic nanovehicle and its drug conjugates: Enhanced efficacy due to clathrin-mediated endocytosis. *Bioconjugate Chemistry* **17**, 1411-1417

63. Rejman, J., Oberle, V., Zuhorn, I. S., and Hoekstra, D. (2004) Size-dependent internalization of particles via the pathways of clathrin-and caveolae-mediated endocytosis. *Biochemical Journal* **377**, 159-169

64. Nakase, I., Tadokoro, A., Kawabata, N., Takeuchi, T., Katoh, H., Hiramoto, K., Negishi, M., Nomizu, M., Sugiura, Y., and Futaki, S. (2007) Interaction of arginine-rich peptides with membrane-associated proteoglycans is crucial for induction of actin organization and macropinocytosis. *Biochemistry* **46**, 492-501

65. Kneuer, C., Ehrhardt, C., Bakowsky, H., Kumar, M., Oberle, V., Lehr, C. M., Hoekstra, D., and Bakowsky, U. (2006) The influence of physicochemical parameters on the efficacy of non-viral DNA transfection complexes: A comparative study. *Journal of Nanoscience and Nanotechnology* **6**, 2776-2782

66. Rao, G. A., Tsai, R., Roura, D., and Hughes, J. A. (2008) Evaluation of the transfection property of a peptide ligand for the fibroblast growth factor receptor as part of PEGylated polyethylenimine polyplex. *Journal of Drug Targeting* **16**, 79-89

67. Midoux, P., and Monsigny, M. (1999) Efficient gene transfer by histidylated polylysine pDNA complexes. *Bioconjugate Chemistry* **10**, 406-411

68. Rejman, J., Bragonzi, A., and Conese, M. (2005) Role of clathrin- and caveolae-mediated endocytosis in gene transfer mediated by lipo- and polyplexes. *Molecular Therapy* **12**, 468-474

69. Douglas, K. L., Piccirillo, C. A., and Tabrizian, M. (2008) Cell line-dependent internalization pathways and intracellular trafficking determine transfection efficiency of nanoparticle vectors. *European Journal of Pharmaceutics and Biopharmaceutics* **68**, 676-687

70. Musch, A. (2004) Microtubule organization and function in epithelial cells. *Traffic (Copenhagen, Denmark)* **5**, 1-9

71. Pollock, N., Koonce, M. P., de Hostos, E. L., and Vale, R. D. (1998) In vitro microtubule-based organelle transport in wild-type Dictyostelium and cells overexpressing a truncated dynein heavy chain. *Cell Motility and the Cytoskeleton* **40**, 304-314

72. Suomalainen, M., Nakano, M. Y., Keller, S., Boucke, K., Stidwill, R. P., and Geber, U. F. (1999) Microtubule-dependent plus- and minus end-

directed motilities are competing processes for nuclear targeting of adenovirus. *Journal of Cell Biology* **144**, 657-672

73. Drake, D. M., and Pack, D. W. (2008) Biochemical investigation of active intracellular transport of polymeric gene-delivery vectors. *Journal of Pharmaceutical Sciences* **97**, 1399-1413

74. Sonawane, N. D., Szoka, F. C., and Verkman, A. S. (2003) Chloride accumulation and swelling in endosomes enhances DNA transfer by polyamine-DNA polyplexes. *Journal of Biological Chemistry* **278**, 44826-44831

75. Mishra, S., Heidel, J. D., Webster, P., and Davis, M. E. (2006) Imidazole groups on a linear, cyclodextrin-containing polycation produce enhanced gene delivery via multiple processes. *Journal of Controlled Release* **116**, 179-191

76. Forrest, M. L., and Pack, D. W. (2002) On the kinetics of polyplex endocytic trafficking: Implications for gene delivery vector design. *Molecular Therapy* **6**, 57-66

77. Akinc, A., and Langer, R. (2002) Measuring the pH environment of DNA delivered using nonviral vectors: Implications for lysosomal trafficking. *Biotechnology and Bioengineering* **78**, 503-508

78. Lukacs, G. L., Haggie, P., Seksek, O., Lechardeur, D., Freedman, N., and Verkman, A. S. (2000) Size-dependent DNA mobility in cytoplasm and nucleus. *Journal of Biological Chemistry* **275**, 1625-1629

79. Mesika, A., Kiss, V., Brumfeld, V., Ghosh, G., and Reich, Z. (2005) Enhanced intracellular mobility and nuclear accumulation of DNA plasmids associated with a karyophilic protein. *Human Gene Therapy* **16**, 200-208

80. Young, J. L., Benoit, J. N., and Dean, D. A. (2003) Effect of a DNA nuclear targeting sequence on gene transfer and expression of plasmids in the intact vasculature. *Gene Therapy* **10**, 1465-1470

81. Miller, A. M., and Dean, D. A. (2008) Cell-specific nuclear import of plasmid DNA in smooth muscle requires tissue-specific transcription factors and DNA sequences. *Gene Therapy* **15**, 1107-1115

82. Pikaart, M. I., Recillas-Targa, F., and Felsenfeld, G. (1998) Loss of transcriptional activity of a transgene is accompanied by DNA methylation and histone deacetylation and is prevented by insulators. *Genes & Development* **12**, 2852-2862

83. Chen, L. F., Fischle, W., Verdin, E., and Greene, W. C. (2001) Duration of nuclear NF-kappa B action regulated by reversible acetylation. *Science* **293**, 1653-1657

84. Yasukawa, K., Sawamura, D., Goto, M., Nakamura, H., and Shimizu, H. (2007) Histone deacetylase inhibitors preferentially augment transient transgene expression in human dermal fibroblasts. *British Journal of Dermatology* **157**, 662-669

85. Nakajima, S. I., Niizeki, H., Tada, M., Nakagawa, K., Kondo, S., Okada, F., and Kobayashi, M. (2009) Trichostatin A with adenovirus-mediated p53 gene transfer synergistically induces apoptosis in breast cancer cell line MDA-MB-231. *Oncology Reports* **22**, 143-148

86. Stein, G. S., Stein, J. L., Vanwijnen, A. J., and Lian, J. B. (1994) Histone gene-transcription - a model for responsiveness to an integrated series of regulatory signals mediating cell-cycle control and proliferation differentiation interrelationships *Journal of Cellular Biochemistry* **54**, 393-404

87. Davie, J. R. (1998) Covalent modifications of histones: expression from chromatin templates. *Current Opinion in Genetics & Development* **8**, 173-178

88. Marks, P. A., Rifkind, R. A., Richon, V. M., Breslow, R., Miller, T., and Kelly, W. K. (2001) Histone deacetylases and cancer: Causes and therapies. *Nature Reviews Cancer* **1**, 194-202

89. Nan, X. S., Hyndman, L., Agbi, N., Porteous, D. J., and Boyd, A. C. (2004) Potent stimulation of gene expression by histone deacetylase

inhibitors on transiently transfected DNA. *Biochemical and Biophysical Research Communications* **324**, 348-354

90. Verdin, E., Dequiedt, F., and Kasler, H. G. (2003) Class II histone deacetylases: versatile regulators. *Trends in Genetics* **19**, 286-293

91. Fabre, C., Grosjean, J., Tailler, M., Boehrer, S., Ades, L., Perfettini, J. L., de Botton, S., Fenaux, P., and Kroemer, G. (2008) A novel effect of DNA methyltransferase and histone deacetylase inhibitors - NF kappa B inhibition in malignant myeloblasts. *Cell Cycle* **7**, 2139-2145

92. Kasman, L., Lu, P., and Voelkel-Johnson, C. (2007) The histone deacetylase inhibitors depsipeptide and MS-275, enhance TRAIL gene therapy of LNCaP prostate cancer cells without adverse effects in normal prostate epithelial cells. *Cancer Gene Therapy* **14**, 327-334

93. El-Zawahry, A., Lu, P., White, S. J., and Voelkel-Johnson, C. (2006) In vitro efficacy of AdTRAIL gene therapy of bladder cancer is enhanced by trichostatin A-mediated restoration of CAR expression and downregulation of cFLIP and Bcl-X-L. *Cancer Gene Therapy* **13**, 281-289

94. Barua, S., and Rege, K. (2009) Cancer-Cell-Phenotype-Dependent Differential Intracellular Trafficking of Unconjugated Quantum Dots. *Small* **5**, 370-376

95. Barua, S., and Rege, K. (2010) The influence of mediators of intracellular trafficking on transgene expression efficacy of polymer-plasmid DNA complexes. *Biomaterials* **31**, 5894-5902

96. Gallop, M. A., Barrett, R. W., Dower, W. J., Fodor, S. P., and Gordon, E. M. (1994) Applications of combinatorial technologies to drug discovery. 1. Background and peptide combinatorial libraries. *J Med Chem* **37**, 1233-1251

97. Gordon, E. M., Barrett, R. W., Dower, W. J., Fodor, S. P., and Gallop, M. A. (1994) Applications of combinatorial technologies to drug discovery. 2. Combinatorial organic synthesis, library screening strategies, and future directions. *J Med Chem* **37**, 1385-1401

98. Brocchini, S., James, K., Tangpasuthadol, V., and Kohn, J. (1998) Structure-property correlations in a combinatorial library of degradable biomaterials. *Journal of biomedical materials research* **42**, 66-75

99. Freeman, A. W., Chrisstoffels, L. A., and Frechet, J. M. (2000) A simple method for controlling dendritic architecture and diversity: A parallel monomer combination approach. *J Org Chem* **65**, 7612-7617

100. Kim, D. Y., and Dordick, J. S. (2001) Combinatorial array-based enzymatic polyester synthesis. *Biotechnol Bioeng* **76**, 200-206

101. Lavastre, O., Illitchev, I., Jegou, G., and Dixneuf, P. H. (2002) Discovery of new fluorescent materials from fast synthesis and screening of conjugated polymers. *Journal of the American Chemical Society* **124**, 5278-5279

102. Vogel, B. M., Cabral, J. T., Eidelman, N., Narasimhan, B., and Mallapragada, S. K. (2005) Parallel synthesis and high throughput dissolution testing of biodegradable polyanhydride copolymers. *Journal of combinatorial chemistry* **7**, 921-928

103. Akinc, A., Lynn, D. M., Anderson, D. G., and Langer, R. (2003) Parallel synthesis and biophysical characterization of a degradable polymer library for gene delivery. *Journal of the American Chemical Society* **125**, 5316-5323

104. Lynn, D. M., Anderson, D. G., Putnam, D., and Langer, R. (2001) Accelerated discovery of synthetic transfection vectors: Parallel synthesis and screening of degradable polymer library. *Journal of the American Chemical Society* **123**, 8155-8156

105. Lynn, D. M., and Langer, R. (2000) Degradable Poly(beta-amino esters): Synthesis, Characterization, and Self-Assembly with Plasmid DNA. *J. Am. Chem. Soc.* **122**, 10761-10768

106. Green, J. J., Langer, R., and Anderson, D. G. (2008) A combinatorial polymer library approach yields insight into nonviral gene delivery. *Accounts of Chemical Research* **41**, 749-759

107. Anderson, D. G., Akinc, A., Hossain, N., and Langer, R. (2005) Structure/property studies of polymeric gene delivery using a library of poly(beta-amino esters). *Mol Ther* **11**, 426-434

108. Raman, V. I., and Palmese, G. R. (2005) Nanoporous thermosetting polymers. *Langmuir* **21**, 1539-1546

109. Boger, D. L., Fink, B. E., Brunette, S. R., Tse, W. C., and Hedrick, M. P. (2001) A simple, high-resolution method for establishing DNA binding affinity and sequence selectivity. *Journal of the American Chemical Society* **123**, 5878-5891

110. Geall, A. J., and Blagbrough, I. S. (2000) Rapid and sensitive ethidium bromide fluorescence quenching assay of polyamine conjugate-DNA interactions for the analysis of lipoplex formation in gene therapy. *Journal of pharmaceutical and biomedical analysis* **22**, 849-859

111. Rege, K., Hu, S., Moore, J. A., Dordick, J. S., and Cramer, S. M. (2004) Chemoenzymatic synthesis and high-throughput screening of an aminoglycoside-polyamine library: identification of high-affinity displacers and DNA-binding ligands. *J Am Chem Soc* **126**, 12306-12315

112. Rege, K., Ladiwala, A., Hu, S., Breneman, C. M., Dordick, J. S., and Cramer, S. M. (2005) Investigation of DNA-binding properties of an aminoglycoside-polyamine library using quantitative structure-activity relationship (QSAR) models. *J Chem Inf Model* **45**, 1854-1863

113. Gong, M. C., Latouche, J. B., Krause, A., Heston, W. D., Bander, N. H., and Sadelain, M. (1999) Cancer patient T cells genetically targeted to prostate-specific membrane antigen specifically lyse prostate cancer cells and release cytokines in response to prostate-specific membrane antigen. *Neoplasia (New York, N.Y* **1**, 123-127

114. Friedman, M. (2004) Applications of the ninhydrin reaction for analysis of amino acids, peptides, and proteins to agricultural and biomedical sciences. *Journal of Agricultural and Food Chemistry* **52**, 385-406

115. Joshi, A., Saraph, A., Poon, V., Mogridge, J., and Kane, R. S. (2006) Synthesis of potent inhibitors of anthrax toxin based on poly-L-glutamic acid. *Bioconjugate chemistry* **17**, 1265-1269

116. Khanam, N., Mikoryak, C., Draper, R. K., and Balkus, K. J., Jr. (2007) Electrospun linear polyethyleneimine scaffolds for cell growth. *Acta biomaterialia* **3**, 1050-1059

117. Swami, A., Kurupati, R. K., Pathak, A., Singh, Y., Kumar, P., and Gupta, K. C. (2007) A unique and highly efficient non-viral DNA/siRNA delivery system based on PEI-bisepoxide nanoparticles. *Biochemical and biophysical research communications* **362**, 835-841

118. Yu, X. X., Wan, C. X., and Chen, H. Q. (2008) Preparation and endothelialization of decellularised vascular scaffold for tissue-engineered blood vessel. *Journal of materials science* **19**, 319-326

119. Segura, T., Chung, P. H., and Shea, L. D. (2005) DNA delivery from hyaluronic acid-collagen hydrogels via a substrate-mediated approach. *Biomaterials* **26**, 1575-1584

120. Soo-Woo Kim, T. O. Y. T. I. N. (2004) Efficacy and cytotoxicity of cationic-agent-mediated nonviral gene transfer into osteoblasts. *Journal of Biomedical Materials Research Part A* **71A**, 308-315

121. Loos, M. R., Coelho, L. A. F., Pezzin, S. H., and Amico, S. C. (2008) The effect of acetone addition on the properties of epoxy. *Polim.: Cienc. Tecnol.* **18**, 76-80

122. Gosselin, M. A., Guo, W., and Lee, R. J. (2001) Efficient gene transfer using reversibly cross-linked low molecular weight polyethylenimine. *Bioconjugate chemistry* **12**, 989-994

123. Akinc, A., Anderson, D. G., Lynn, D. M., and Langer, R. (2003) Synthesis of poly(beta-amino ester)s optimized for highly effective gene delivery. *Bioconjugate chemistry* **14**, 979-988

124. Anderson, D. G., Peng, W., Akinc, A., Hossain, N., Kohn, A., Padera, R., Langer, R., and Sawicki, J. A. (2004) A polymer library approach to suicide gene therapy for cancer. *Proceedings of the National Academy of Sciences of the United States of America* **101**, 16028-16033

125. Thomas, M., Lu, J. J., Zhang, C., Chen, J., and Klibanov, A. M. (2007) Identification of novel superior polycationic vectors for gene delivery by high-throughput synthesis and screening of a combinatorial library. *Pharmaceutical research* **24**, 1564-1571

126. Apodaca, G. (2001) Endocytic traffic in polarized epithelial cells: role of the actin and microtubule cytoskeleton. *Traffic (Copenhagen, Denmark)* **2**, 149-159

127. Musch, A. (2004) Microtubule organization and function in epithelial cells. *Traffic (Copenhagen, Denmark)* **5**, 1-9

128. Bonaccorsi, L., Nosi, D., Muratori, M., Formigli, L., Forti, G., and Baldi, E. (2007) Altered endocytosis of epidermal growth factor receptor in androgen receptor positive prostate cancer cell lines. *Journal of molecular endocrinology* **38**, 51-66

129. Guimaraes, A. R., Tabatabei, S., Dahl, D., McDougal, W. S., Weissleder, R., and Harisinghani, M. G. (2008) Pilot study evaluating use of lymphotrophic nanoparticle-enhanced magnetic resonance imaging for assessing lymph nodes in renal cell cancer. *Urology* **71**, 708-712

130. Johannsen, M., Gneveckow, U., Thiesen, B., Taymoorian, K., Cho, C. H., Waldofner, N., Scholz, R., Jordan, A., Loening, S. A., and Wust, P. (2007) Thermotherapy of prostate cancer using magnetic nanoparticles: feasibility, imaging, and three-dimensional temperature distribution. *European urology* **52**, 1653-1661

131. Maier-Hauff, K., Rothe, R., Scholz, R., Gneveckow, U., Wust, P., Thiesen, B., Feussner, A., von Deimling, A., Waldoefner, N., Felix, R., and Jordan, A. (2007) Intracranial thermotherapy using magnetic nanoparticles combined with external beam radiotherapy: results of a feasibility study on patients with glioblastoma multiforme. *Journal of neuro-oncology* **81**, 53-60

132. Lidke, D. S., Nagy, P., Heintzmann, R., Arndt-Jovin, D. J., Post, J. N., Grecco, H. E., Jares-Erijman, E. A., and Jovin, T. M. (2004) Quantum dot ligands provide new insights into erbB/HER receptor-mediated signal transduction. *Nature biotechnology* **22**, 198-203

133. Vasir, J. K., and Labhasetwar, V. (2007) Biodegradable nanoparticles for cytosolic delivery of therapeutics. *Advanced drug delivery reviews* **59**, 718-728

134. Serda, R. E., Adolphi, N. L., Bisoffi, M., and Sillerud, L. O. (2007) Targeting and cellular trafficking of magnetic nanoparticles for prostate cancer imaging. *Mol Imaging* **6**, 277-288

135. Emmanuel Chang, N. T. William W. Y. Vicki L. C. R. D. (2006) Evaluation of Quantum Dot Cytotoxicity Based on Intracellular Uptake13. *Small (Weinheim an der Bergstrasse, Germany)* **2**, 1412-1417

136. Tanya S. Hauck, Arezou A. G. Warren C. W. C. (2008) Assessing the Effect of Surface Chemistry on Gold Nanorod Uptake, Toxicity, and Gene Expression in Mammalian Cells. *Small (Weinheim an der Bergstrasse, Germany)* **4**, 153-159

137. Ruan, G., Agrawal, A., Marcus, A. I., and Nie, S. (2007) Imaging and Tracking of Tat Peptide-Conjugated Quantum Dots in Living Cells: New Insights into Nanoparticle Uptake, Intracellular Transport, and Vesicle Shedding. *Journal of the American Chemical Society* **129**, 14759-14766

138. Tkachenko, A. G., Xie, H., Liu, Y., Coleman, D., Ryan, J., Glomm, W. R., Shipton, M. K., Franzen, S., and Feldheim, D. L. (2004) Cellular trajectories of peptide-modified gold particle complexes: comparison of nuclear localization signals and peptide transduction domains. *Bioconjugate chemistry* **15**, 482-490

139. Delehanty, J. B., Medintz, I. L., Pons, T., Brunel, F. M., Dawson, P. E., and Mattoussi, H. (2006) Self-assembled quantum dot-peptide bioconjugates for selective intracellular delivery. *Bioconjugate chemistry* **17**, 920-927

140. Chithrani, B. D., and Chan, W. C. (2007) Elucidating the mechanism of cellular uptake and removal of protein-coated gold nanoparticles of different sizes and shapes. *Nano letters* **7**, 1542-1550

141. Jiang, W., KimBetty, Y. S., Rutka, J. T., and ChanWarren, C. W. (2008) Nanoparticle-mediated cellular response is size-dependent. *Nat Nano* **3**, 145-150

142. Lai, S. K., Hida, K., Man, S. T., Chen, C., Machamer, C., Schroer, T. A., and Hanes, J. (2007) Privileged delivery of polymer nanoparticles to the perinuclear region of live cells via a non-clathrin, non-degradative pathway. *Biomaterials* **28**, 2876-2884

143. Jemal, A., Siegel, R., Xu, J., and Ward, E. (2010) Cancer Statistics, 2010. *CA Cancer J Clin*, caac.20073

144. Miyamoto, H., Messing, E. M., and Chang, C. (2004) Androgen deprivation therapy for prostate cancer: current status and future prospects. *Prostate* **61**, 332-353

145. Gu, F., Zhang, L., Teply, B. A., Mann, N., Wang, A., Radovic-Moreno, A. F., Langer, R., and Farokhzad, O. C. (2008) Precise engineering of targeted nanoparticles by using self-assembled biointegrated block copolymers. *Proceedings of the National Academy of Sciences of the United States of America* **105**, 2586-2591

146. Stern, J. M., Stanfield, J., Kabbani, W., Hsieh, J. T., and Cadeddu, J. A. (2008) Selective prostate cancer thermal ablation with laser activated gold nanoshells. *The Journal of urology* **179**, 748-753

147. Sahoo, S. K., Ma, W., and Labhasetwar, V. (2004) Efficacy of transferrin-conjugated paclitaxel-loaded nanoparticles in a murine model of prostate cancer. *International journal of cancer* **112**, 335-340

148. Michalet, X., Pinaud, F. F., Bentolila, L. A., Tsay, J. M., Doose, S., Li, J. J., Sundaresan, G., Wu, A. M., Gambhir, S. S., and Weiss, S. (2005) Quantum Dots for Live Cells, in Vivo Imaging, and Diagnostics. *science* **307**, 538-544

149. Medintz, I. L., Uyeda, H. T., Goldman, E. R., and Mattoussi, H. (2005) Quantum dot bioconjugates for imaging, labelling and sensing. *Nat Mater* **4**, 435-446

150. Rasband, and W.S. (2004) ImageJ. National Institutes of Health, Bethesda, Maryland, USA

151. Silver, J., and Ou, W. (2005) Photoactivation of quantum dot fluorescence following endocytosis. *Nano letters* **5**, 1445-1449

152. Zhang, L. W., and Monteiro-Riviere, N. A. (2009) Mechanism of Quantum Dot Nanoparticle Cellular Uptake. *Toxicological Sciences*

153. Baravalle, G., Schober, D., Huber, M., Bayer, N., Murphy, R. F., and Fuchs, R. (2005) Transferrin recycling and dextran transport to lysosomes is differentially affected by bafilomycin, nocodazole, and low temperature. *Cell and tissue research* **320**, 99-113

154. Vossenkamper, A., Nedvetsky, P. I., Wiesner, B., Furkert, J., Rosenthal, W., and Klussmann, E. (2007) Microtubules are needed for the perinuclear positioning of aquaporin-2 after its endocytic retrieval in renal principal cells. *American journal of physiology* **293**, C1129-1138

155. Maxfield, F. R., and McGraw, T. E. (2004) Endocytic recycling. *Nature reviews* **5**, 121-132

156. Perner, S., Hofer, M. D., Kim, R., Shah, R. B., Li, H., Moller, P., Hautmann, R. E., Gschwend, J. E., Kuefer, R., and Rubin, M. A. (2007) Prostate-specific membrane antigen expression as a predictor of prostate cancer progression. *Human pathology* **38**, 696-701

157. Mhawech-Fauceglia, P., Zhang, S., Terracciano, L., Sauter, G., Chadhuri, A., Herrmann, F. R., and Penetrante, R. (2007) Prostate-specific membrane antigen (PSMA) protein expression in normal and neoplastic tissues and its sensitivity and specificity in prostate adenocarcinoma: an immunohistochemical study using mutiple tumour tissue microarray technique. *Histopathology* **50**, 472-483

158. Chu, T. C., Marks, J. W., 3rd, Lavery, L. A., Faulkner, S., Rosenblum, M. G., Ellington, A. D., and Levy, M. (2006) Aptamer:toxin conjugates that specifically target prostate tumor cells. *Cancer Res* **66**, 5989-5992

159. Henry, M. D., Wen, S., Silva, M. D., Chandra, S., Milton, M., and Worland, P. J. (2004) A prostate-specific membrane antigen-targeted monoclonal antibody-chemotherapeutic conjugate designed for the treatment of prostate cancer. *Cancer research* **64**, 7995-8001

160. Bander, N. H., Nanus, D. M., Milowsky, M. I., Kostakoglu, L., Vallabahajosula, S., and Goldsmith, S. J. (2003) Targeted systemic therapy of prostate cancer with a monoclonal antibody to prostate-specific membrane antigen. *Seminars in Oncology* **30**, 667-677

161. Farokhzad, O. C., Jon, S., Khademhosseini, A., Tran, T. N., Lavan, D. A., and Langer, R. (2004) Nanoparticle-aptamer bioconjugates: a new approach for targeting prostate cancer cells. *Cancer Res* **64**, 7668-7672

162. Rege, K., Patel, S. J., Megeed, Z., and Yarmush, M. L. (2007) Amphipathic peptide-based fusion peptides and immunoconjugates for the targeted ablation of prostate cancer cells. *Cancer Res* **67**, 6368-6375

163. Lawrence, C. M., Ray, S., Babyonyshev, M., Galluser, R., Borhani, D. W., and Harrison, S. C. (1999) Crystal structure of the ectodomain of human transferrin receptor. *Science (New York, N.Y* **286**, 779-782

164. Kawabata, H., Yang, R., Hirama, T., Vuong, P. T., Kawano, S., Gombart, A. F., and Koeffler, H. P. (1999) Molecular cloning of transferrin receptor 2. A new member of the transferrin receptor-like family. *The Journal of biological chemistry* **274**, 20826-20832

165. Davis, M. I., Bennett, M. J., Thomas, L. M., and Bjorkman, P. J. (2005) Crystal structure of prostate-specific membrane antigen, a tumor marker and peptidase. *Proceedings of the National Academy of Sciences of the United States of America* **102**, 5981-5986

166. Liu, H., Rajasekaran, A. K., Moy, P., Xia, Y., Kim, S., Navarro, V., Rahmati, R., and Bander, N. H. (1998) Constitutive and antibody-induced internalization of prostate-specific membrane antigen. *Cancer Res* **58**, 4055-4060

167. Anilkumar, G., Rajasekaran, S. A., Wang, S., Hankinson, O., Bander, N. H., and Rajasekaran, A. K. (2003) Prostate-specific membrane antigen association with filamin A modulates its internalization and NAALADase activity. *Cancer research* **63**, 2645-2648

168. Shah, R. B., Mehra, R., Chinnaiyan, A. M., Shen, R., Ghosh, D., Zhou, M., MacVicar, G. R., Varambally, S., Harwood, J., Bismar, T. A., Kim, R., Rubin, M. A., and Pienta, K. J. (2004) Androgen-Independent Prostate

Cancer Is a Heterogeneous Group of Diseases. *Cancer Research* **64**, 9209-9216

169. Freytag, S. O., Stricker, H., Pegg, J., Paielli, D., Pradhan, D. G., Peabody, J., DePeralta-Venturina, M., Xia, X., Brown, S., Lu, M., and Kim, J. H. (2003) Phase I Study of Replication-Competent Adenovirus-Mediated Double-Suicide Gene Therapy in Combination with Conventional-Dose Three-Dimensional Conformal Radiation Therapy for the Treatment of Newly Diagnosed, Intermediate- to High-Risk Prostate Cancer. *Cancer Research* **63**, 7497-7506

170. Khuri, F. R., Nemunaitis, J., Ganly, I., Arseneau, J., Tannock, I. F., Romel, L., Gore, M., Ironside, J., MacDougall, R. H., Heise, C., Randlev, B., Gillenwater, A. M., Bruso, P., Kaye, S. B., Hong, W. K., and Kirn, D. H. (2000) A controlled trial of intratumoral ONYX-015, a selectively-replicating adenovirus, in combination with cisplatin and 5-fluorouracil in patients with recurrent head and neck cancer. *Nature Medicine* **6**, 879-885

171. Richon, V. M., Sandhoff, T. W., Rifkind, R. A., and Marks, P. A. (2000) Histone deacetylase inhibitor selectively induces p21(WAF1) expression and gene-associated histone acetylation. *Proceedings of the National Academy of Sciences of the United States of America* **97**, 10014-10019

172. Xiao, H. Y., Hasegawa, T., and Isobe, K. (2000) p300 collaborates with Sp1 and Sp3 in p21(waf1/cip1) promoter activation induced by histone deacetylase inhibitor. *Journal of Biological Chemistry* **275**, 1371-1376

173. Dompierre, J. P., Godin, J. D., Charrin, B. C., Cordelieres, F. P., King, S. J., Humbert, S., and Saudou, F. (2007) Histone deacetylase 6 inhibition compensates for the transport deficit in Huntington's disease by increasing tubulin acetylation. *Journal of Neuroscience* **27**, 3571-3583

174. Roth, D. M., Moseley, G. W., Glover, D., Pouton, C. W., and Jans, D. A. (2007) A microtubule-facilitated nuclear import pathway for cancer regulatory proteins. *Traffic* **8**, 673-686

175. Marks, P. A., Richon, V. M., and Rifkind, R. A. (2000) Histone deacetylase inhibitors: Inducers of differentiation or apoptosis of transformed cells. *Journal of the National Cancer Institute* **92**, 1210-1216

176. Johnstone, R. W. (2002) Histone-deacetylase inhibitors: Novel drugs for the treatment of cancer. *Nature Reviews Drug Discovery* **1**, 287-299

177. Peart, M. J., Tainton, K. M., Ruefli, A. A., Dear, A. E., Sedelies, K. A., O'Reilly, L. A., Waterhouse, N. J., Trapani, J. A., and Johnstone, R. W. (2003) Novel mechanisms of apoptosis induced by histone deacetylase inhibitors. *Cancer Research* **63**, 4460-4471

178. Rasheed, W. K., Johnstone, R. W., and Prince, H. M. (2007) Histone deacetylase inhibitors in cancer therapy. *Expert Opinion on Investigational Drugs* **16**, 659-678

179. Haggarty, S. J., Koeller, K. M., Wong, J. C., Grozinger, C. M., and Schreiber, S. L. (2003) Domain-selective small-molecule inhibitor of histone deacetylase 6 (HDAC6)-mediated tubulin deacetylation. *Proceedings of the National Academy of Sciences of the United States of America* **100**, 4389-4394

180. Barua, S., Joshi, A., Banerjee, A., Matthews, D., Sharfstein, S. T., Cramer, S. M., Kane, R. S., and Rege, K. (2009) Parallel Synthesis and Screening of Polymers for Nonviral Gene Delivery. *Molecular Pharmaceutics* **6**, 86-97

181. Hideshima, T., Bradner, J. E., Wong, J., Chauhan, D., Richardson, P., Schreiber, S. L., and Anderson, K. C. (2005) Small-molecule inhibition of proteasome and aggresome function induces synergistic antitumor activity in multiple myeloma. *Proceedings of the National Academy of Sciences of the United States of America* **102**, 8567-8572

182. Johnston, J. A., Ward, C. L., and Kopito, R. R. (1999) Aggresomes: A cellular response to misfolded proteins. *Faseb Journal* **13**, 1883-1898

183. Simms-Waldrip, T., Rodriguez-Gonzalez, A., Lin, T., Ikeda, A. K., Fu, C., and Sakamoto, K. M. (2008) The aggresome pathway as a target for therapy in hematologic malignancies. *Molecular Genetics and Metabolism* **94**, 283-286

184. Olzmann, J. A., Li, L., and Chin, L. S. (2008) Aggresome formation and neurodegenerative diseases: Therapeutic implications. *Current Medicinal Chemistry* **15**, 47-60

185. Chou, T. C., and Talalay, P. (1984) Quantitative analysis of dose-effect relationships: the combined effects of multiple drugs or enzyme inhibitors. *Adv Enzyme Regul* **22**, 27-55

186. Haggarty, S. J., Koeller, K. M., Wong, J. C., Grozinger, C. M., and Schreiber, S. L. (2003) Domain-selective small-molecule inhibitor of histone deacetylase 6 (HDAC6)-mediated tubulin deacetylation. *Proceedings of the National Academy of Sciences of the United States of America* **100**, 4389-4394

187. Vaughan, E. E., and Dean, D. A. (2006) Intracellular trafficking of plasmids during transfection is mediated by microtubules. *Mol Ther* **13**, 422-428

188. Miller, A. M., and Dean, D. A. (2009) Tissue-specific and transcription factor-mediated nuclear entry of DNA. *Advanced drug delivery reviews* **61**, 603-613

189. Bishop, C. L., Ramalho, M., Nadkarni, N., May Kong, W., Higgins, C. F., and Krauzewicz, N. (2006) Role for centromeric heterochromatin and PML nuclear bodies in the cellular response to foreign DNA. *Mol Cell Biol* **26**, 2583-2594

190. Reed, N. A., Cai, D., Blasius, T. L., Jih, G. T., Meyhofer, E., Gaertig, J., and Verhey, K. J. (2006) Microtubule acetylation promotes kinesin-1 binding and transport. *Curr Biol* **16**, 2166-2172

191. Vaughan, E. E., Geiger, R. C., Miller, A. M., Loh-Marley, P. L., Suzuki, T., Miyata, N., and Dean, D. A. (2008) Microtubule Acetylation Through HDAC6 Inhibition Results in Increased Transfection Efficiency. *Molecular Therapy* **16**, 1841-1847

192. Soppina, V., Rai, A. K., Ramaiya, A. J., Barak, P., and Mallik, R. (2009) Tug-of-war between dissimilar teams of microtubule motors regulates transport and fission of endosomes. *Proceedings of the National Academy of Sciences of the United States of America* **106**, 19381-19386

193. Wolffe, A. P., and Pruss, D. (1996) Targeting chromatin disruption: Transcription regulators that acetylate histones. *Cell* **84**, 817-819

194. Ishiguro, K., and Sartorelli, A. C. (2004) Activation of transiently transfected reporter genes in 3T3 Swiss cells by the inducers of differentiation/apoptosis - dimethylsulfoxide, hexamethylene bisacetamide and trichostatin A. *European Journal of Biochemistry* **271**, 2379-2390

195. Nan, X., Hyndman, L., Agbi, N., Porteous, D. J., and Boyd, A. C. (2004) Potent stimulation of gene expression by histone deacetylase inhibitors on transiently transfected DNA. *Biochemical and biophysical research communications* **324**, 348-354

196. Davis, M. E., Zuckerman, J. E., Choi, C. H. J., Seligson, D., Tolcher, A., Alabi, C. A., Yen, Y., Heidel, J. D., and Ribas, A. (2010) Evidence of RNAi in humans from systemically administered siRNA via targeted nanoparticles. *Nature* **464**, 1067-U1140

197. Green, J. J., Zhou, B. Y., Mitalipova, M. M., Beard, C., Langer, R., Jaenisch, R., and Anderson, D. G. (2008) Nanoparticles for Gene Transfer to Human Embryonic Stem Cell Colonies. *Nano Letters* **8**, 3126-3130

198. Farokhzad, O. C., Cheng, J., Teply, B. A., Sherifi, I., Jon, S., Kantoff, P. W., Richie, J. P., and Langer, R. (2006) Targeted nanoparticle-aptamer bioconjugates for cancer chemotherapy in vivo. *Proc Natl Acad Sci U S A* **103**, 6315-6320

199. Lynn, D. M., and Langer, R. (2000) Degradable poly(beta-amino esters): Synthesis, characterization, and self-assembly with plasmid DNA. *Journal of the American Chemical Society* **122**, 10761-10768

200. Wu, D. C., Liu, Y., Jiang, X., He, C. B., Goh, S. H., and Leong, K. W. (2006) Hyperbranched poly(amino ester)s with different terminal amine groups for DNA delivery. *Biomacromolecules* **7**, 1879-1883

201. Lo, C. T., Van Tassel, P. R., and Saltzman, W. M. (2010) Poly(lactide-co-glycolide) nanoparticle assembly for highly efficient delivery of potent therapeutic agents from medical devices. *Biomaterials* **31**, 3631-3642

202. Bryson, J. M., Fichter, K. M., Chu, W. J., Lee, J. H., Li, J., Madsen, L. A., McLendon, P. M., and Reineke, T. M. (2009) Polymer beacons for luminescence and magnetic resonance imaging of DNA delivery.

Proceedings of the National Academy of Sciences of the United States of America **106**, 16913-16918

203. Gasiorowski, J. Z., and Dean, D. A. (2007) Intranuclear trafficking of episomal DNA is transcription-dependent. *Molecular Therapy* **15**, 2132-2139

204. Dean, D. A. (2009) Cytoplasmic and Nuclear Trafficking of Plasmids During Gene Delivery. *In Vitro Cellular & Developmental Biology-Animal* **45**, S2-S2

205. Miller, A. M., and Dean, D. A. (2009) Tissue-specific and transcription factor-mediated nuclear entry of DNA. *Advanced Drug Delivery Reviews* **61**, 603-613

206. Barua, S., and Rege, K. The influence of mediators of intracellular trafficking on transgene expression efficacy of polymer-plasmid DNA complexes. *Biomaterials* **31**, 5894-5902

207. Maeshima, K., Iino, H., Hihara, S., Funakoshi, T., Watanabe, A., Nishimura, M., Nakatomi, R., Yahata, K., Imamoto, F., Hashikawa, T., Yokota, H., and Imamoto, N. (2010) Nuclear pore formation but not nuclear growth is governed by cyclin-dependent kinases (Cdks) during interphase. *Nat Struct Mol Biol* **17**, 1065-1071

208. Maeshima, K., Yahata, K., Sasaki, Y., Nakatomi, R., Tachibana, T., Hashikawa, T., Imamoto, F., and Imamoto, N. (2006) Cell-cycle-dependent dynamics of nuclear pores: pore-free islands and lamins. *J Cell Sci* **119**, 4442-4451

209. Tseng, W. C., Haselton, F. R., and Giorgio, T. D. (1999) Mitosis enhances transgene expression of plasmid delivered by cationic liposomes. *Biochimica Et Biophysica Acta-Gene Structure and Expression* **1445**, 53-64

210. Zhou, H. Y., Kuang, J., Zhong, L., Kuo, W. L., Gray, J. W., Sahin, A., Brinkley, B. R., and Sen, S. (1998) Tumour amplified kinase STK15/BTAK induces centrosome amplification, aneuploidy and transformation. *Nature Genetics* **20**, 189-193

211. Bischoff, J. R., and Plowman, G. D. (1999) The Aurora/Ipi1p kinase family: regulators of chromosome segregation and cytokinesis. *Trends in Cell Biology* **9**, 454-459

212. Bischoff, J. R., Anderson, L., Zhu, Y. F., Mossie, K., Ng, L., Souza, B., Schryver, B., Flanagan, P., Clairvoyant, F., Ginther, C., Chan, C. S. M., Novotny, M., Slamon, D. J., and Plowman, G. D. (1998) A homologue of Drosophila aurora kinase is oncogenic and amplified in human colorectal cancers. *Embo Journal* **17**, 3052-3065

213. Tatsuka, M., Katayama, H., Ota, T., Tanaka, T., Odashima, S., Suzuki, F., and Terada, Y. (1998) Multinuclearity and increased ploidy caused by overexpression of the aurora- and Ipl1-like midbody-associated protein mitotic kinase in human cancer cells. *Cancer Research* **58**, 4811-4816

214. Prabha, S., and Labhasetwar, V. (2004) Nanoparticle-mediated wild-type p53 gene delivery results in sustained antiproliferative activity in breast cancer cells. *Mol Pharm* **1**, 211-219

215. Harrington, E. A., Bebbington, D., Moore, J., Rasmussen, R. K., Ajose-Adeogun, A. O., Nakayama, T., Graham, J. A., Demur, C., Hercend, T., Diu-Hercend, A., Su, M., Golec, J. M. C., and Miller, K. M. (2004) VX-680, a potent and selective small-molecule inhibitor of the Aurora kinases, suppresses tumor growth in vivo. *Nature Medicine* **10**, 262-267

216. Romé, P., Montembault, E., Franck, N., Pascal, A., Glover, D. M., and Giet, R. (2010) Aurora A contributes to p150glued phosphorylation and function during mitosis. *The Journal of Cell Biology* **189**, 651-659

217. Brunner, S., Sauer, T., Carotta, S., Cotten, M., Saltik, M., and Wagner, E. (2000) Cell cycle dependence of gene transfer by lipoplex polyplex and recombinant adenovirus. *Gene Therapy* **7**, 401-407

218. Akita, H., Ito, R., Kamiya, H., Kogure, K., and Harashima, H. (2007) Cell cycle dependent transcription, a determinant factor of heterogeneity in cationic tipid-mediated transgene expression. *Journal of Gene Medicine* **9**, 197-207

219. Chaudhary, N., and Courvalin, J. C. (1993) Stepwise reassembly of the nuclear envelope at the end of mitosis. *Journal of Cell Biology* **122**, 295-306

220. Beaudouin, J., Gerlich, D., Daigle, N., Eils, R., and Ellenberg, J. (2002) Nuclear envelope breakdown proceeds by microtubule-induced tearing of the lamina. *Cell* **108**, 83-96

221. Salina, D., Bodoor, K., Eckley, D. M., Schroer, T. A., Rattner, J. B., and Burke, B. (2002) Cytoplasmic dynein as a facilitator of nuclear envelope breakdown. *Cell* **108**, 97-107

222. Lin, D., Shields, M. T., Ullrich, S. J., Appella, E., and Mercer, W. E. (1992) Growth arrest induced by wild-type p53 protein blocks cells prior to or near the restriction point in late G1 phase. *Proceedings of the National Academy of Sciences of the United States of America* **89**, 9210-9214

223. Miyashita, T., Krajewski, S., Krajewska, M., Wang, H. G., Lin, H. K., Liebermann, D. A., Hoffman, B., and Reed, J. C. (1994) Tumor-suppressor p53 is a regulator of bcl-2 and Bax gene-expression *in vitro* and *in vivo*. *Oncogene* **9**, 1799-1805

224. Miyashita, T., and Reed, J. C. (1995) Tumor-suppresor p53 is a direct transcriptional activator of the human Bax gene. *Cell* **80**, 293-299

225. Yang, C. L., Cirielli, C., Capogrossi, M. C., and Passaniti, A. (1995) Adenovirus-mediated wild-type p53 expression induces apoptosis and suppresses tumorigenesis of prostatic tumor cells *Cancer Research* **55**, 4210-4213

226. Lee, J. M., and Bernstein, A. (1993) p53 mutations increase resistance to ionizing-radiation. *Proceedings of the National Academy of Sciences of the United States of America* **90**, 5742-5746

227. Toffoli, G., Doglioni, C., Cernigoi, C., Frustaci, S., Perin, T., Canal, B., and Boiocchi, M. (1994) p53 overexpression in human soft-tissue sarcomas- relation to biological aggressiveness. *Annals of Oncology* **5**, 167-172

228. Srivastava, S., Katayose, D., Tong, Y. A., Craig, C. R., McLeod, D. G., Moul, J. W., Cowan, K. H., and Seth, P. (1995) Recombinant adenovirus vector expressing wild-type p53 is a potent inhibitor of prostate cancer cell proliferation. *Urology* **46**, 843-848

229. Nielsen, L. L., Lipari, P., Dell, J., Gurnani, M., and Hajian, G. (1998) Adenovirus-mediated p53 gene therapy and paclitaxel have synergistic efficacy in models of human head and neck, ovarian, prostate, and breast cancer. *Clinical Cancer Research* **4**, 835-846

230. Eastham, J. A., Grafton, W., Martin, C. M., and Williams, B. J. (2000) Suppression of primary tumor growth and the progression to metastasis with p53 adenovirus in human prostate cancer. *Journal of Urology* **164**, 814-819

231. Morris, M. J., and Scher, H. I. (2002) Novel therapies for the treatment of prostate cancer: current clinical trials and development strategies. *Surg Oncol* **11**, 13-23

232. Haupt, S., Berger, M., Goldberg, Z., and Haupt, Y. (2003) Apoptosis - the p53 network. *Journal of Cell Science* **116**, 4077-4085

233. Katayama, H., Sasai, K., Kawai, H., Yuan, Z. M., Bondaruk, J., Suzuki, F., Fujii, S., Arlinghaus, R. B., Czerniak, B. A., and Sen, S. (2004) Phosphorylation by aurora kinase A induces Mdm2-mediated destabilization and inhibition of p53. *Nature Genetics* **36**, 55-62

234. Li, M. L., Jung, A., Ganswindt, U., Marini, P., Friedl, A., Daniel, P. T., Lauber, K., Jendrossek, V., and Belka, C. (2010) Aurora kinase inhibitor ZM447439 induces apoptosis via mitochondrial pathways. *Biochemical Pharmacology* **79**, 122-129

235. Zelphati, O., Uyechi, L. S., Barron, L. G., and Szoka, F. C. (1998) Effect of serum components on the physico-chemical properties of cationic lipid/oligonucleotide complexes and on their interactions with cells. *Biochimica Et Biophysica Acta-Lipids and Lipid Metabolism* **1390**, 119-133

236. Ogris, M., Brunner, S., Schuller, S., Kircheis, R., and Wagner, E. (1999) PEGylated DNA/transferrin-PEI complexes: reduced interaction with

blood components, extended circulation in blood and potential for systemic gene delivery. *Gene Therapy* **6**, 595-605

237. Zhang, Y. Q., Chen, J. J., Zhang, Y. D., Pan, Y. F., Zhao, J. F., Ren, L. F., Liao, M. M., Hu, Z. Y., Kong, L., and Wang, J. W. (2007) A novel PEGylation of chitosan nanoparticles for gene delivery. *Biotechnology and Applied Biochemistry* **46**, 197-204

238. Ravina, M., Cubillo, E., Olmeda, D., Novoa-Carballal, R., Fernandez-Megia, E., Riguera, R., Sanchez, A., Cano, A., and Alonso, M. J. (2010) Hyaluronic Acid/Chitosan-g-Poly(ethylene glycol) Nanoparticles for Gene Therapy: An Application for pDNA and siRNA Delivery. *Pharmaceutical Research* **27**, 2544-2555

239. Huang, F. W., Wang, H. Y., Li, C., Wang, H. F., Sun, Y. X., Feng, J., Zhang, X. Z., and Zhuo, R. X. (2010) PEGylated PEI-based biodegradable polymers as non-viral gene vectors. *Acta Biomaterialia* **6**, 4285-4295

240. Sung, S. J., Min, S. H., Cho, K. Y., Lee, S., Min, Y. J., Yeom, Y. I., and Park, J. K. (2003) Effect of polyethylene glycol on gene delivery of polyethylenimine. *Biological & Pharmaceutical Bulletin* **26**, 492-500

241. Lin, C., Zhong, Z. Y., Lok, M. C., Jiang, X. L., Hennink, W. E., Feijen, J., and Engbersen, J. F. J. (2006) Linear poly(amido amine)s with secondary and tertiary amino groups and variable amounts of disulfide linkages: Synthesis and in vitro gene transfer properties. *Journal of Controlled Release* **116**, 130-137

242. Tanaka, K., Kanazawa, T., Ogawa, T., Takashima, Y., Fukuda, T., and Okada, H. (2010) Disulfide crosslinked stearoyl carrier peptides containing arginine and histidine enhance siRNA uptake and gene silencing. *International Journal of Pharmaceutics* **398**, 219-224

243. Germershaus, O., Merdan, T., Bakowsky, U., Behe, M., and Kissel, T. (2006) Trastuzumab-polyethylenimine-polyethylene glycol conjugates for targeting Her2-expressing tumors. *Bioconjugate Chemistry* **17**, 1190-1199

244. Petersen, H., Merdan, T., Kunath, F., Fischer, D., and Kissel, T. (2002) Poly(ethylenimine-co-L-lactamide-co-succinamide): A biodegradable polyethylenimine derivative with an advantageous pH-dependent

hydrolytic degradation for gene delivery. *Bioconjugate Chemistry* **13**, 812-821

245. Moffatt, S., and Cristiano, R. J. (2006) PEGylated J591 mAb loaded in PLGA-PEG-PLGA tri-block copolymer for targeted delivery: in vitro evaluation in human prostate cancer cells. *Int J Pharm* **317**, 10-13

246. Moffatt, S., Papasakelariou, C., Wiehle, S., and Cristiano, R. (2006) Successful in vivo tumor targeting of prostate-specific membrane antigen with a highly efficient J591/PEI/DNA molecular conjugate. *Gene Ther* **13**, 761-772

247. Nanus, D. M., Milowsky, M. I., Kostakoglu, L., Smith-Jones, P. M., Vallabahajosula, S., Goldsmith, S. J., and Bander, N. H. (2003) Clinical use of monoclonal antibody HuJ591 therapy: Targeting prostate specific membrane antigen. pp. S84-S88

248. Zhang, K. X., Moussavi, M., Kim, C., Chow, E., Chen, I. S., Fazli, L., Jia, W., and Rennie, P. S. (2009) Lentiviruses with trastuzumab bound to their envelopes can target and kill prostate cancer cells. *Cancer Gene Therapy* **16**, 820-831

249. Seki, M., Iwakawa, J., Cheng, H., and Cheng, P. W. (2002) p53 and PTEN/MMAC1/TEP1 gene therapy of human prostate PC-3 carcinoma xenograft, using transferrin-facilitated lipofection gene delivery strategy. *Human Gene Therapy* **13**, 761-773

250. Murphy, M., Ahn, J., Walker, K. K., Hoffman, W. H., Evans, R. M., Levine, A. J., and George, D. L. (1999) Transcriptional repression by wild-type p53 utilizes histone deacetylases, mediated by interaction with mSin3a. *Genes & Development* **13**, 2490-2501

251. Vaziri, H., Dessain, S. K., Eagon, E. N., Imai, S. I., Frye, R. A., Pandita, T. K., Guarente, L., and Weinberg, R. A. (2001) hSIR2(SIRT1) functions as an NAD-dependent p53 deacetylase. *Cell* **107**, 149-159

252. Roy, S., Packman, K., Jeffrey, R., and Tenniswood, M. (2005) Histone deacetylase inhibitors differentially stabilize acetylated p53 and induce cell cycle arrest or apoptosis in prostate cancer cells. *Cell Death and Differentiation* **12**, 482-491

253. Blagosklonny, M. V., Robey, R., Sackett, D. L., Du, L., Traganos, F., Darzynkiewicz, Z., Fojo, T., and Bates, S. E. (2002) Histone Deacetylase Inhibitors All Induce p21 but Differentially Cause Tubulin Acetylation, Mitotic Arrest, and Cytotoxicity. *Molecular Cancer Therapeutics* **1**, 937-941

254. Henley, D., Isbill, M., Fernando, R., Foster, J. S., and Wimalasena, J. (2007) Paclitaxel induced apoptosis in breast cancer cells requires cell cycle transit but not Cdc2 activity. *Cancer Chemotherapy and Pharmacology* **59**, 235-249

255. North, B. J., and Verdin, E. (2004) Sirtuins: Sir2-related NAD-dependent protein deacetylases. *Genome Biology* **5**

256. Kruszewski, M., and Szumiel, I. (2005) Sirtuins (histone deacetylases III) in the cellular response to DNA damage - Facts and hypotheses. *DNA Repair* **4**, 1306-1313

257. van Leeuwen, I., and Lain, S. (2009) Sirtuins and p53. In *Advances in Cancer Research, Vol 102* Vol. 102 pp. 171-195

258. North, B. J., Marshall, B. L., Borra, M. T., Denu, J. M., and Verdin, E. (2003) The human Sir2 ortholog, SIRT2, is an NAD(+)-dependent tubulin deacetylase. *Molecular Cell* **11**, 437-444

259. Grozinger, C. M., Chao, E. D., Blackwell, H. E., Moazed, D., and Schreiber, S. L. (2001) Identification of a class of small molecule inhibitors of the sirtuin family of NAD-dependent deacetylases by phenotypic screening. *Journal of Biological Chemistry* **276**, 38837-38843

260. Lara, E., Mai, A., Calvanese, V., Altucci, L., Lopez-Nieva, P., Martinez-Chantar, M. L., Varela-Rey, M., Rotili, D., Nebbioso, A., Ropero, S., Montoya, G., Oyarzabal, J., Velasco, S., Serrano, M., Witt, M., Villar-Garea, A., Inhof, A., Mato, J. M., Esteller, M., and Fraga, M. F. (2009) Salermide, a Sirtuin inhibitor with a strong cancer-specific proapoptotic effect. *Oncogene* **28**, 781-791

261. Outeiro, T. F., Kontopoulos, E., Altmann, S. M., Kufareva, I., Strathearn, K. E., Amore, A. M., Volk, C. B., Maxwell, M. M., Rochet, J. C., McLean, P. J., Young, A. B., Abagyan, R., Feany, M. B., Hyman, B. T.,

and Kazantsev, A. G. (2007) Sirtuin 2 inhibitors rescue alpha-synuclein-mediated toxicity in models of Parkinson's disease. *Science* **317**, 516-519

262. Wood, K. W., Lad, L., Luo, L., Qian, X., Knight, S. D., Nevins, N., Brejc, K., Sutton, D., Gilmartin, A. G., Chua, P. R., Desai, R., Schauer, S. P., McNulty, D. E., Annan, R. S., Belmont, L. D., Garcia, C., Lee, Y., Diamond, M. A., Faucette, L. F., Giardiniere, M., Zhang, S., Sun, C.-M., Vidal, J. D., Lichtsteiner, S., Cornwell, W. D., Greshock, J. D., Wooster, R. F., Finer, J. T., Copeland, R. A., Huang, P. S., Morgans, D. J., Dhanak, D., Bergnes, G., Sakowicz, R., and Jackson, J. R. (2010) Antitumor activity of an allosteric inhibitor of centromere-associated protein-E. *Proceedings of the National Academy of Sciences* **107**, 5839-5844

263. Fasbender, A., Zabner, J., Chillon, M., Moninger, T. O., Puga, A. P., Davidson, B. L., and Welsh, M. J. (1997) Complexes of adenovirus with polycationic polymers and cationic lipids increase the efficiency of gene transfer in vitro and in vivo. *The Journal of biological chemistry* **272**, 6479-6489

264. Dodds, E., Piper, T. A., Murphy, S. J., and Dickson, G. (1999) Cationic Lipids and Polymers Are Able to Enhance Adenoviral Infection of Cultured Mouse Myotubes. *Journal of Neurochemistry* **72**, 2105-2112

265. Kasman, L. M., Barua, S., Lu, P., Rege, K., and Voelkel-Johnson, C. (2009) Polymer-Enhanced Adenoviral Transduction of CAR-Negative Bladder Cancer Cells. *Molecular Pharmaceutics* **6**, 1612-1619

266. Eastham, J. A., Hall, S. J., Sehgal, I., Wang, J. X., Timme, T. L., Yang, G., Connellcrowley, L., Elledge, S. J., Zhang, W. W., Harper, J. W., and Thompson, T. C. (1995) In-vivo gene therapy with p53 or p21 adenovirus for prostate cancer *Cancer Research* **55**, 5151-5155

267. Gurnani, M., Lipari, P., Dell, J., Shi, B., and Nielsen, L. L. (1999) Adenovirus mediated p53 gene therapy has greater efficacy when combined with chemotherapy against human head and neck, ovarian, prostate, and breast cancer. *Cancer Chemotherapy and Pharmacology* **44**, 143-151

268. Meunier-Durmort, C., Grimal, H., Sachs, L. M., Demeneix, B. A., and Forest, C. (1997) Adenovirus enhancement of polyethylenimine-mediated transfer of regulated genes in differentiated cells. *Gene therapy* **4**, 808-814

269. Meunier-Durmort, C., Picart, R., Ragot, T., Perricaudet, M., Hainque, B., and Forest, C. (1997) Mechanism of adenovirus improvement of cationic liposome-mediated gene transfer. *Biochim Biophys Acta* **1330**, 8-16

270. Toyoda, K., Ooboshi, H., Chu, Y., Fasbender, A., Davidson, B. L., Welsh, M. J., and Heistad, D. D. (1998) Cationic polymer and lipids enhance adenovirus-mediated gene transfer to rabbit carotid artery. *Stroke* **29**, 2181-2188

271. Chillon, M., Lee, J. H., Fasbender, A., and Welsh, M. J. (1998) Adenovirus complexed with polyethylene glycol and cationic lipid is shielded from neutralizing antibodies in vitro. *Gene therapy* **5**, 995-1002

272. Dodds, E., Piper, T. A., Murphy, S. J., and Dickson, G. (1999) Cationic lipids and polymers are able to enhance adenoviral infection of cultured mouse myotubes. *J Neurochem* **72**, 2105-2112

273. Toyoda, K., Nakane, H., and Heistad, D. D. (2001) Cationic polymer and lipids augment adenovirus-mediated gene transfer to cerebral arteries in vivo. *J Cereb Blood Flow Metab* **21**, 1125-1131

274. Subr, V., Kostka, L., Selby-Milic, T., Fisher, K., Ulbrich, K., Seymour, L. W., and Carlisle, R. C. (2009) Coating of adenovirus type 5 with polymers containing quaternary amines prevents binding to blood components. *J Control Release* **135**, 152-158

275. (2002) Assessment of adenoviral vector safety and toxicity: Report of the National Institutes of Health Recombinant DNA Advisory Committee. *Human Gene Therapy* **13**, 3-13

276. Yamanaka, T., Shiraki, K., Sugimoto, K., Ito, T., Fujikawa, K., Ito, M., Takase, K., Moriyama, M., Nakano, T., and Suzuki, A. (2000) Chemotherapeutic agents augment TRAIL-induced apoptosis in human hepatocellular carcinoma cell lines. *Hepatology* **32**, 482-490

277. Norris, J. S., Hyer, M. L., Voelkel-Johnson, C., Lowe, S. L., Rubinchik, S., and Dong, J. Y. (2001) The use of Fas Ligand, TRAIL and Bax in gene therapy of prostate cancer. *Curr Gene Ther* **1**, 123-136

278. Voelkel-Johnson, C., King, D. L., and Norris, J. S. (2002) Resistance of prostate cancer cells to soluble TNF-related apoptosis-inducing ligand (TRAIL/Apo2L) can be overcome by doxorubicin or adenoviral delivery of full-length TRAIL. *Cancer Gene Therapy* **9**, 164-172

279. Naldini, L. (1998) Lentiviruses as gene transfer agents for delivery to non-dividing cells. *Current Opinion in Biotechnology* **9**, 457-463

280. Quinonez, R., and Sutton, R. E. (2002) Lentiviral vectors for gene delivery into cells. *DNA and Cell Biology* **21**, 937-951

281. Lever, A. M. L., Strappe, P. M., and Zhao, J. (2004) Lentiviral vectors. *Journal of Biomedical Science* **11**, 439-449

282. Pfeifer, A. (2006) Lentiviral transgenesis - A versatile tool for basic research and gene therapy. *Current Gene Therapy* **6**, 535-542

283. Naldini, L., Blömer, U., Gage, F. H., Trono, D., and Verma, I. M. (1996) Efficient transfer, integration, and sustained long-term expression of the transgene in adult rat brains injected with a lentiviral vector. *Proceedings of the National Academy of Sciences of the United States of America* **93**, 11382-11388

284. Pham, P. L., Kamen, A., and Durocher, Y. (2006) Large-scale Transfection of mammalian cells for the fast production of recombinant protein. *Molecular Biotechnology* **34**, 225-237

285. Hay, N. (2005) The Akt-mTOR tango and its relevance to cancer. *Cancer Cell* **8**, 179-183

286. Rodriguezviciana, P., Warne, P. H., Dhand, R., Vanhaesebroeck, B., Gout, I., Fry, M. J., Waterfield, M. D., and Downward, J. (1994) Phosphatidylinosition-3-OH Kinase as a Direct Target of Ras. *Nature* **370**, 527-532

287. Park, I. H., Bachmann, R., Shirazi, H., and Chen, J. (2002) Regulation of ribosomal S6 kinase 2 by mammalian target of rapamycin. *Journal of Biological Chemistry* **277**, 31423-31429

288. Hara, K., Yonezawa, K., Kozlowski, M. T., Sugimoto, T., Andrabi, K., Weng, Q. P., Kasuga, M., Nishimoto, I., and Avruch, J. (1997) Regulation of eIF-4E BP1 phosphorylation by mTOR. *Journal of Biological Chemistry* **272**, 26457-26463

289. Sonenberg, N., and Gingras, A. C. (1998) The mRNA 5 ' cap-binding protein eIF4E and control of cell growth. *Current Opinion in Cell Biology* **10**, 268-275

290. Li, S., Takasu, T., Perlman, D. M., Peterson, M. S., Burrichter, D., Avdulov, S., Bitterman, P. B., and Polunovsky, V. A. (2003) Translation factor eIF4E rescues cells from Myc-dependent apoptosis by inhibiting cytochrome c release. *Journal of Biological Chemistry* **278**, 3015-3022

291. Muise-Helmericks, R. C., Grimes, H. L., Bellacosa, A., Malstrom, S. E., Tsichlis, P. N., and Rosen, N. (1998) Cyclin D expression is controlled post-transcriptionally via a phosphatidylinositol 3-kinase Akt-dependent pathway. *Journal of Biological Chemistry* **273**, 29864-29872

292. Tan, A., Bitterman, P., Sonenberg, N., Peterson, M., and Polunovsky, V. (2000) Inhibition of Myc-dependent apoptosis by eukaryotic translation initiation factor 4E requires cyclin D1. *Oncogene* **19**, 1437-1447

293. Hidalgo, M., and Rowinsky, E. K. (2000) The rapamycin-sensitive signal transduction pathway as a target for cancer therapy. *Oncogene* **19**, 6680-6686

294. Paglin, S., Lee, N.-Y., Nakar, C., Fitzgerald, M., Plotkin, J., Deuel, B., Hackett, N., McMahill, M., Sphicas, E., Lampen, N., and Yahalom, J. (2005) Rapamycin-Sensitive Pathway Regulates Mitochondrial Membrane Potential, Autophagy, and Survival in Irradiated MCF-7 Cells. *Cancer Research* **65**, 11061-11070

295. Hashemolhosseini, S., Nagamine, Y., Morley, S. J., Desrivieres, S., Mercep, L., and Ferrari, S. (1998) Rapamycin inhibition of the G(1) to S

transition is mediated by effects on cyclin D1 mRNA and protein stability. *Journal of Biological Chemistry* **273**, 14424-14429

296. Aguirre, D., Boya, P., Bellet, D., Faivre, S., Troalen, F., Benard, J., Saulnier, P., Hopkins-Donaldson, S., Zangemeister-Wittke, U., Kroemer, G., and Raymond, E. (2004) Bcl-2 and <i>CCND1/CDK4</i> expression levels predict the cellular effects of mTOR inhibitors in human ovarian carcinoma. *Apoptosis* **9**, 797-805

297. Ke, N., Zhou, D., E. Chatterton, J., Liu, G., Chionis, J., Zhang, J., Tsugawa, L., Lynn, R., Yu, D., Meyhack, B., Wong-Staal, F., and Li, Q.-X. (2006) A new inducible RNAi xenograft model for assessing the staged tumor response to mTOR silencing. *Experimental Cell Research* **312**, 2726-2734

APPENDIX A

POLYMER-VIRUS HYBRID VECTOR FOR GENE DELIVERY

In contrast to non-viral vectors, viruses are highly effective in infecting cells and transferring their genetic materials to the nucleus where it is expressed. However, viral vectors suffer from toxicity, immunogenicity and specificity to target cells that decrease their efficiency. The melding of viral delivery components with non-viral systems represents a new approach to enhance viral infection by overcoming the repulsion between the negatively charged viral surfaces and anionic glycosaminoglycan coated epithelial cells (263, 264). Cationic polymers that were synthesized in our laboratory and described in Chapter 2 of this thesis were evaluated to enhance viral infection in bladder, breast and prostate cancer cells. The researches were carried out in collaboration with Professors Christina Voelkel-Johnson and Joshua LaBaer's laboratories at Medical University of South Carolina (MUSC) in Charleston, SC and the Biodesign Institute at ASU, respectively. The works are summarized below.

App.1. Polymer-enhanced Adenoviral Transduction of CAR-negative Bladder Cancer Cells (265)

Adenoviruses (Ad) have been applied for gene therapy in multiple applications because of their high transduction efficiencies *in vivo* (228, 266, 267). However, the commonly used Ad vectors suffer from two fundamental problems: the high transduction of untargeted cells and low transduction of the target cells. The second problem is associated with the cells that express low or no coxsackie adenovirus receptors (CAR) for efficient Ad infection. As a result, transduction efficiency of those cells is extremely poor using Ad vectors. One method of Ad retargeting is to coat the viral capsid using cationic lipids and

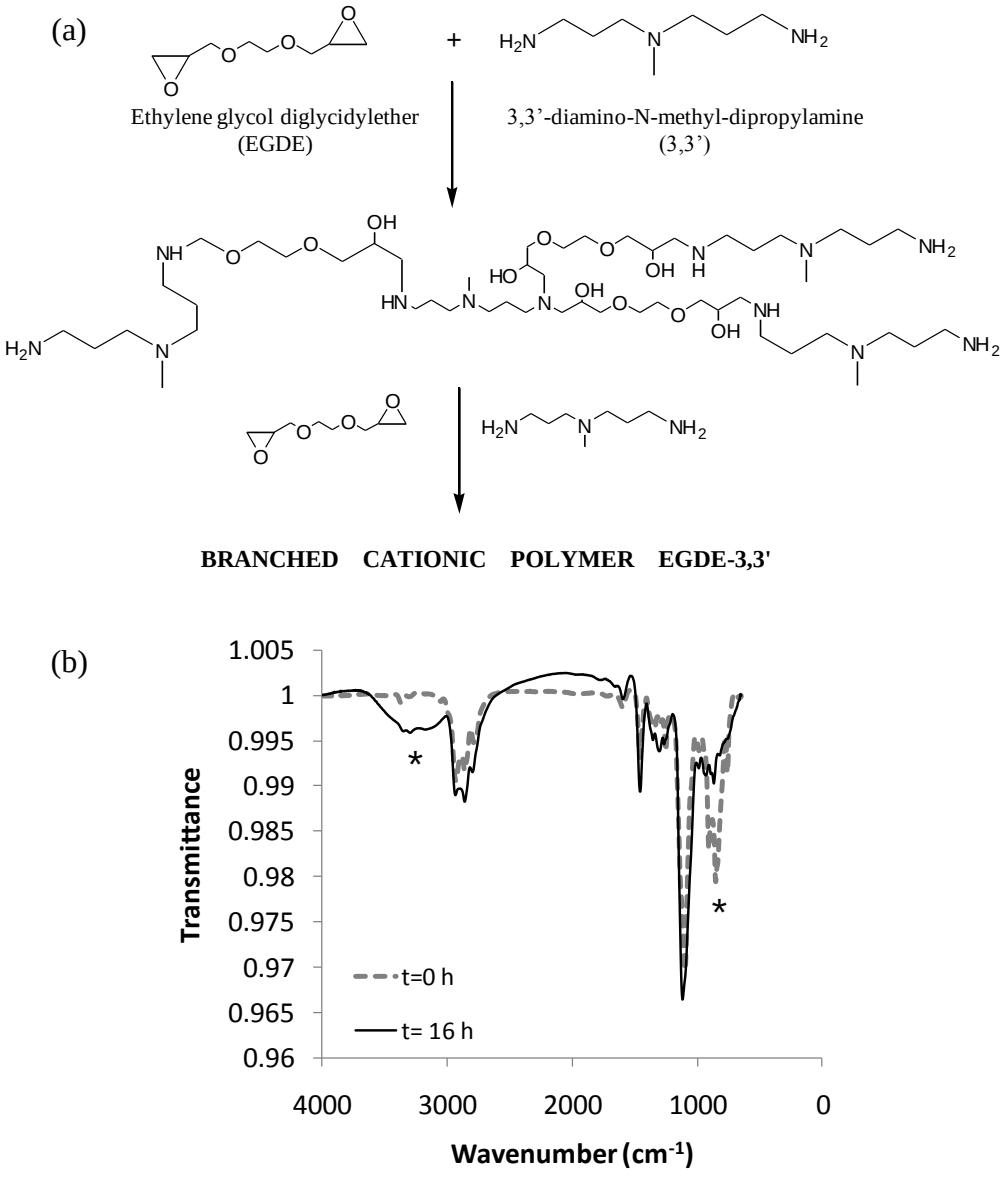

Figure A1: (a) Schematic representation of synthesis of the EGDE-3,3' polymer based on ethyleneglycol diglycidyl ether (EGDE) and 3,3'-diamino-N-methyl dipropylamine (3,3') monomers. (b) Fourier Transform Infrared (FT-IR) Spectroscopy of EGDE-3,3' polymerization at t= 0 and 16 h. Polymerization reaction can be seen by the emergence of the hydroxyl peak from 3000-4000 cm^{-1} and the disappearance of the epoxide peak in the 860-950 cm^{-1} region of the FT-IR spectrum. These regions are marked with asterisks in the figure. Adopted from Ref. (265).

polymers for efficient interactions between cationic Ad-polymer hybrid vectors with anionic glycosaminoglycan coated epithelial cells and thus enhancing their

cellular internalization (263, 268-274). Based on these previous reports, one of the lead cationic polymers from the library described in Chapter 2 was investigated to enhance adenoviral transduction in CAR-negative bladder cancer cells (265). The polymer ethyleneglycol diglycidyl ether(EGDE)-3,3'-diamino-N-methyl dipropylamine (3,3') or EGDE-3,3' (Figure A1) was used to deliver green fluorescent protein (GFP) containing Ad (Ad-GFP) to CAR-negative TCCSUP human bladder cancer cells (265). pEI-25 was used as a polymer standard.

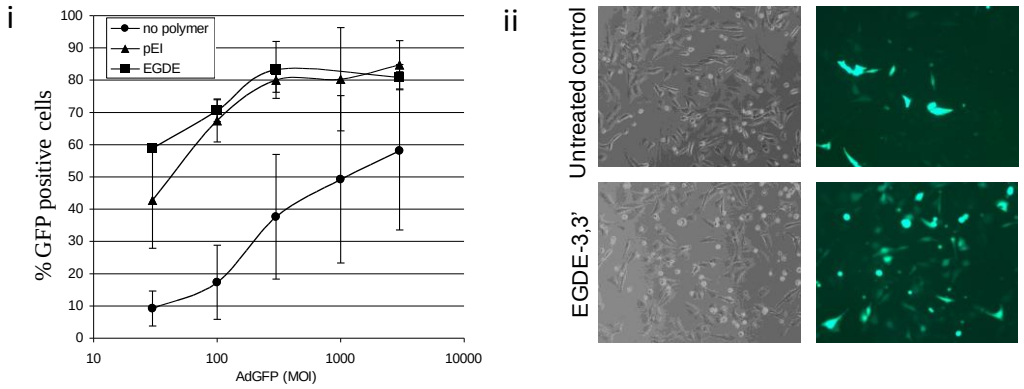

Figure A2. Effects of polymers on infectivity and transgene expression. TCCSUP bladder cancer cells were plated overnight and exposed to Ad.GFP either alone or complexed with polymers. GFP expression was quantified by flow cytometry at 48h post-infection. (i) % infectivity based on the number of GFP positive cells; (ii) Representative images under brightfield and fluorescent microscopy of TCCSUP cells exposed to 30 MOI of Ad.GFP without (control) and with (EGDE-3,3') polymer pre-incubation.

GFP gene expression was detected in 20% of TCCSUP cells when the multiplicity of infection (MOI=number of viral particles per target cell) of Ad-GFP was used as 100 (Figure A2 (i)) (265). Higher MOI at 3000 showed 50-60% GFP expressing cells (Figure A2 (i)), whereas the MOI was not physiologically relevant, can stimulate immune responses, and can be fatal for the host (275). Incorporation of the EGDE-3,3' polymer into the Ad.GFP enhanced their

infectivity in TCCSUP cells with 60% and 80% GFP expressing cells at MOI=30 and 500, respectively . pEI-25 also improved the Ad.GFP infectivity to the same level like EGDE-3,3', although transgene expression in individual cells was not consistent using pEI-25 compared to those using EGDE-3,3'. The polymer-Ad.GFP complexes did not show any adverse effects or toxicity to the cells.

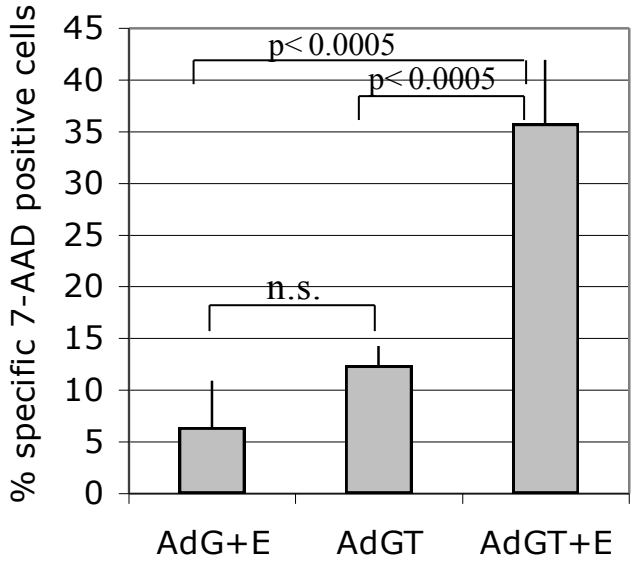

Figure A3. Effects of polymer on the efficacy of Ad.GFP-TRAIL induced cell death in TCCSUP bladder cancer cells. Cells were infected with 30 MOI Ad.GFP (AdG) or Ad.GFP-TRAIL (AdGT) either in the absence or presence of the EGDE-3,3' polymer. Membrane integrity was stained using 7-AAD and quantified using flow cytometry. % specific 7-AAD uptake was calculated by subtracting background staining in Ad.GFP infected cells. All data shown are the mean ± SD from at least three independent experiments. Statistical significance between groups was calculated using the Student's t-test (n.s. = not significant).

The EGDE-3,3' polymer-Ad complexes were then tested to deliver a gene of human tumor necrosis factor-related apoptosis inducing ligand (TRAIL) that induces apoptotic cancer cell death by binding with death receptors (276). The Ad.GFP-TRAIL gene was generated by the fusion of TRAIL to the GFP vector

(Ad.GFP-TRAIL) (277, 278). The EGDE-3,3' and Ad.GFP-TRAIL construct caused cell death of TCCSUP cells by 35-40%, while the Ad.GFP-TRAIL alone, EGDE-3,3' alone, and Ad.GFP with EGDE-3,3' induced only 12, 5 and 5% cell death, respectively (Figure A3). The combination treatments with Ad.GFP TRAIL and EGDE-3,3' resulted in synergistic cell death compared to their individual treatments. These data indicate that polymer coated virus delivery can confer CAR-independent infection and infectivity enhancement. Further studies to restore the viral infectivity in target cells are underway in Professor Voelkel-Johnson's laboratory at MUSC in Charleston, SC.

App. 2. Improvement of Lentivirus Production and Transduction using Cationic Polymer

App.2.1 Introduction

Lentiviruses (LV) are a subclass of retroviral vectors that contain a diploid positive-strand viral RNA genome. LV are used in many gene therapy applications because of their replication in both dividing and non-dividing cells (279-282). Assembly of the capsids of these viruses requires three proteins: *gag*, *pol* and *env*, which are viral capsid proteins, reverse transcriptase and envelope proteins, respectively. The viral capsid protein forms a virion for viral packaging. The reverse transcriptase converts the RNA genome to double-stranded DNA which is permanently integrated into the chromosomes of host cells. The envelope proteins help to bind to the receptors on target cells and mediate cellular entry. One of the important challenges for LV gene delivery applications is the production of high titer viral stocks. One approach to obtain high viral titer stocks

is to transiently transfect human embryonic kidney (293T) cells using cotransfection of the three pDNA containing gene of *gag-pol*, *env* and any gene of interest (283) (Figure A4). The pDNAs of *gag-pol* and *env* express viral packaging and envelope glycoproteins, respectively. The third pDNA expresses replication-defective LV vector genomes containing the gene of interest, e.g., a reporter gene that provides a quantitative evaluation of viral particles production. However, delivery of genes into 293T cells requires an efficient delivery vehicle.

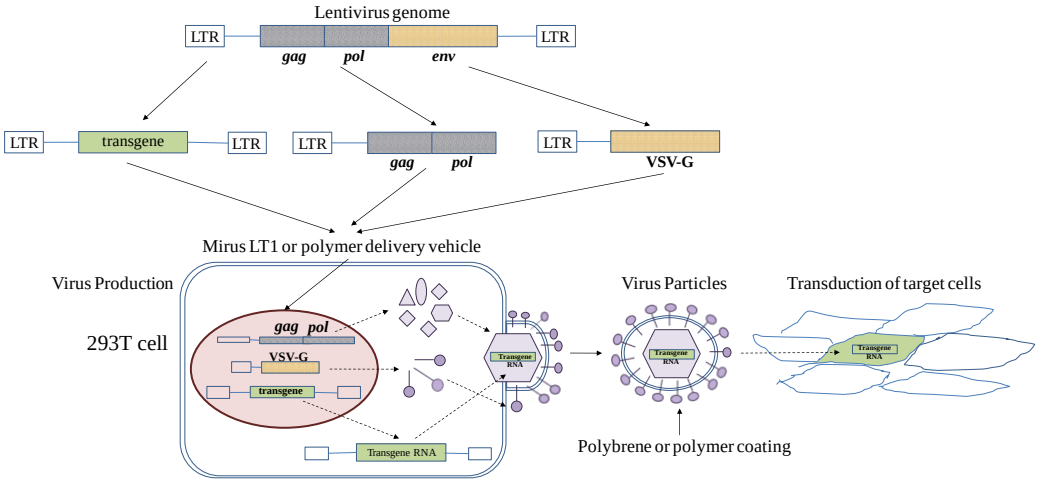

Figure A4. Lentivirus production and lentiviral-vector mediated transduction. The *gag-pol* structural genes, *env* packaging constructs and a transgene expression vector are delivered together into 293T cells using Mirus LT1 or cationic polymer vectors. The virus particles produced from the 293T cells contain the gene of interest (transgene) which is then used for infecting target cells (transduction) in order to express or knock down the gene of interest. Polybrene or cationic polymers are used to facilitate the viral transduction of targeted cells.

App.2.2 Production of High Titer LV Vectors by Transient Transfection

Production of LV by transient transfection using several plasmid constructs are classically used in small scale transfection experiments. The commonly used gene delivery vectors used are Lipofectamine, FuGENE and

Mirus LT1 reagents etc. which are commercially available and expensive (284), and thus are not economically feasible for large scale virus production. An economically viable feature of LV production had been proposed using the cationic polymers produced in our laboratory. The motivation was to substitute the expensive commercially available transfection reagents with the easily synthesized and cheap polymers for increasing virus production and transduction efficiency of the viruses. Therefore, the first objective of this study is to develop a cost-effective, reliable and scalable LV production process using the transient transfection method and the lead polymer vectors that were synthesized in our laboratory (details are in Chapter 2). The second objective is to produce LV short hairpin RNA (shRNA) vectors to knock down a known cancer therapeutic target protein, the mammalian target of rapamycin (mTOR) in human breast and prostate cancer cells *in vitro*.

App.2.2.1 Generation of Lentiviruses

The polymers 1,4C-3,3'; NPGDE-DT; NPGDE-1,4Bis; NPGDE-N2 Amino; EGDE-3,3', 1,4C-1,4Bis; and BDGE-1,4Bis were tested at different concentrations to generate LV in 293T cells in a 96-well plate format. The cells were seeded and grown overnight in the DMEM medium at a density of 60,000cells/100µl/well in a 96-well plate. Following 24h of growth, a master mix of 100ng *gag-pol* pDNA and 20ng LV envelope expressing vector VSV-G DNA was prepared in 6.5µl of serum-free DMEM. The pDNA of GFP was diluted to 5ng/µl in 10µl 1X PBS. Transfection reagents Mirus LT1 and the polymers were

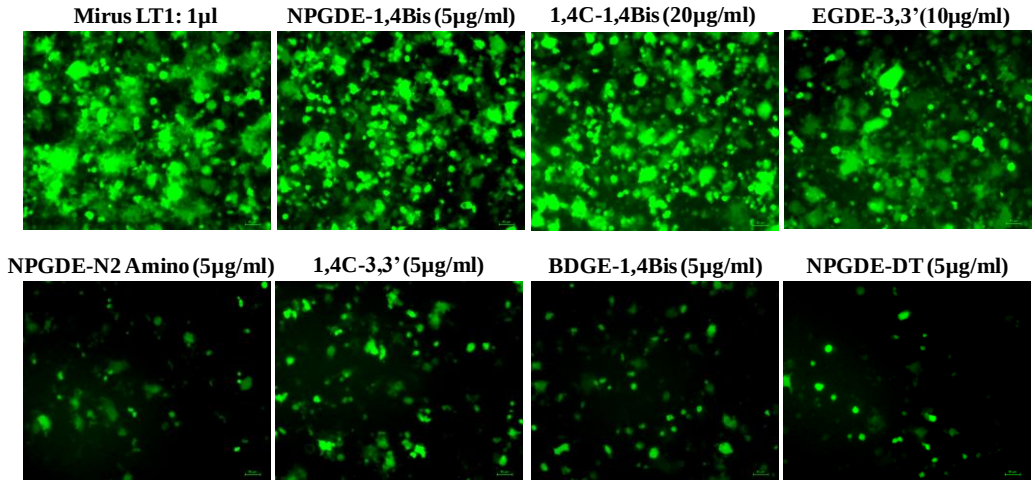

Figure A5. Representative fluorescence images of 293T cells used for the production of GFP-coding LV. Cells were transfected using a packaging plasmid expressing *gag-pol*, an envelope plasmid expressing the *env* glycoprotein and the GFP vector plasmid DNA delivered using Mirus LT1 or cationic polymers synthesized in our laboratory. The GFP expressing cells were imaged 72 h of post-transfection.

prepared at different concentrations (the final concentrations are shown in Figure A5) in 6.5µl of serum-free DMEM. The viral packaging DNA solution, GFP DNA and Mirus LT1 or polymer solution were mixed together and incubated for 20 min at R.T. The mixture was added to the cells per well of a 96-well plate following which the plates were centrifuged for 30 min at 2000 rpm and incubated at 37°C. Viral supernatant of 180µl was collected in every 24 h of post-transfection till 72 h by replacing the cell culture medium with fresh 200µl DMEM medium after each collection. The viruses were aliquoted and stored at -20°C for transduction experiments. The virus production was assessed from GFP fluorescence images after 72h of transfection of 293T cells. The preliminary results showed that NPGDE-1,4 Bis (5µg/ml); EGDE-3,3' (10µg/ml) and 1,4C-1,4Bis (20µg/ml) polymers produced GFP expression levels equal to or greater than those produced using Mirus LT1 reagents without causing any toxicity to the

cells (Figure A5). The results indicate the polymers to be more suitable and cost-effective alternatives than the commercially available reagents to produce 10^6-10^7 titer units/ml of LV. Further evaluation of this strategy is under investigation in collaboration with Dr. Laura Gonzalez and Professor Joshua LaBaer at the Center for Personalized Diagnostics Laboratory in the Biodesign Institute of ASU.

App.2.3 Silencing the Mammalian Target of Rapamycin (mTOR) using LV-shmTOR and Polymer

Cancer cells, including breast and prostate cancer cells, frequently induce the phosphatidylinositol-3 kinase (PI3K)/AKT signaling pathway that triggers activation of cytoplasmic mTOR serine/threonine kinases (285). In cancer cells, mTOR can also be activated by other receptor tyrosine kinase pathways such as overexpression of human epidermal growth factor receptors (HER 1-4) and platelet-derived growth factor receptors (PDGFR) etc. (286). mTOR forms mTORC1 complexes by interacting with regulatory associated protein of mTOR (Raptor). mTORC1 phosphorylates two downstream proteins: ribosomal p70s6 kinase (S6K1) (287) and eukaryotic initiation factor (eIF4E) binding proteins (4EBP1) (288, 289). Phosphorylation of S6K1 and eIF4E enhances translation of growth factors, anti-apoptotic proteins (Bcl2 and Bad) (290), cell cycle regulators (cyclin D1) of G1 to S phase transition (291, 292), ribosomal proteins and elongation factors in a variety of cancer cells (293). Inhibition of mTOR activity using rapamycin molecules and its derivatives (CCI-779, RAD 001 and AP23573) has been demonstrated to dephosphorylate S6K1 and 4EBP1(294), block G1 to S phase traverse (295), and inactivate Bcl2 and Bad anti-apoptotic proteins (296).

Silencing of mTOR using LV-shmTOR constructs had been shown to induce apoptosis upon induction with Doxycycline (Dox) in PC3-MC-luc prostate cancer cells both *in vitro* and *in vivo* (297). Cultured cells treated with shmTOR in presence of 1µg/ml Dox showed 60% reduction in mTOR protein and mRNA levels after four days of Dox-induction. The control shRNA did not show any reduction in the mTOR levels. A 10-15% increase of cells in the G1/G0 phase was observed for the cells transduced with shmTOR in the presence of Dox compared to the untreated cells. *In vivo* evaluation of mTOR silencing with Dox induction in PC3-MC-luc xenografts of athymic nude mice showed a complete regression of the tumors at the early stage of tumors. However, tumor volume was not reduced from the original volume in the advanced staged tumors.

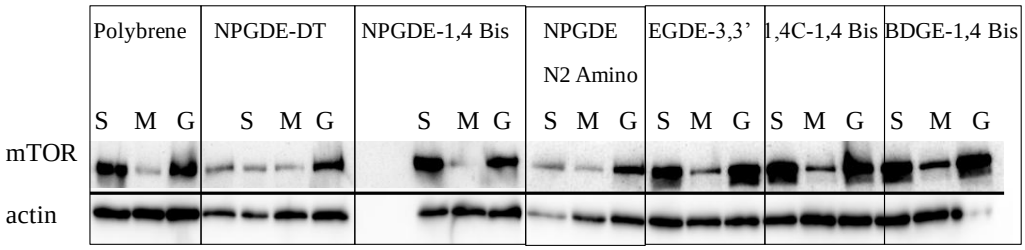

Figure A6: mTOR silencing in MCF-7 breast cancer cells. Cells (80,000/well) were transduced using either scramble shRNA control (S), or shmTOR (M), or GFP transgene (G) expressing lentiviral vectors at MOI=25. Western blot analysis of mTOR and actin protein expression was carried out after 72h of transduction. Actin was used as a loading control.

In our study, we tested the efficacy of LV-shmTOR constructs in MCF-7 breast cancer cells by delivering them using 5µg/ml of the following polymers: 1,4C-3,3'; NPGDE-DT; NPGDE-1,4Bis; NPGDE-N2 Amino; EGDE-3,3', 1,4C-1,4Bis; and BDGE-1,4Bis. Polybrene (8µg/ml) was used as a control polymer

vector. The preliminary results showed that NPGDE-1,4Bis deleted the mTOR protein expression levels significantly in MCF-7 cells, while a faint levels of mTOR were detected for cells transduced using polybrene polymer and LV-shmTOR constructs (Figure A6). Though NPGDE-DT and NPGDE-N2 Amino showed similar efficacy as polybrene, the polymers were toxic to cells which was seen from the lower levels of actin and mTOR expression in scramble shRNA and GFP DNA transduced cells than that of the shmTOR transduced cells. Further studies on mTOR knockdown are underway in Dr. Joshua LaBaer's laboratory in the Biodesign Institute of ASU.

APPENDIX B

LIST OF PUBLICATIONS

B.1 List of Publications Derived from this Thesis

- Barua, S.; Rege, K., The influence of Mediators of Intracellular Trafficking on Transgene Expression Efficacy of Polymer-plasmid DNA Complexes. Biomaterials, 2010, 31 (22), 5894-5902
- Barua, S.; Joshi, A.; Banerjee, A.; Matthews, D.; Sharfstein, S. T.; Cramer, S. M.; Kane, R. S.; Rege, K., Parallel Synthesis and Screening of Polymers for Nonviral Gene Delivery. Molecular Pharmaceutics, 2009, 6 (1), 86-97
- Barua, S.; Rege, K., Cancer-Cell-Phenotype-Dependent Differential Intracellular Trafficking of Unconjugated Quantum Dots. Small, 2009, 5 (3), 370-376
- Kasman, L.M.; Barua, S.; Lu, P.; Rege, K.; Voelkel-Johnson, C., Polymer-enhanced Adenoviral Transduction of CAR-negative Bladder Cancer Cells. Molecular Pharmaceutics, 2009, 6 (5), 1612-1619

B.2 Manuscripts in Preparation

- Barua, S.; Voelkel-Johnson, C.; Han, H.; Von Hoff, D. D.; Rege, K., Inhibition of Aurora Kinases Enhances Transgene Expression and Cancer Cell Apoptosis following delivery of Polymer-Plasmid DNA Complexes. In Preparation, 2011

B.3 Manuscripts in Revision

- Barua, S.; Ramos, J.; Potta, T.; Taylor, D.; Huang, H.C.; Montanez, G.; Rege, K., Review on Discovery of Cationic Polymers for Non-viral Gene

Delivery. In Revision, Combinatorial Chemistry & High Throughput Screening, 2011

- Huang, H.C.; Barua, S.; Sharma, G; Dey, S.K.; Rege, K., Review on Inorganic Nanoparticles for Cancer Imaging and Therapy. In Revision, Journal of Controlled Release, 2011

B.4 Research Work in Progress

- Gonzalez, L.; Barua, S.; LaBaer, J; Rege, K., Generation of Lentiviruses using Cationic Polymers and Transduction using Lentivirus-Polymer Hybrids

B.5 Other Research Papers

- Barua, S.; Bullard, R.S.; Banerjee, I.; Yarmush M. L.; Rege, K., Lytic Peptide-Mediated Sensitization of TRAIL-Resistant Prostate Cancer Cells to Death Receptor Agonists. Cancer Letters, 2010, 293 (2), 240-253
- Chavez, V.L.; Song, L.; Barua, S.; Wu, Q.; Zhao, D.; Rege, K.; Vogt, B.D., Impact of Nanopure Morphology on Cell Viability on Mesoporous Polymer and Carbon Surfaces. Acta Biomaterialia, 2010, 6(8), 3035-3043
- Huang, H.C.; Barua, S.; Kay, D.B.; Rege, K., Simultaneous Enhancement of Photothermal Stability and Gene Delivery Efficacy of Gold Nanorods Using Polyelectrolytes. *ACS Nano*, 2009, 3 (10), 2941–2952
- Li, X. X.; Barua, S.; Rege, K.; Vogt, B. D., Tuning Stability of Mesoporous Silica Films under Biologically Relevant Conditions through Processing with Supercritical CO_2. Langmuir, 2008, 24 (20), 11935-11941

- Şengör, S.S.; Barua, S.; Gikas, P.; Ginn, T.R.; Peyton, B.M.; Sani, R.K.; Spycher, N.F., Influence of Heavy Metals on Microbial Growth Kinetics Including Lag Time: Mathematical Modeling and Experimental Verification. Environmental Toxicology and Chemistry, 2009, 28(10), 2020-2029
- Rastogi, G; Barua, S.; Sani, K.; Peyton, B.M., Investigation of Microbial Populations in the Extremely Metal-Contaminated Coeur d'Alene River Sediments. Microbial Ecology, 2011